THE ASTROPHYSICAL JOURNAL

AN INTERNATIONAL REVIEW OF SPECTROSCOPY AND ASTRONOMICAL PHYSICS

VOLUME 79 MARCH 1934 NUMBER 2

PHOTO-ELECTRIC PHOTOMETRY IN THE INFRA-RED WITH THE LOOMIS TELESCOPE

By JOHN S. HALL

ABSTRACT

It is shown that a caesium oxide photo-electric cell may be used to measure stellar radiation in the infra-red, if cooled to approximately -40° C. At this, and lower, temperatures an obnoxious dark current is much weaker than the photo-current. The photometer, as attached to the Loomis telescope of the Yale University Observatory, differs from others chiefly in two respects: the cell is mounted in a thermos bottle in such a way as to be well insulated from heat and all drying is done chemically.

The Pleiades were observed on several different nights for calibration purposes. ζ Geminorum was observed on thirty-three nights. Comparison with other data shows that the maximum and minimum observed in the infra-red are later than those observed in the visual. There is a corresponding phase difference between observations made in the blue and in the visual, the former being earlier.

Color observations, numbering 1240, were made on 347 stars by making intensity measurements at three effective wave-lengths. This list of stars, with the exception of Polaris, includes all those north of the equator brighter than 4.4 visual mag. The data show that the colors of these stars, measured in the infra-red, are closely related to those measured in the blue region of the spectrum. The obvious exceptions are stars of very early or very late spectral types. The observed *c* stars are slightly redder than the other stars of the same spectral class. The color excesses of the observed early-type stars are not noticeably influenced by possible scattering due to the presence of interstellar matter. The possibility of finding the absolute magnitudes of giant stars later than F8 from their color excesses, as observed in the infra-red, appears promising.

A brief description, together with a photograph, of the Loomis coelostat telescope has been given by Dr. F. Schlesinger.[1]

The telescope consists of a plane mirror 30 inches in diameter, mounted equatorially and driven by clockwork. The mirror can be set in such a way that it will reflect the light from a particular star-field upward through a steel tube parallel to the earth's axis. A

[1] *Popular Astronomy*, **31**, 77, 1923.

15-inch photographic objective and a 10-inch visual objective are mounted at the lower end of this tube. Each lens is made of Jena glass and each has a focal length of 50 feet, or about 15 m. The transparency of these lenses is excellent for the blue as well as for the visual light. When this instrument was used for photographic observations, the plate-holder was rotated about the optical axis of the instrument by means of a clockwork. When only one star is under observation, as is generally the case with photo-electric photometry, the mirror can be pointed in such a way that the image of the star falls on this axis of rotation. The clockwork is then unnecessary. An observing room at the top of a 60-foot brick tower houses the photo-electric equipment. Although this room could easily be heated, this was not done for reasons that will soon be evident.

The general requirements for any photo-electric photometer are that it shall be highly insulated at all strategic points, that it shall be as light-tight as possible, thoroughly shielded, and light enough to be carried by the telescope for which it is designed. The cell chamber in this case must also be insulated against heat. The weight of the apparatus obviously did not have to be taken into consideration.

Although photo-electric photometers have been described elsewhere, the one used to collect all the material in this paper differs radically from the others, and I shall describe it in detail.[2]

Figure 1 shows a cross-section of the apparatus. An iris and its shutter are at A. Just behind this iris is a negative lens which enlarges the stellar image to a little over 1 cm. at the distance of the cathode of the photo-cell. Two filter slides are each held by a pair of gibs. A wooden box covered on all six sides with tinfoil contains a thermos bottle. The latter is large enough to hold the cell and about 300 cc. of solid carbon dioxide or "dry ice." In order to be sure that the outer surface of the thermos bottle would not be coated with moisture or frost at the window, owing to the very low temperature of the dry ice within the bottle, a copper ring was fitted to the contour of the bottle and connected through the wood to the aluminum base by two copper springs. These are not shown in the diagram.

[2] A preliminary description is given in *Proceedings of the National Academy of Sciences*, **18**, 365, 1932.

Conduction of heat from this base helps to keep the outside of the bottle free from frost.

The cork *d* has a cylindrical shape and was made to fit the inner surface of the thermos bottle and the outer surface of the cell. A

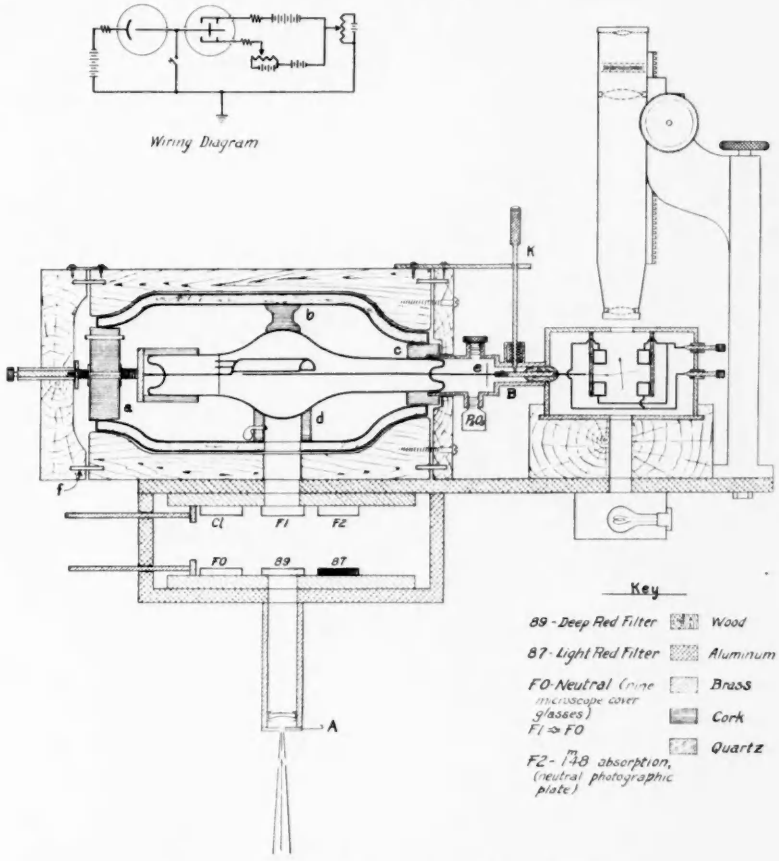

FIG. 1.—The apparatus and the wiring diagram

small glass tube in its side filled with a drying agent keeps this chamber dry. Although dry ice at $-80°$ C sometimes surrounded this cork for many hours, no difficulty was encountered due to the formation of frost on the cell or thermos bottle window. Except for a small window, the inner walls of the thermos bottle were completely silvered. The space between these walls was then evacuated to 0.002

mm. The cork *b* between the top of the bottle and the cell is used as a support. The anode end of the cell fits rather tightly in the cork *c*, which in turn fits snugly into the end of the thermos bottle. The outer surface of this end of the cell is wrapped in tinfoil and grounded. The conduit *B* is dried by the use of phosphorus pentoxide, replaced every few weeks. The disk *e* is a piece of black paper and keeps out possible light from the electrometer lamp. Unless the key *K* is pulled out, the electrometer needle is grounded. The catch attached to it enables the operator to record observations and observe at the same time.

The left end of the cell is inclosed in a cork cylinder, to the end of which a brass plate is attached. The cathode lead wire is soldered to this plate. Two brass springs are attached to cork *a*, which closes the thermos bottle. In addition to making reasonably good contacts (a megohm resistance is in the circuit), these springs lengthen the path over which the heat must travel in order to reach the photo-cell. Despite this fact, the cathode binding post, just outside the box, in general became quite cold. This binding post, together with the exposed end of the lead wire, is coated with paraffin. On the night of November 10, 1932, the air was so damp in the observing room that drops of water occasionally fell from the end of this post, yet the apparatus worked smoothly. Circular strips of metal *f* help to make the cell chamber light-tight.

The microscope is fitted with a 16-mm objective, and an eyepiece giving a combined magnification of about 125. The scale in the eyepiece is divided into tenths of a millimeter. The deflection was usually timed over ten eyepiece divisions with a stop-watch which reads to one-fifth of a second.

THE PHOTO-ELECTRIC CELL

The photo-electric cell used in the Yale photometer is commonly designated as a *CsO* cell. Its real photo-sensitive surface, however, is believed to be a layer of *Cs* on *CsO* on *Ag*. It is also sometimes designated as *Cs*$-$*O*.

The Bell Telephone Laboratory in New York kindly gave us a gas-filled *CsO* photo-cell which it had developed for use in connection with talking motion pictures. The electrodes of this first cell

came out at the same end, and consequently it was found that a large current flowed when no light struck the cathode, owing presumably to leakage. Dr. Holden Prescott, of the Bell Laboratories, then kindly offered to make up another of these cells, this time bringing the two electrodes out at opposite ends.

This current was still far too large for stellar photometry, but when the polarity was reversed it was no longer detectable with a sensitive galvanometer. Dr. Prescott then suggested that this effect was due to thermionic emission from the cathode at room temperatures. On the following day (January 23, 1931) I was given the opportunity to test this theory at the Sloane Physics Laboratory. At a temperature of $-10°$ C the "dark current," that is, the current which flows when no visible radiation strikes the cathode, was less than 3×10^{-11} amp. Kingsbury and Stillwell,[3] also of the Bell Laboratories, confirmed these results, using an equally sensitive galvanometer. When the cell was packed in dry ice, the dark current decreased to a value that made stellar measurements possible. A thermocouple showed that the equilibrium temperature of the gas about the cell was near $-40°$ C. A half-dozen *CsO* cells were tried before one was finally chosen for the observing program. In each case the dark current could be made less than 5×10^{-14} amp. by cooling the cell in this way. The cell finally adopted nearly always has a dark current which is less than one division in thirty seconds, or less than 10^{-15} amp. Dry ice may be obtained from the local ice cream companies at five to ten cents a pound.

Since the operating potential for the cell was around 125 volts, it is easily seen that the resistance of the soda-lime glass, of which the photo-cell was made, must be enormously great, and that quartz glass is not necessary. If Ohm's law is obeyed (it may not hold for thin films), the effective resistance between the two ends of the cell must be of the order of 10^{17} ohms. Dr. Bronson[4] has found that the better grades of commercial glasses are insulators of high quality provided the glass is clean and properly polarized. He found that as soon as the potential is applied polarization begins, at first rapidly and after a few minutes much more slowly, several hours being necessary to complete the process. In like manner, when the potential is

[3] *Physical Review*, **37**, 1549, 1931.

[4] *Physics*, **2**, 420, 1932.

first applied to this cell the dark current at first is quite appreciable, but in a few minutes it reaches a value which is less than the photo-electric current, owing to background. Since the cell is presumably as cold as it ever gets when the potential is first applied, this initial current is apparently due to a change in the polarization of the glass. When the potential across the cell is removed, this process is reversed, the current flowing in the opposite direction.

Figure 2 shows an approximate color-curve for a *CsO* cell together with a color-curve for a *KH* cell. The former is taken from the manufacturer's data for a typical cell of this kind, while the latter is that given by Ives and Kingsbury.[5] Since for a group of *CsO* cells the color curves may vary from cell to cell, and for a particular cell its color curve may vary with the time, the *CsO* curve in Figure 2 can be regarded as only an approximation. *KH* and similar cells have been used extensively in astronomy by several observers. The color sensitivity of a particular photometric arrangement is sometimes roughly given by the color equation or the observed color index of a Ko star. The color equation (*CsO* − Visual) for the Yale photometer is approximately −0.8 mag. With Wratten filter 89 it becomes −1.2 mag., and for Wratten filter 87 it is −1.4 mag. The color equation (Radiometric − Visual) of the thermocouple used by Nicholson and Pettit[6] at Mount Wilson was −1.2 mag.

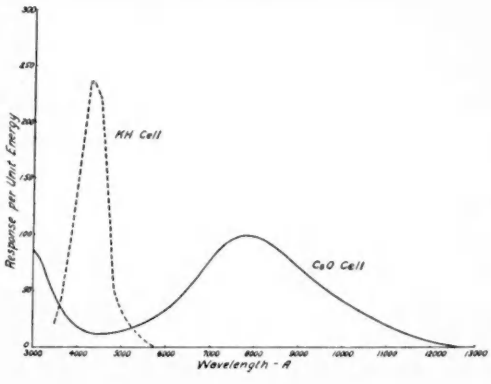

FIG. 2.—Color-curve of a *CsO* photo-electric cell compared with that of a *KH* cell.

In general, during the summer months the cell sensitivity would gradually decrease until the chamber was refilled with ice. It would then usually return to the same value that it was at the beginning of the evening. During the winter months the cell chamber did not

[5] *Journal of the Optical Society of America*, **21**, 541, 1931.

[6] *Contributions of the Mount Wilson Observatory*, No. 369, 459, 1928.

have to be refilled with ice and the sensitivity of the cell remained large enough for the scheduled observing program. The order in which the readings were taken automatically eliminated this factor.

The change of spectral response with the time, although usually small, had to be taken into consideration when the reductions were made. Fortunately, on only one night, August 14, 1932, was there definite evidence that the cell changed its color-curve while observations were in progress. When the program for this night was about half finished, the photo-current became erratic and the cell less sensitive. When the colors of the stars observed on this night are plotted against the mean colors of the same stars as observed on other nights, those that constituted the first part of the program follow a straight line with the usual regularity. The star observed when the cell began to be unstable, and all succeeding stars, form a curve which is displaced from the straight line by 0.1 to 0.3 mag. The evidence is strong that this change took place suddenly. In general, the spectral response of the cell changed slightly from night to night, particularly during the summer months. Changes in spectral response with the time are not peculiar to *CsO* cells alone. Becker,[7] working with a potassium photo-cell, observed such a change.

The actual sensitivity of the *CsO* cell was found by comparing its response with that of a Weston illumination meter which had been calibrated to light from a tungsten filament at 3000° K. After making due allowance for the difference in the color-curves of the photronic and *CsO* cells for the particular temperature of the comparison source (near 2600° K in this case), the derived sensitivity of this *CsO* cell is about 20 micro-amp. per lumen at 22.5 volts. This value may be called the "vacuum sensitivity" since the gas amplification begins at this voltage for these cells. For the voltages at which the cell was actually used, its sensitivity is between 250 and 400 micro-amp./lumen. When this datum is compared with that given by Stebbins,[8] one concludes that this cell is fully as sensitive to late-type stars as an excellent *KH* cell is to an Ao star of the same visual magnitude.

In order to be sure that the photo-current is directly proportional

[7] *Veröffentlichungen Berlin-Babelsberg*, **10**, Heft 3, 1933.

[8] *Astrophysical Journal*, **76**, 222, 1932.

to the light intensity incident on the cathode of the cell, eleven bright stars in the Pleiades were observed on several different nights in January, February, and March, 1932. Electra was used as the comparison star, and in general three readings were made for each star. The rates of deflection varied from three divisions per second for a 3.0-mag. star to about one-tenth of a division per second for a 6.5-mag. star. This range in photo-current is greater than that which applies to any observation in the body of this paper. These observations are reduced in such a way that the sum of the HR magnitudes equals the sum of the Yale magnitudes. Figure 3 shows that a 45° line fits the observations satisfactorily.

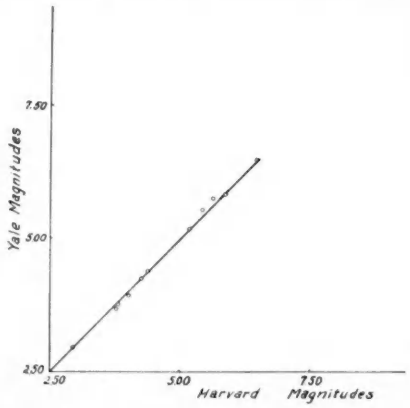

FIG. 3.—The magnitudes of eleven stars in the Pleiades, observed with a *CsO* cell, plotted against the Harvard visual magnitudes. The sum of each set of magnitudes is the same. A 45° straight line is drawn through the origin.

Table I gives the HR number and magnitude, the Yale magnitude (in the infra-red), the probable error of the mean magnitude, and the number of nights on which each star was observed. These magnitudes are plotted in Figure 3. The residuals, Yale *minus* Harvard Revised, do not appear to be systematically influenced by spectral subclass differences. The probable errors show the accuracy with which the magnitudes of blue stars can be measured with this red-sensitive photo-cell. The table shows that the light-intensity of a B-type star of 6.5 mag. may be compared with that of a brighter star with reasonable accuracy. Approximately the same rate of deflection would be obtained from an 8.0-mag. Ma star as from a 6.5-mag. B5 star. Since these Pleiades observations were made, the effective sensitivity of the electrometer has been doubled by the use of suitable potentiometers.

THE ELECTROMETER

Two potentiometers are used to adjust the potential of the knives of the Lindemann electrometer. One of these changes the zero point

of the needle without sensibly affecting the sensitivity of the electrometer, while the other changes both the sensitivity and the zero point.

The capacity of the anode-electrometer system was found by measuring the rate of deflection of the electrometer needle with and

TABLE I

OBSERVATIONS OF THE PLEIADES

HR	HR Mag.	Yale Mag.	P.E. Mag.	N
1165	2.96	2.966	±0.005	14
1178	3.80	3.685	7	15
1142	3.81	3.787	1	15
1149	4.02	3.930	4	12
1156	4.25	4.224	4	13
1145	4.37	4.390	5	14
1180	5.18	5.159	8	13
1140	5.43	5.541	5	6
1144	5.63	5.749	7	12
1151	5.85	5.838	11	6
1152	6.46	6.488	±0.015	5
Total	51.76	51.757	.....	.....

without a calibrated condenser attached to the anode. This capacity was found to be very nearly 9 cm.

The sensitivity of the electrometer as it is usually employed is 250 eyepiece divisions per volt. One division per second therefore corresponds to a current of 4×10^{-14} amp. On one or two occasions the electrometer has been used at four hundred divisions per volt, but the needle then takes several seconds to return to the zero point.

OBSERVATIONS OF ζ GEMINORUM

				Period
ζ Gem.	$6^h58^m.2$, $+20°.7$	($3^m.7$)	Gop	$10^d.15$
δ Gem.	7 14.2, +22.2	3.51	Fo	.....
ϵ Gem.	6 37.8, +25.2	3.18	G5	.....

The variable star ζ Geminorum was observed on thirty-three nights between January 28 and November 27, 1932; δ Geminorum was the comparison star, but the variable is plotted against ϵ Geminorum in Figure 4 in order to compare it more readily with two other light-curves. The magnitude difference ($\delta-\epsilon$) was observed on two

nights and found to be 1.10 mag. The transparency on all but two of these thirty-three nights was rated fair or good. The other two nights (March 16 and April 15) were called poor and given half-

TABLE II

OBSERVATIONS OF ζ GEMINORUM

G.M.T.	Phase	$\zeta-\delta$ Mag.	N
1932 Jan. 28.631	0.387	+0.221	2.5
30.613	.583	+ .308	3.0
31.602	.680	+ .212	3.0
Feb. 1.632	.782	+ .135	3.0
8.619	.470	+ .291	3.0
13.618	.962	− .039	3.0
15.582	.156	+ .013	3.0
20.551	.645	+ .234	3.0
23.580	.943	+ .004	2.0
24.598	.044	− .049	2.0
Mar. 3.604	.832	+ .096	3.0
5.553	.024	− .058	3.0
9.550	.418	+ .257	3.0
10.550	.517	+ .333	3.0
12.534	.712	+ .193	3.0
14.535	.909	+ .047	3.0
15.548	.009	− .035	3.0
16.544	.107	− .013	1.0
18.505	.300	+ .151	3.0
Apr. 1.533	.682	+ .198	2.5
3.523	.878	+ .044	4.0
4.541	.978	− .010	3.5
6.533	.175	+ .048	1.5
15.531	.062	.000	1.0
19.534	.456	+ .309	2.0
20.543	.559	+ .343	4.0
22.538	.752	+ .146	3.0
23.534	.850	+ .088	3.0
Oct. 27.802	.296	+ .134	4.0
30.905	.602	+ .298	2.0
Nov. 3.841	.990	− .020	3.0
26.813	.253	+ .136	2.0
27.749	0.345	+0.233	2.0

weight. Since one of these nights follows the other directly in phase, the two are plotted as a single normal at phase 0.084. The other normals average 2.7 comparisons taken on a single night. Each com-

parison represents ten or twelve separate readings. Three comparisons were usually made in less than a half-hour. The variation in magnitude of ζ Geminorum is so slow that there is no necessity of reducing the observations to heliocentric time.

The residuals derived from a smoothed curve show no systematic tendency when plotted against the variable's zenith distance. The sum of the residuals of the nights that are rated fair is substantially zero. If two straight lines are drawn through the normals of Figure 4, and if five residuals (one near maximum and four near minimum) are disregarded, the average probable error of a single normal is ±0.012

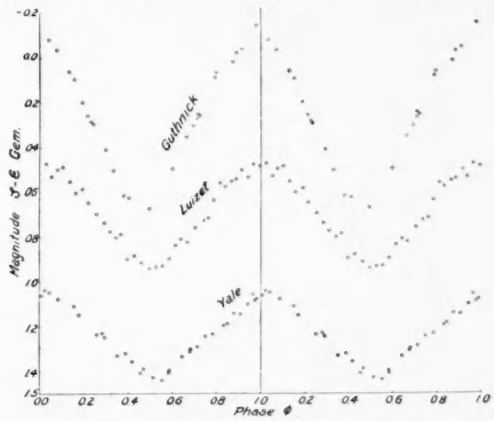

FIG. 4.—Three light-curves of ζ Geminorum observed in three different effective wave-lengths. These wave-lengths are roughly 4500 A (Guthnick), 5500 A (Luizet), and 7400 A for the Yale observations.

mag. The average probable error of a single normal as derived internally from the agreement of the individual comparisons is ±0.007 mag.

The phases given in Table II were computed from elements derived by Nielsen:

$$\text{Max} = \text{J.D. } 2410639.801 + 10^{d}.153527E - 0^{d}.575 \times 10^{-6}E^{2}.$$

The column designated by N shows the number of comparisons. When the photo-cell was not working smoothly, the comparisons were given half-weight.

Guthnick's[9] light-curve, given in Figure 4, was observed in the

[9] *Astronomische Nachrichten* (*Jubilaumsnummer*), 1921.

winter of 1919–1920 with a blue-sensitive potassium photo-cell. Luizet's[10] light-curve was observed visually within the interval 1898–1918, and reduced by Hertzsprung. Each normal represents the observations of twenty-six separate nights. Hertzsprung showed that Luizet's observations are well represented by a sine curve.

The distribution of effective energy with respect to wave-length was roughly obtained for the Yale observations of this star by making use of given filter calibrations. When the light-intensity of ζ Geminorum was measured with and without Wratten filters 89 and 87,[11] it was found, on the average, that 65 per cent of the total effective energy is of longer wave-length than 6900 A and 30 per cent is beyond 8000 A. The wave-length which equally divides the total effective energy is near 7400 A. The observed color index (*CsO* – Visual) for an average Go star is -0.5 mag.

Nielsen[12] has shown that the period of ζ Geminorum has been decreasing at the rate of 0.099 ± 0.006 sec. per period or 3.6 sec. per year. His discussion is based on forty-six sets of visual observations taken within the interval 1849–1926. His separate discussion of three photo-electric light-curves (in the blue) and one photographic light-curve shows that the maxima of these four curves were, on the average, 0.023 ± 0.006 periods earlier than the others. Luizet's observed maximum is very close to that derived from Nielsen's elements.

The Yale observations show that the maximum of the light-curve of ζ Geminorum for an effective wave-length near 7400 A is about 0.024 periods later than the maximum determined visually. The displacement in the minimum is in the same direction but somewhat larger.

Dr. Meldrum Stewart has very kindly informed me by letter that contemporary photo-electric observations (in the blue), made at Ottawa by Dr. Henroteau, show a maximum that is in good agreement with that formerly observed in this region of the spectrum. The shift in phase depending on wave-length therefore cannot be ascribed to a neglected change in period.

[10] *Lyon Bulletin*, **11**, 33A, 1929.

[11] *Wratten Light Filters*, Eastman Kodak Co., 1928.

[12] *Ole Romer-Observatoriet*, **5**, 1930.

The infra-red and visual range in magnitude are both very nearly one-half the range in the blue. If the variation were due to a pure temperature change of a black-body radiator, this could not be the case. The color observations of ζ Geminorum, given in a following section, are not sufficiently numerous to justify a computation of a variation in the star's diameter.

COLOR OBSERVATIONS OF 347 STARS

Every observation in this paper was made by the author, using a gas-filled caesium oxide photo-electric cell which is designated as No. 43808.

In order to determine the relative colors of these bright stars in the infra-red, the light-intensity of each star was measured in three effective wave-lengths. I was unable to find a satisfactory filter that transmits the yellow and not the infra-red. Accordingly, two red filters were selected: Wratten filter 89, which has a rather sharp yellow cut-off at 6900 A, and Wratten filter 87, which has an equally sharp cut-off at 8000 A. These figures represent the wave-lengths at which the transmission is approximately half the total energy. At longer wave-lengths these filters absorb a small fraction of the energy, probably 15 per cent. Filter 89 transmits one-half of 1 per cent of visual daylight energy. These two gelatin filters were each mounted between two microscope cover-glasses. The third effective wave-length was obtained by using no filter at all.

The colors observed by comparing the intensities with and without filter 89 have a range of nearly 0.9 mag. (Bo–Mb), and the corresponding colors using filter 87 have a range of 1.6 mag.

In order to equalize the electrometer deflections to some extent, a neutral filter consisting of nine microscope cover-glasses was used. This filter absorbed very nearly 0.74 mag. regardless of whether the light-source was a B-type or a K-type star. A similar filter used to decrease the stellar intensities in all three effective wave-lengths was found to be far from neutral. In addition to equalizing the electrometer deflections and therefore increasing the accuracy of the timing, the neutral filter reduced the strain on the photo-cell and made the background current more nearly the same for each of the three effective wave-lengths.

Observations had to be interrupted on several nights because the cell delivered large numbers of electrons after the starlight had been shut off. This effect is produced by allowing the light of too bright a star to strike the cathode of the cell at the high potential at which the cell is being used. If the potential is taken off and the cell is allowed to remain in the dark for several hours, it was noticed that this effect does not persist when the potential is again applied. In one case, after I had waited for only one hour, it still persisted. For this reason no attempt was made to decrease the rate of deflection of the electrometer for bright stars by decreasing its sensitivity.

With the exception of Polaris, all stars brighter than 4.40 visual mag. and north of the equator and several others were observed. Three of the 347 stars were observed on only one night; 17 were observed on two nights. The total number of observations is 1240. At least eleven readings constitute one observation of each star: two with the neutral filter, two with 89, three with 87, two with 89, and finally two again with the neutral filter. The dark current, which includes sky, leakage, and possibly other effects, was in general measured once for each star.

For the sake of brevity let us define the set of relative colors obtained by comparing the stellar intensity with and without filter 89 as colors 89, and similarly those relative colors obtained by comparing the intensity with and without filter 87 we shall designate as colors 87. Let us call Fo the neutral filter used to help equalize the rates of electrometer deflection, and let us call F1 the similar filter sometimes used in addition to the two color filters and Fo. The heavy neutral filter (F2 in Fig. 1) was used in the same rôle as F1. This filter is a developed photographic plate and is remarkably colorless. The few very bright stars were observed with a rotating sector.

THE REDUCTIONS

1. *Filter corrections.*—The first corrections which were applied to the relative colors expressed in magnitudes were those due to the fact that F1 is not neutral. A special series of observations was made on stars of different spectral type in order to determine the difference in color for a star of a given spectral class when observed with and without F1. In this way a good approximation to the corrections finally

adopted was obtained for both sets of colors. The final corrections were obtained from a discussion of the residuals after all other systematic errors had been eliminated from both sets of colors. In the case of colors 89, the total corrections vary from +0.060 mag. for a B-type star to +0.104 mag. for an M-type star. For colors 87, the corresponding corrections are +0.098 and +0.125 mag. The observed color of the star was used as the argument in each case. Less than a third of the observations were made with F1 in place.

2. *Reduction to the zenith.*—The observations were reduced to the zenith in the usual fashion,

$$\text{Color at zenith} = I_t - I_r + (E_t - E_r)\ (\sec z - 1),$$

where I_t differs from the total intensity by a constant, owing to the absorption of Fo (0.74 mag.), and I_r is the intensity (in magnitudes) with a red filter. This intensity differs from that with the filter alone since the two cover-glasses inclosing each red filter absorb about 0.17 mag. E_t and E_r are the corresponding extinctions at the zenith. Observations were made on six different nights for the purpose of determining the coefficient $(E_t - E_r)$. These nights as a whole may be considered as having the mean transparency of all the nights used in making the observations. Three stars of widely different colors were observed first three hours east of the meridian, then on the meridian, and then three hours west. Two such sets of stars were usually under observation at the same time in order to detect any possible differences depending on azimuth. The mean of the east and west coefficients was always adopted. In order to obtain as rapid variations in sec z as possible, these stars were chosen near the equator. The Loomis telescope cannot be used for stars at large hour angles or for stars much below the equator. The range in sec z used to determine the corrections was much larger than the average observed value of $(\sec z - 1)$.

Since only those nights were used which were rated as fair or better, the extinction coefficient was assumed to be constant from night to night for a star of a given color. More than 90 per cent of the nights were called good or better.

For colors 89 $(E_t - E_r) = -0.11 \pm 0.02$ mag. for B-type stars and $+0.02 \pm 0.01$ mag. for Ma stars. The positive coefficient is probably

accidental, but it seems possible that it may be due to atmospheric absorption bands in the infra-red. It simply means that to the photocell an M-type star is bluer at large zenith distances than at the zenith. For colors 87 the corresponding values of $(E_i - E_r)$ are -0.15 ± 0.05 mag. and -0.06 ± 0.03 mag., respectively. The observations show that these coefficients may be considered to be a linear function of the color itself. They are relatively small when compared to those found by Guthnick, his coefficients being five or six times larger on a comparable scale of colors.

A count of one quarter of all the stars observed shows that the zenith distance of 85 per cent of them was less than 33° at the time of observation. The correction to the zenith was in general so small that, as a matter of convenience, the spectral type was used as the argument instead of the color. Perhaps a half-dozen stars whose spectral types do not indicate their color were given a special correction depending on color. The extinction corrections when applied to B-type stars, observed during the course of the regular observations, brought their colors into such good agreement that the author feels that the other coefficients are sufficiently accurate for their respective spectral classes.

3. *Reduction to the standard night.*—With the exception of the night of August 14, 1932 (already mentioned), the cell apparently retained the same color-curve throughout the night after it had once been cooled. The observed relative colors for any one night are related to those observed for the same stars on any other night by a simple linear relation. While during the summer months the observed colors might depart systematically from their average values for a given spectral class by as much as 0.10 mag., during the colder winter months this departure was usually less than 0.02 mag. About two-thirds of the total number of observations were made during the fall or winter months. November 3, 1932 was arbitrarily chosen as the standard night and all observations were reduced to it. This night was chosen because it was near the mean date of the observations and the color-curve of the cell appeared to be near normal. It was a night of good transparency and a relatively large number of stars were observed.

The principle underlying the reductions was to make enough ap-

proximations such that still another one would not change the mean value of the color of any star by as much as half its probable error. The two sets of colors, 89 and 87, were reduced to the standard night independently. We shall first discuss the reduction of set 89.

An effort was made to arrange the observing program in such a way that observations were made of some stars formerly observed as well as of some new stars on each night. Since in general each star was observed on at least three different nights, special calibration stars were unnecessary. However, a few stars were observed over a period of several months. In the reductions these stars were given the same weight as the others.

The colors of the stars observed on any one night were plotted against the accumulating mean colors of the same stars which had already been reduced either directly or indirectly to the standard night, these reductions being made graphically. The first time that this process was carried completely around the sky, the accumulated error was 0.06 mag. for B-type stars, and less for other types, after more than twenty linear transformations. Rather than retrace one's steps and assign each night its share of the accumulated difference, it was easier and more accurate to reobserve stars on the same night which had formerly been observed in widely different months. On March 5, 1933, I reobserved stars first observed in September, 1932. These reobservations were made in the early evening and also just before dawn, in this way connecting the winter and the summer stars more closely. Three other nights were used for the same purpose, although the number of months covered on these nights was not as great. These observations show that this accumulated error is present in the reduction of the observations made from June to September, and is not present in the fall and winter observations. The original observations of the fall and winter stars were now plotted against the mean color of each of these stars as obtained from the first reduction, and a second approximation was made for these stars in the same way. The mean colors for the summer stars, derived from the first approximation, were disregarded (because of the accumulative errors) and the original observations were plotted against the accumulating means as before. This time, however, there were four nights' observations available connecting the summer stars di-

rectly with the November stars, in addition to the connecting links that formerly existed.

A third approximation was then made for the stars observed in the summer months, similar to that used in the second approximation for the winter observations.

Since the four nights used primarily to eliminate systematic errors were all of high quality with regard to transparency, and since the stars observed on these nights were usually selected for their favorable position and color, the errors due to possible changes in transparency should be small.

The reduction of colors 87 was carried out in the same general way. Since all the observations were available when the reduction of this set of colors was started, only two approximations were necessary, and the inconvenience due to accumulated errors was avoided. The mean colors derived from the first approximation were used as the standard (the same as November 3) for the second approximation for all stars.

If the color excesses (observed color *minus* mean color for spectral class) given in the accompanying general catalogue are summed up over two-hour intervals of right ascension for each set of colors, the systematic differences for any interval do not exceed 0.011 mag. on scale 89. Both sets show a slight tendency for the stars in right ascension 2^h–12^h to be redder than stars of the same spectral type in other regions of the northern sky. Greenstein[13] obtained the same general result from a discussion of Hertzsprung's[14] compilation of colors. Whether or not this tendency is real, it is evident that the systematic differences between colors 89 and 87 are small.

Each set of colors shows a definite change in the color-curve of the cell on the night of August 14, 1932, which has already been referred to under the section entitled "The Photo-electric Cell." All observations on this night after this change were discarded. Five observations on other nights were discarded because clouds were threatening to stop the observations entirely. Three were rejected because the dark current was unusually large. In another case the wrong filter was certainly tabulated, and in another there is good evidence that

[13] *Bulletin of the Harvard Observatory*, **876**, 32, 1930.

[14] *Annalen van de Sterrewacht te Leiden*, **14**, 1922.

the wrong star was observed. All observations made on September 9 and 10 were given half-weight because the dark current was large enough to influence the readings. A few other observations were given half-weight for similar reasons. I believe that I have erred on the side of inclusion rather than on the side of exclusion in this matter.

VARIATION OF SPECULAR REFLECTION WITH ANGLE OF INCIDENCE

Light from stars having different declinations strikes the 30-inch mirror of the Loomis telescope at different angles. It is therefore important to know if the variation of specular reflection with angle of incidence is the same for different wave-lengths. Similar problems have been thoroughly investigated by Chant,[15] Coblentz,[16] and Wilsey.[17] Chant found practically no variation in the reflecting power of silver for angles of incidence less than 50°. The work of Wilsey showed that the reflecting power of a metal for a beam of radiation incident at an angle of 0° is only about 1 per cent higher than for an angle of 45°. And, finally, Coblentz concludes his paper with the statement: "From this it is evident that the correction to spectral energy-curves owing to the difference in reflecting power for different angles of incidence is negligibly small."

The angles of incidence for the stars included in this paper vary from 6° to 45°. The variation of specular reflection with angle of incidence was assumed to be the same for all effective wave-lengths.

Although the mirror had not been re-silvered for ten months at the time the last observations were made, the silver remained free from obvious tarnish during this period. It had been burnished but once (March 10, 1933) during the course of the observations.

THE GENERAL CATALOGUE

The general catalogue requires little explanation. In the first column is Schlesinger's "Bright Star" number. In the case of double stars, where the integrated light has been observed, the number of the preceding component is given and is marked with two asterisks. The second column gives the number from the *Preliminary General*

[15] *Astrophysical Journal*, **21**, 211, 1905.

[16] *Bulletin of the Bureau of Standards*, **9**, 319, 1913.

[17] *Physical Review*, **8**, 396, 1916.

GENERAL CATALOGUE

BS	PGC	RA 1900	Decl. 1900	Mag.	Sp.	Color		Color Excess		N
						89	87	89	87	
15...	10	$0^h\ 3^m.2$	$+28°32'$	2.15	Aop	$-0^M.528$	$-1^M.485$	$-0^M.135$	$-0^M.142$	6.0
21...	12	3.8	58 36	2.42	F5	− .285	1.180	− .126	− .136	2.0
39...	27	8.1	14 38	2.87	B2	− .643	1.683	.....	.....	1.5
45...	31	9.4	19 39	4.94	Ma	+ .230	0.470	− .023	− .077	3.0
130...	103	27.3	62 23	4.24	Bo	− .297	1.227	.....	.....	3.0
153...	122	31.4	53 21	3.72	B3	− .553	1.547	− .057	− .080	3.0
163...	130	33.3	28 46	4.52	G5	− .020	0.865	− .016	− .023	4.0
165...	132	34.0	30 19	3.49	K2	+ .060	0.762	− .058	− .120	5.0
168...	135	34.8	55 59	2.47	Ko	+ .010	0.820	− .040	− .056	2.0
215...	164	42.0	23 43	4.30	Ko	+ .075	0.750	+ .025	+ .014	4.0
219...	168	43.0	57 17	3.64	F8	− .083	0.967	+ .041	+ .025	3.0
224...	173	43.5	7 2	4.55	K5	+ .177	0.567	+ .001	− .044	3.0
253...	193	49.1	58 26	4.95	Ko	+ .110	0.707	+ .060	+ .057	3.0
264...	199	50.7	60 11	2.25	Bop	− .385	1.310	.....	.....	1.0
265...	200	50.7	58 38	4.83	Ko	+ .003	0.793	− .047	− .029	3.0
269...	203	51.2	37 57	3.94	A2	− .313	1.253	+ .033	+ .019	3.0
294...	226	57.8	7 21	4.45	Ko	+ .045	0.840	− .005	− .076	4.0
335...	257	1 3.7	46 42	4.28	B8	− .413	1.373	+ .035	+ .012	3.0
337...	259	4.1	35 5	2.37	Ma	+ .194	0.458	− .059	− .065	5.0
351...	270	6.1	20 30	4.89	Ko	+ .013	0.840	− .037	− .076	3.0
360...	281	8.3	24 3	4.64	Ko	+ .063	0.773	+ .013	− .009	3.0
403...	314	19.3	59 43	2.80	A5	− .324	1.202	− .035	− .017	5.0
437...	335	26.1	14 50	3.72	G5	+ .012	0.804	+ .016	+ .038	5.0
458...	350	30.9	40 54	4.18	Go	− .085	0.955	− .030	− .055	4.0
464...	357	31.9	48 7	3.77	Ko	+ .070	0.728	+ .020	+ .036	4.0
496...	384	37.4	50 11	4.19	Bop	− .330	1.290	.....	.....	3.0
542...	419	47.2	63 11	3.44	B3	− .512	1.462	− .016	+ .005	4.0
544...	421	47.4	29 6	3.58	F5	− .088	0.980	+ .071	+ .064	4.0
545**.	422	48.0	18 48	4.04	Aop	− .438	1.385	− .045	− .042	4.0
553...	428	49.1	20 19	2.72	A5	− .327	1.256	− .038	− .071	3.0
580...	449	54.9	71 56	4.06	A2	− .363	1.323	− .017	− .051	3.0
595...	463	56.9	2 17	3.94	A2p	− .385	1.380	− .039	− .108	2.0
603...	468	57.8	41 51	2.28	Ko	+ .140	0.643	+ .090	+ .121	3.0
617...	477	2 1.5	22 59	2.23	K2	+ .080	0.713	− .038	− .071	3.0
622...	482	3.6	34 31	3.08	A5	− .318	1.248	− .029	− .063	4.0
664...	517	11.4	33 23	4.07	Ao	− .415	1.300	− .022	+ .043	4.0
718...	560	22.8	8 1	4.34	Ao	− .400	1.410	− .007	− .067	3.0
779...	604	34.4	− 0 6	4.04	B2	− .587	1.630	.....	.....	3.0
799...	617	37.4	+48 48	4.22	F8	− .140	1.017	− .016	− .025	3.0
804...	622	38.1	2 49	3.58	A2	− .373	1.293	− .027	− .021	3.0
813...	629	39.5	9 42	4.36	Fo	− .190	1.117	+ .024	− .011	3.0
834...	639	43.4	55 29	3.93	Ko	+ .190	0.526	+ .140	+ .238	5.0
838...	643	44.1	26 51	3.68	B8	− .470	1.433	− .022	− .048	3.0
840...	644	44.3	37 54	4.27	Fo	− .210	1.055	+ .004	+ .051	4.0
843...	646	45.4	+34 39	4.67	K5	+0.208	−0.495	+0.032	+0.028	4.0

GENERAL CATALOGUE—*Continued*

BS	PGC	RA 1900	Decl. 1900	Mag.	Sp.	Color		Color Excess		N
						89	87	89	87	
854	653	2^h47^m2	+52°21′	4.06	Go, A5	−0M010	−0M860	.....	.....	3.0
882	670	52.9	34 47	4.97	Ko	+ .090	0.715	+0M040	+0M049	4.0
911	691	57.1	3 42	2.82	Ma	+ .233	0.423	− .020	− .030	3.0
915	694	57.6	53 7	3.08	F5, A3	− .043	0.867	.....	.....	3.0
921	698	58.8	38 27	(3.4)	Mb	+ .382	0.220	.....	.....	4.0
936	708	3 1.7	40 34	(2.1)	B8	− .347	1.247	+ .101	+ .138	3.0
937	710	1.8	49 14	4.17	Go	− .107	0.967	− .052	− .067	3.0
941	713	2.7	44 29	4.00	Ko	− .007	0.827	− .057	− .063	3.0
1017	772	17.2	49 30	1.90	F5	− .133	0.940	+ .026	+ .104	3.0
1030	778	19.4	8 41	3.80	G5	− .007	0.863	− .003	− .021	3.0
1038	784	21.7	9 23	3.75	B8	− .477	1.387	− .029	− .002	3.0
1066	804	25.4	12 36	4.28	Ko	+ .055	0.695	+ .005	+ .069	2.0
1087	817	29.4	47 52	4.26	B5p	− .397	1.343	+ .079	+ .088	3.0
1101	825	31.8	0 5	4.40	G5	− .106	1.018	− .102	− .176	2.5
1122	838	35.8	47 28	3.10	B5	− .490	1.433	− .014	− .002	3.0
1131	844	38.0	31 58	3.94	B1	− .358	1.245	.....	.....	4.0
1135	847	38.4	42 16	3.93	F5	− .170	1.067	− .011	− .023	3.0
1142	852	38.9	23 48	3.81	B5p	− .468	1.422	+ .008	+ .009	4.0
1145	856	39.3	24 9	4.37	B5	− .517	1.440	− .041	− .009	3.0
1149	860	39.9	24 3	4.02	B5	− .473	1.350	+ .003	+ .081	3.0
1156	865	40.4	23 38	4.25	B5	− .438	1.372	+ .038	+ .059	4.0
1165	869	41.5	23 48	2.96	B5p	− .488	1.385	− .012	+ .046	4.0
1178	877	43.2	23 45	3.80	B8	− .483	1.413	− .035	− .028	3.0
1203	894	47.8	31 35	2.91	B1	− .340	1.213	.....	.....	3.0
1220	910	51.1	39 43	2.96	B1	− .530	1.492	.....	.....	4.0
1228	913	52.5	35 30	4.05	Oe5	− .368	1.293	.....	.....	4.0
1239	920	55.1	12 12	(3.3)	B3	− .483	1.373	+ .013	+ .094	3.0
1251	932	57.8	5 43	3.94	A0	− .390	1.350	+ .003	− .007	4.0
1261	938	59.1	50 5	4.33	A0	− .359	1.283	+ .034	+ .060	3.5
1273	947	4 1.4	47 27	4.03	B3p	− .407	1.313	+ .089	+ .154	3.0
1303	967	7.6	48 9	4.28	Go	+ .010	0.775	+ .065	+ .125	4.0
1320	981	10.1	8 39	4.32	B3	− .430	1.408	+ .066	+ .059	4.0
1346	1000	14.1	15 23	3.86	K0	+ .020	0.840	− .030	− .076	4.0
1373	1017	17.2	17 18	3.93	K0	+ .023	0.800	− .027	− .036	3.0
1387	1026	19.4	22 4	4.36	A3	− .283	1.223	+ .029	+ .012	3.0
1389	1029	19.7	17 42	4.24	A2	− .383	1.297	− .037	− .025	3.0
1392	1033	20.3	22 35	4.40	A5	− .240	1.122	+ .049	+ .063	4.0
1409	1044	22.8	18 58	3.63	K0	+ .037	0.787	− .013	− .023	3.0
1411	1045	22.9	15 44	4.04	K0	+ .022	0.825	− .028	− .061	4.0
1412	1046	23.0	15 39	3.62	F0	− .255	1.135	− .041	− .029	4.0
1457	1077	30.2	16 18	1.06	K5	+ .167	0.487	− .009	+ .036	3.0
1458	1076	30.2	9 57	4.38	A3	− .293	1.233	+ .019	+ .002	3.0
1473	1087	32.6	12 19	4.30	A3	− .340	1.257	− .028	− .022	3.0
1497	1107	36.2	22 46	4.33	B5	− .468	1.462	+0.008	−0.031	4.0
1542	1139	44.1	+ 66 10	4.38	B0	−0.340	−1.340	.....	.....	2.0

GENERAL CATALOGUE—*Continued*

BS	PGC	RA 1900	Decl. 1900	Mag.	Sp.	Color		Color Excess		N
						89	87	89	87	
1543...	1140	4^h44^m4	+ 6°47′	3.31	F8	−0M180	−1M030	−0M056	−0M038	3.0
1544...	1141	45.2	8 44	4.35	Ao	− .373	1.333	+ .020	+ .010	3.0
1552...	1147	45.9	5 26	3.78	B3	− .507	1.490	− .011	− .023	3.0
1567...	1159	49.0	2 17	3.87	B3	− .517	1.513	− .021	− .046	3.0
1577...	1167	50.5	33 0	2.90	K2	+ .132	0.612	+ .014	+ .030	4.0
1580...	1169	50.7	13 21	4.28	Ko	+ .070	0.727	+ .020	+ .037	3.0
1603...	1185	54.5	60 18	4.22	Gop	+ .010	0.845	+ .065	+ .055	2.0
1605...	1187	54.8	43 41	(3.18)	F5p	− .067	0.880	+ .092	+ .164	3.0
1612...	1190	55.5	40 56	3.94	Ko, B1	+ .146	0.590	.....	.....	5.0
1641...	1204	59.5	41 6	3.28	B3	− .520	1.526	− .024	− .059	5.0
1708...	1246	5 9.3	45 54	0.21	Go	+ .010	0.772	+ .065	+ .128	4.0
1790...	1303	19.8	6 16	1.70	B2	− .517	1.547	.....	.....	3.0
1791...	1304	20.0	28 31	1.78	B8	− .430	1.387	+ .018	− .002	3.0
1839...	1331	25.4	5 52	4.32	B3	− .523	1.473	− .027	− .006	3.0
1879**.	1357	29.6	9 52	3.49	Oe5	− .527	1.540	.....	.....	3.0
1907...	1373	31.4	9 14	4.39	Ko	+ .047	0.780	− .003	− .016	3.0
1910...	1375	31.7	21 5	3.00	B3p	− .498	1.410	− .002	+ .057	4.0
2012...	1442	44.6	39 7	4.18	Ko	+ .076	0.722	+ .026	+ .042	5.0
2061...	1468	49.8	7 23	0.92	Ma	+ .317	0.283	+ .064	+ .110	3.0
2077...	1472	51.3	54 17	3.88	Ko	+ .035	0.755	− .015	+ .009	2.0
2088...	1478	52.2	44 56	2.07	Aop	− .392	1.292	+ .001	+ .051	4.0
2095...	1482	52.9	37 12	2.71	Aop	− .410	1.363	− .017	− .020	3.0
2124...	1501	56.9	9 39	4.19	A2	− .292	1.160	+ .054	+ .112	4.0
2134...	1508	58.0	23 16	4.30	G5	− .020	0.870	− .016	− .028	3.0
2159...	1525	6 1.9	14 47	4.40	B2	− .513	1.537	.....	.....	3.0
2199...	1548	6.3	14 14	4.35	B3	− .523	1.483	− .027	− .016	3.0
2216...	1561	8.8	22 32	(3.2)	Ma	+ .307	0.263	+ .054	+ .130	3.0
2286...	1604	16.9	22 34	3.19	Ma	+ .287	0.307	+ .034	+ .086	3.0
2298**.	1611	18.5	4 39	4.33	A5	− .260	1.182	+ .029	+ .003	4.0
2343...	1635	23.0	20 17	4.06	B5	− .463	1.463	+ .013	− .032	3.0
2421...	1690	31.9	16 29	1.93	Ao	− .337	1.263	+ .056	+ .080	3.0
2473...	1717	37.8	25 14	3.18	G5	+ .067	0.713	+ .071	+ .129	3.0
2484...	1725	39.7	13 0	3.40	F5	− .163	1.053	− .004	− .009	3.0
2540...	1763	46.2	34 5	3.64	A2	− .345	1.265	+ .001	+ .007	2.0
2650...	1815	58.2	20 43	(3.7)	Gop	− .043	0.873	+ .012	+ .027	6.0
2763...	1886	7 12.3	16 43	3.65	A2	− .340	1.252	+ .006	+ .020	4.0
2777...	1898	14.2	22 10	3.51	Fo	− .193	1.083	+ .021	+ .023	3.0
2821...	1931	19.5	28 0	3.89	Ko	+ .038	0.788	− .012	− .024	5.0
2845...	1944	21.7	8 29	3.09	B8	− .470	1.465	− .022	− .080	2.0
2852...	1952	22.7	31 59	4.18	Fo	− .230	1.103	− .016	+ .003	3.0
2890**.	1979	28.2	32 6	1.58	Ao	− .383	1.303	+ .010	+ .040	3.0
2905...	1987	29.8	27 7	4.22	K5	+ .223	0.497	+ .047	+ .026	3.0
2943...	2008	34.1	5 29	0.48	F5	− .117	0.963	+ .042	+ .081	3.0
2973...	2023	37.1	29 8	4.26	Ko	+ .046	0.758	− .004	+ .006	5.0
2985...	2029	38.4	+24 38	3.68	G5	+0.017	−0.830	+0.021	+0.012	3.0

GENERAL CATALOGUE—*Continued*

BS	PGC	RA 1900	Decl. 1900	Mag.	Sp.	Color		Color Excess		N
						89	87	89	87	
2990...	2031	$7^h39^m.2$	+28°16′	1.21	Ko	+0.M013	−0.M780	−0.M037	−0.M016	3.0
3249...	2195	8 11.1	9 30	3.76	K2	+ .167	0.563	+ .049	+ .079	3.0
3275...	2208	16.0	43 31	4.43	K5	+ .193	0.520	+ .027	+ .003	3.0
3323...	2247	22.0	61 3	3.47	Go	− .007	0.830	+ .048	+ .070	3.0
3410...	2295	32.4	6 3	4.18	Ao	− .370	1.313	+ .023	+ .030	3.0
3454...	2330	38.0	3 45	4.32	B3	− .540	1.553	− .044	− .086	3.0
3461...	2336	39.0	18 31	4.17	Ko	+ .037	0.803	− .013	− .039	3.0
3475...	2348	40.6	29 8	4.20	G5	+ .037	0.770	+ .041	+ .072	3.0
3482...	2354	41.5	6 47	3.48	F8	− .080	0.927	+ .044	+ .065	3.0
3492...	2361	43.1	6 12	4.42	Ao	− .367	1.360	+ .026	− .017	3.0
3547...	2393	50.1	6 20	3.30	Ko	+ .023	0.790	− .027	− .026	3.0
3569...	2404	52.4	48 26	3.12	A5	− .285	1.202	+ .004	− .017	4.0
3572...	2407	53.0	12 15	4.27	A3	− .317	1.263	− .005	− .028	3.0
3579...	2413	54.2	42 11	4.09	F5	− .162	1.042	− .003	+ .002	4.0
3594...	2424	56.8	47 33	3.68	Ao	− .355	1.312	+ .038	+ .031	4.0
3665...	2479	9 9.2	2 44	3.84	Ao	− .417	1.420	− .024	− .077	3.0
3690...	2495	12.6	37 14	3.82	A2	− .348	1.280	− .002	− .008	4.0
3705...	2507	15.0	34 49	3.30	K5	+ .188	0.490	+ .012	+ .033	5.0
3757...	2540	23.7	63 30	3.75	Fo	− .177	1.033	+ .041	+ .073	3.0
3775...	2552	26.2	52 8	3.26	F8p	− .105	0.965	+ .019	+ .027	2.0
3852...	2602	35.8	10 21	3.76	F5, A3	− .150	1.023	.....	.....	3.0
3873...	2618	40.2	24 14	3.12	Gop	− .048	0.882	+ .007	+ .018	4.0
3888...	2632	43.9	59 31	3.89	Fo	− .210	1.140	+ .004	− .034	3.0
3905...	2648	47.1	26 29	4.10	Ko	+ .088	0.728	+ .038	+ .036	4.0
3975...	2694	10 1.9	17 15	3.58	Aop	− .325	1.295	+ .068	+ .048	4.0
3982...	2698	3.0	12 27	1.34	B8	− .430	1.370	+ .018	+ .015	3.0
4031...	2730	11.1	23 55	3.67	Fo	− .200	1.090	+ .014	+ .016	3.0
4033...	2729	11.1	43 25	3.52	A2	− .377	1.347	− .031	− .075	3.0
4057**	2742	14.5	20 21	2.30	Ko	+ .110	0.670	+ .060	+ .094	4.0
4069...	2751	16.4	42 0	3.21	K5	+ .187	0.440	+ .013	+ .083	3.0
4133...	2804	27.5	9 49	3.85	Bop	− .503	1.550	.....	.....	3.0
4247...	2899	47.7	34 45	3.92	Ko	+ .065	0.745	+ .015	+ .019	4.0
4259**	2909	50.2	25 17	4.32	Ao	− .340	1.290	+ .053	+ .053	3.0
4295...	2930	55.8	56 55	2.44	Ao	− .353	1.327	+ .040	+ .016	3.0
4301...	2933	57.6	62 17	1.95	Ko	+ .037	0.743	− .013	+ .021	3.0
4335...	2958	11 4.0	45 2	3.15	Ko	+ .060	0.713	+ .010	+ .051	3.0
4357...	2972	8.8	21 4	2.58	A3	− .283	1.235	+ .029	.000	6.0
4359...	2974	9.0	15 59	3.41	Ao	− .407	1.362	− .014	− .019	6.0
4374**	2984	12.9	32 6	3.86	Go	− .090	0.930	− .035	− .030	3.0
4377...	2985	13.1	33 38	3.71	Ko	+ .137	0.650	+ .087	+ .114	3.0
4386...	2990	16.0	6 35	4.13	Ao	− .420	1.407	− .027	− .064	3.0
4399...	2999	18.7	11 5	4.03	F5	− .157	1.073	+ .002	− .029	3.0
4434...	3031	25.5	69 53	4.06	Ma	+ .203	0.507	− .050	− .114	3.0
4517...	3089	40.7	7 5	4.20	Ma	+ .243	0.503	− .010	− .110	3.0
4518...	3090	40.8	+48 20	3.85	Ko	+0.107	−0.743	+0.057	+0.021	3.0

GENERAL CATALOGUE—*Continued*

BS	PGC	RA 1900	Decl. 1900	Mag.	Sp.	Color		Color Excess		N
						89	87	89	87	
4534	3101	11h44m0	+15° 8′	2.23	A2	−0M352	−1M286	−0M006	−0M014	5.0
4540	3105	45.5	2 20	3.80	F8	− .140	0.997	− .016	− .005	3.0
4554	3117	48.6	54 15	2.54	Ao	− .352	1.308	+ .041	+ .035	4.0
4608	3155	12 .1	9 17	4.24	G5	+ .032	0.805	+ .036	+ .037	6.0
4660	3190	10.5	57 35	3.44	A2	− .337	1.290	+ .009	− .018	4.0
4785	3279	29.0	41 54	4.32	Go	− .082	0.983	− .027	− .083	6.0
4787	3281	29.2	70 20	3.88	B5p	− .470	1.457	+ .006	− .026	3.0
4905	3363	49.6	56 30	1.68	Aop	− .387	1.333	+ .006	+ .010	3.0
4910	3367	50.6	3 56	3.66	Ma	+ .298	0.362	+ .045	+ .031	5.0
4914**	3371	51.4	38 52	2.80	Aop	− .423	1.378	− .030	− .035	6.0
4932	3383	57.2	11 30	2.95	Ko	+ .018	0.818	− .032	− .054	5.0
4983	3424	13 7.2	28 23	4.32	Go	− .104	0.996	− .049	− .096	5.0
5054**	3474	19.9	55 27	2.17	A2p	− .417	1.320	− .071	− .048	3.0
5062	3480	21.2	55 31	4.02	A5	− .272	1.240	+ .017	− .055	4.0
5191	3566	43.6	49 49	1.91	B3	− .491	1.467	+ .005	.000	7.0
5200	3572	44.6	16 18	4.28	K5	+ .192	0.500	.....	.....	1.0
5235	3596	49.9	18 54	2.80	Go	− .138	0.998	− .083	− .098	4.0
5264	3612	56.6	2 2	4.34	A2	− .303	1.260	+ .043	+ .012	3.0
5291	3626	14 1.7	64 51	3.64	Aop	− .418	1.342	− .025	+ .001	4.0
5340	3662	11.1	19 42	0.24	Ko	+ .150	0.557	+ .100	+ .207	3.0
5351	3666	12.6	46 33	4.26	Ao	− .350	1.320	+ .043	+ .023	3.0
5404	3704	21.8	52 19	4.06	F8	− .170	1.030	− .046	− .038	4.0
5429	3717	27.5	30 49	3.78	Ko	+ .094	0.679	+ .044	+ .085	13.0
5430	3718	27.7	76 8	4.37	K2	+ .130	0.635	+ .012	+ .007	4.0
5435	3722	28.1	38 45	3.00	Fo	− .280	1.190	− .066	− .084	3.0
5447	3729	30.3	30 11	4.48	Fo	− .120	0.990	+ .094	+ .116	5.0
5477**	3752	36.4	14 9	3.86	A2	− .388	1.318	− .042	− .046	5.0
5505	3771	40.6	27 30	2.59	Ko, Ao	+ .004	0.814	.....	.....	5.0
5511	3772	41.2	2 19	3.76	Ao	− .368	1.356	+ .025	− .013	5.0
5563	3809	51.0	74 34	2.24	K5	+ .103	0.570	− .073	− .047	3.0
5602	3836	58.2	40 47	3.63	G5	+ .013	0.830	+ .017	+ .012	3.0
5681	3887	15 11.5	33 41	3.54	Ko	− .015	0.825	− .065	− .061	4.0
5735	3928	20.9	72 11	3.14	A2	− .278	1.145	+ .068	+ .127	4.0
5744	3936	22.7	59 19	3.47	Ko	+ .058	0.728	+ .008	+ .036	5.0
5747	3940	23.7	29 27	3.72	Fop	− .277	1.184	− .063	− .078	9.0
5778	3953	28.9	31 42	4.17	B5	− .494	1.454	− .018	− .023	5.0
5788**	3960	30.0	10 52	3.85	Fo	− .258	1.168	− .044	− .062	4.0
5793	3961	30.5	27 3	2.31	Ao	− .434	1.344	− .041	− .001	8.0
5849	3998	38.5	26 37	3.93	Ao	− .397	1.353	− .004	− .010	3.0
5854	4001	39.3	6 44	2.75	Ko	+ .042	0.765	− .008	− .001	4.0
5867	4009	41.6	15 44	3.74	A2	− .330	1.207	+ .016	+ .065	4.0
5879	4015	44.2	18 27	4.28	K5	+ .215	0.485	+ .039	+ .038	4.0
5892	4026	45.8	4 47	3.75	A2	− .337	1.270	+ .009	+ .002	3.0
5903	4035	47.6	78 6	4.34	A2	− .313	1.240	+ .033	+ .032	3.0
5933	4055	51.8	+ 15 59	3.86	F5	−0.200	−1.093	−0.041	−0.049	3.0

GENERAL CATALOGUE—*Continued*

BS	PGC	RA 1900	Decl. 1900	Mag.	Sp.	Color		Color Excess		N
						89	87	89	87	
5947...	4063	15h53m4	+ 27°10′	4.22	Ko	+0M055	−0M732	+0M005	+0M032	4.0
5986...	4090	16 .0	58 50	4.11	F8	− .144	1.058	− .020	− .066	5.0
6023...	4112	5.6	45 12	4.26	B9p	− .410	1.335	.....	.....	4.0
6092...	4162	16.7	46 33	3.91	B5	− .502	1.505	− .026	− .074	4.0
6095...	4165	17.5	19 23	3.79	Fo	− .210	1.107	+ .004	− .001	3.0
6132...	4192	22.6	61 44	2.89	G5	− .024	0.844	− .020	− .002	5.0
6148...	4204	25.9	21 42	2.81	Ko	+ .020	0.810	− .030	− .046	3.0
6149...	4203	25.9	2 12	3.85	Ao	− .335	1.222	+ .058	+ .121	4.0
6168...	4220	30.9	42 39	4.25	Ao	− .367	1.313	+ .026	+ .030	3.0
6212...	4246	37.5	31 47	3.00	Go	− .070	0.895	− .015	+ .005	4.0
6220...	4255	39.5	39 7	3.61	Ko	+ .002	0.800	− .048	− .036	4.0
6281...	4302	49.3	10 20	4.29	B8	− .457	1.320	− .009	+ .065	3.0
6299...	4315	52.9	9 32	3.42	Ko	+ .062	0.740	+ .012	+ .024	5.0
6324...	4328	56.5	31 4	3.92	Ao	− .453	1.447	− .060	− .104	3.0
6396...	4368	17 8.5	65 50	3.22	B5	− .478	1.470	− .002	− .039	4.0
6406**	4373	10.1	14 30	3.31	Mb	+ .368	0.012	.....	.....	4.0
6410...	4376	10.9	24 57	3.16	A2	− .322	1.217	+ .024	+ .055	3.0
6418...	4381	11.6	36 55	3.36	K5	+ .123	0.660	− .053	− .137	3.0
6536...	4443	28.2	52 23	2.99	Go	− .033	0.847	+ .022	+ .053	3.0
6556...	4459	30.3	12 38	2.14	A5	− .306	1.160	− .017	+ .025	5.0
6588...	4479	36.6	46 4	3.79	B3	− .506	1.438	− .010	+ .029	2.5
6603...	4487	38.5	4 37	2.94	Ko	+ .052	0.782	+ .002	− .018	4.0
6623...	4497	42.5	27 47	3.48	G5	− .040	0.863	− .036	− .021	3.0
6629...	4500	42.9	2 45	3.74	Ao	− .357	1.287	+ .036	+ .056	3.0
6688...	4531	51.8	56 53	3.90	Ko	+ .047	0.748	− .003	+ .016	3.0
6695...	4535	52.8	37 16	3.99	Ko	+ .077	0.720	+ .027	+ .044	3.0
6703...	4538	53.9	29 16	3.82	Ko	+ .007	0.810	− .043	− .046	3.0
6705...	4541	54.3	51 30	2.42	K5	+ .123	0.513	− .053	+ .010	3.0
6714...	4548	55.6	2 56	3.92	B5p	− .313	1.167	.....	.....	3.0
6752...	4571	18 .4	2 31	4.07	Ko	+ .017	0.860	− .033	− .096	3.0
6771...	4581	2.6	9 33	3.73	A3	− .347	1.220	− .035	+ .013	3.0
6779...	4584	3.6	28 45	3.83	Ao	− .407	1.340	− .014	+ .003	3.0
6787...	4590	4.5	20 48	4.32	B3	− .497	1.503	− .001	− .036	3.5
6872...	4639	16.4	36 1	4.34	Ko	+ .074	0.732	+ .024	+ .032	2.5
6895...	4656	19.4	21 43	3.92	Ko	+ .052	0.717	+ .002	+ .047	3.0
6902...	4660	20.8	7 59	5.69	Go, A3	+ .050	0.730	.....	.....	2.0
6920...	4670	22.2	71 17	4.24	Aop	− .422	1.360	− .029	− .017	4.0
6927...	4672	22.9	72 41	3.69	F8	− .106	0.958	+ .018	+ .034	5.0
7001...	4722	33.6	38 41	0.14	Ao	− .392	1.375	+ .001	− .032	2.0
7056...	4752	41.3	37 30	4.06	A3	− .300	1.182	+ .012	+ .053	3.0
7061...	4753	41.4	20 27	4.26	F5	− .120	1.020	+ .039	+ .024	1.0
7069...	4761	42.6	18 4	4.37	A3	− .354	1.294	− .042	− .059	3.5
7106...	4776	46.4	33 15	(3.4)	B2p	− .377	1.303	.....	.....	3.0
7157...	4814	52.3	43 49	4.32	Mb	+ .388	0.103	.....	.....	3.0
7176...	4823	55.1	+14 56	4.21	Ko	+0.051	−0.762	+0.001	+0.002	6.0

GENERAL CATALOGUE—*Continued*

BS	PGC	RA 1900	Decl. 1900	Mag.	Sp.	Color		Color Excess		N
						89	87	89	87	
7178...	4824	$18^h55^m.2$	+ 32°33′	3.30	Aop	$-0^M.377$	$-1^M.350$	$+0^M.016$	$-0^M.007$	3.0
7235...	4858	19 .8	13 43	3.02	Ao	− .360	1.280	+ .033	+ .063	3.0
7310...	4909	12.5	67 29	3.24	Ko	+ .072	0.752	+ .022	+ .012	4.0
7328...	4923	14.8	53 11	3.98	Ko	+ .013	0.807	− .037	− .043	3.0
7377...	4953	20.5	2 55	3.44	Fo	− .200	1.070	+ .014	+ .036	3.0
7417...	4986	26.7	27 45	3.24	Ko, Ao	+ .028	0.825	.....	.....	2.0
7420...	4988	27.2	51 31	3.94	A2	− .297	1.220	+ .049	+ .052	3.0
7479...	5023	35.6	17 47	4.37	Go	− .050	0.933	+ .005	− .033	3.0
7525...	5047	41.5	10 22	2.80	K2	+ .142	0.565	+ .024	+ .077	4.0
7528...	5048	41.9	44 53	2.97	Ao	− .438	1.398	− .045	− .055	2.0
7536...	5052	42.9	18 17	3.78	Ma, Ao	+ .238	0.532	.....	.....	2.0
7557...	5062	45.9	8 36	0.89	A5	− .295	1.110	− .006	+ .075	2.0
7570...	5071	47.4	0 45	(3.7)	Gop	− .053	0.940	+ .002	− .040	3.0
7582...	5079	48.5	70 1	3.99	Ko	+ .003	0.810	− .047	− .046	3.0
7602...	5093	50.4	6 9	3.90	Ko	− .023	0.847	− .073	− .083	3.0
7615...	5103	52.6	34 49	4.03	Ko	+ .002	0.825	− .048	− .061	4.0
7635...	5118	54.3	19 13	3.71	K5	+ .203	0.557	+ .027	− .034	3.0
7735...	5187	20 10.5	46 26	3.95	Ko, B8	+ .097	0.643	.....	.....	3.0
7740...	5191	11.1	56 16	4.32	A3	− .295	1.210	+ .017	+ .025	4.0
7751...	5200	12.4	47 24	4.16	Ko, A3	+ .180	0.503	.....	.....	3.0
7796...	5229	18.6	39 56	2.32	F8p	− .095	0.985	+ .029	+ .007	2.0
7834...	5255	25.3	30 2	4.09	F5p	− .173	1.113	− .014	− .069	3.0
7850...	5270	27.9	62 39	4.28	A5	− .273	1.163	+ .016	+ .022	3.0
7852...	5272	28.4	10 58	3.98	B5	− .513	1.477	− .037	− .046	3.0
7866...	5279	30.0	34 54	4.85	K5, A3	+ .156	0.528	.....	.....	2.5
7882...	5291	32.9	14 15	3.72	F5	− .130	0.993	+ .029	+ .051	3.0
7906...	5310	35.0	15 34	3.86	B8	− .420	1.373	+ .028	+ .012	3.0
7924...	5320	38.0	44 55	1.33	A2p	− .341	1.261	+ .005	+ .011	3.5
7942...	5331	41.5	30 21	4.34	Ko	− .010	0.873	− .060	− .109	3.0
7947**.	5334	42.0	15 46	4.12	G5, F8	− .040	0.870	− .036	− .028	3.0
7949...	5336	42.0	33 36	2.64	Ko	+ .043	0.797	− .007	− .033	3.0
7957...	5346	43.3	61 27	3.59	Ko	+ .023	0.770	− .027	− .006	3.0
8028...	5393	53.4	40 57	4.04	Ao	− .383	1.290	+ .010	+ .053	3.0
8079...	5431	21 1.3	43 32	3.92	K5	+ .167	0.547	− .009	− .024	3.0
8115...	5452	8.7	29 49	3.40	Ko	− .010	0.820	− .060	− .056	3.0
8130...	5460	10.8	37 37	3.82	Fo	− .193	1.103	+ .021	+ .003	3.0
8131...	5461	10.8	4 50	4.14	F8, A3	− .120	0.992	.....	.....	3.0
8143...	5469	13.5	38 59	4.28	Aop	− .313	1.267	+ .080	+ .076	3.0
8146...	5471	13.8	34 29	4.42	B3p	− .473	1.517	+ .023	− .050	3.0
8162...	5480	16.2	62 10	2.60	A5	− .280	1.153	+ .009	+ .032	3.0
8173...	5489	17.5	19 23	4.24	Ko	+ .013	0.802	− .037	− .038	3.0
8238...	5532	27.4	70 7	3.32	B1	− .557	1.507	.....	.....	3.0
8252...	5543	30.2	45 9	4.22	Ko	− .010	0.845	− .060	− .081	2.0
8308...	5584	39.3	9 25	2.54	Ko	+ .120	0.715	+ .070	+ .049	2.0
8315...	5592	40.1	+ 25 11	4.27	F5	−0.233	−1.117	−0.074	−0.074	3.0

GENERAL CATALOGUE—*Continued*

BS	PGC	RA 1900	Decl. 1900	Mag.	Sp.	Color		Color Excess		*N*
						89	87	89	87	
8316...	5593	21h40m4	+ 58°19′	(4.5)	Ma	+0M330	−0M267	+0M077	+0M126	3.0
8335...	5609	43.1	48 51	4.26	B3	− .457	1.453	+ .039	+ .014	3.0
8417...	5677	22 .9	64 8	4.40	A3, G	− .187	1.080	.....	.....	3.0
8430...	5688	2.4	24 51	3.96	F5	− .157	1.087	+ .002	− .043	3.0
8450...	5703	5.2	5 52	3.70	A2	− .412	1.364	− .066	− .092	2.5
8454...	5709	5.5	32 41	4.38	F5	− .157	1.080	+ .002	− .036	3.0
8465...	5714	7.4	57 42	3.62	Ko	+ .117	0.651	+ .067	+ .103	10.5
8494...	5742	11.3	56 33	4.23	Fo	− .214	1.128	.000	− .022	11.0
8498...	5746	11.6	37 15	4.22	Ko	+ .130	0.687	+ .080	+ .077	3.0
8571...	5805	25.4	57 54	(3.7)	Go	− .065	0.919	.....	.....	18.5
8585...	5813	27.2	49 46	3.85	Ao	− .405	1.303	− .012	+ .040	8.5
8634...	5853	36.5	10 19	3.61	B8	− .507	1.490	− .059	− .105	3.0
8650...	5865	38.3	29 42	3.10	Go	− .060	0.887	− .005	+ .013	3.0
8665...	5874	41.7	11 40	4.31	F5	− .173	1.063	− .014	− .019	3.0
8667...	5875	41.7	23 22	4.14	Ko	+ .010	0.832	− .040	− .068	2.5
8684...	5885	45.2	24 4	3.67	Ko	− .003	0.863	− .053	− .099	3.0
8694...	5891	46.1	65 40	3.68	Ko	+ .033	0.820	− .017	− .056	3.0
8762...	5933	57.3	41 47	3.63	B5, A2p	− .467	1.392	.....	.....	4.0
8775...	5940	58.9	27 32	2.61	Mb	+ .277	0.337	.....	.....	3.0
8781...	5944	59.8	14 40	2.57	Ao	− .482	1.428	− .089	− .085	2.5
8795...	5952	23 2.0	8 52	4.69	Ma	+ .180	0.560	− .073	− .167	3.0
8796...	5954	2.2	24 56	4.98	Ko	+ .110	0.743	+ .060	+ .021	3.0
8852...	5988	12.0	2 44	3.85	Ko	+ .020	0.827	− .030	− .063	3.0
8860...	5993	13.1	48 28	4.99	Ma	+ .260	0.348	+ .007	+ .045	2.5
8916...	6037	22.9	5 50	4.45	G5	+ .020	0.837	+ .024	+ .005	3.0
8961...	6071	32.7	45 55	4.00	Ko	+ .025	0.770	− .025	− .006	2.0
8965...	6073	33.2	42 43	4.28	B8	− .475	1.365	− .027	+ .020	2.0
8969...	6077	34.8	5 5	4.28	F8	− .120	0.980	+ .004	+ .012	3.0
8974...	6078	35.2	77 4	3.42	Ko	+ .090	0.730	+ .040	+ .034	3.0
8976...	6080	35.5	43 47	4.33	Ao	− .540	1.500	− .147	− .157	2.0
9064...	6150	52.7	24 35	4.75	Ma	+ .205	0.370	− .048	+ .023	2.0
9072...	6156	54.2	+ 6 19	4.03	F5	−0.180	−1.070	−0.021	−0.026	3.0

Catalogue of Boss. The visual magnitude and the spectrum are those of the *Henry Draper Catalogue*. The values given under 89 and 87 are the mean colors derived with and without these two filters. The magnitude difference due to the neutral cover-glass filter, Fo, and the cover-glasses enclosing filters 89 and 87, may be eliminated by subtracting 0.58 mag. from all colors. In order to find the observed effective energy beyond the filter cut-offs, one must also allow for the general absorption of these filters in the infra-red. This absorption

is probably 15 per cent or 0.18 mag. Therefore the observed ratio of the intensity of light of wave-length longer than the filter cut-offs, to total light, expressed in magnitudes, may be found by subtracting approximately 0.40 mag. from all the colors in the accompanying catalogue. The color excesses (already defined) were computed by using the Henry Draper classification of spectra. The last column shows the number of nights on which the star was observed. The average number of stars observed each night is twenty-eight.

DISCUSSION OF THE DATA

1. An effort was made to determine at least roughly how the effective energy from a star of a given temperature is distributed throughout the spectrum.

The response curve of the photo-cell, given in Figure 2, was combined with the energy curve of a black-body radiator at a given temperature, by multiplying together the ordinates corresponding to certain wave-lengths. The resultant curve was then corrected for atmospheric, mirror, and lens absorptions in the blue end of the spectrum. The band absorptions in the infra-red were neglected. The computed fraction of the total effective energy that is of longer wave-length than the filter cut-offs (6900 and 8000 A) was then found for each filter from this graph, using the transmission coefficients given in *Wratten Filters*.[11] These coefficients were first multiplied by a constant factor in order to make the transmission of each filter equal to unity at wave-lengths beyond the cut-offs. This fraction was computed in this way for seven black-body temperatures, ranging from 3000° to 10,000°. It was not computed for still higher temperatures because uncertainties in the absorption coefficients would then become increasingly important and tend to vitiate the results.

It has already been mentioned that about 0.40 mag. must first be subtracted from the observed colors in order to reduce them to the fraction of the total effective energy that is of wave-length longer than that at which the filters may be considered to cut off the energy abruptly. The mean color observed for stars of each spectral type was plotted against the "adopted temperature" for that type, as given by Russell, Dugan, and Stewart.[18] The observed color cor-

[18] *Astronomy*, **2**, 753.

responding to a given temperature was read from this curve. These colors *minus* 0.40 mag. were then expressed as fractions, and are given in columns 2 and 5 in Table III. This table shows that the computed and observed ratios are in good agreement if the computed values are all multiplied by a constant.

Several factors might cause the observed ratios to be systematically shifted from the computed. The color-curve for the cell used in the computations probably attributes too much red sensitivity (beyond 8000 A) to the cell. I believe that this is the most important of the many possibilities and that this systematic difference is not pri-

TABLE III

T	89/Clear Observed	89/Clear Computed	Column 3 ×0.90	87/Clear Observed	87/Clear Computed	Column 6 ×0.74
3000°.....	0.85	0.88	0.79	0.44	0.59	0.44
4000.....	.77	.80	.72	.36	.49	.36
5000.....	.68	.75	.68	.32	.42	.31
6000.....	.62	.69	.62	.29	.39	.29
7000.....	.57	.65	.59	.26	.37	.27
8000.....	.52	.60	.54	.23	.31	.23
10,000.....	0.50	0.58	0.52	0.21	0.30	0.22

marily due to systematic errors in the adopted temperatures or to deviations of the stars from black- or gray-body radiators.

The graphs used to derive the ratios given in Table III show that the computed wave-length which equally divides the total effective energy in the case of a Go star is near 7500 A for no filter, 8100 A for filter 89, and 8800 A for filter 87. Comparison of the observed and computed ratios indicates that these wave-lengths are actually somewhat less than those computed, probably near 7400, 7950, and 8600 A, respectively, provided the filter calibrations are correct, and these stars are black- or gray-body radiators.

It might be mentioned in passing that the color-curve of the cell was determined by the manufacturer at room temperature a year before my standard night. Further, the source of light used by the manufacturer was many millions of times brighter than the average star at the focus of the 15-inch lens of the Loomis telescope. The discrepancies shown above are therefore not at all surprising.

2. Figure 5 shows the relation between mean colors 89 and 87

for all observed stars which have bright-star numbers between 000 and 400 in each thousand. The very nearly linear relationship between the two sets of colors for all stars within the limits −0.6 and +0.1 mag. on scale 89 is at once apparent. It was decided to make use of this linear relationship in an effort to determine whether the scatter within this range is partly due to peculiarities in the stars' energy curves or entirely due to errors of observation.

The average probable error for one observation determined from the internal agreement of 398 observations of 118 stars is ±0.020

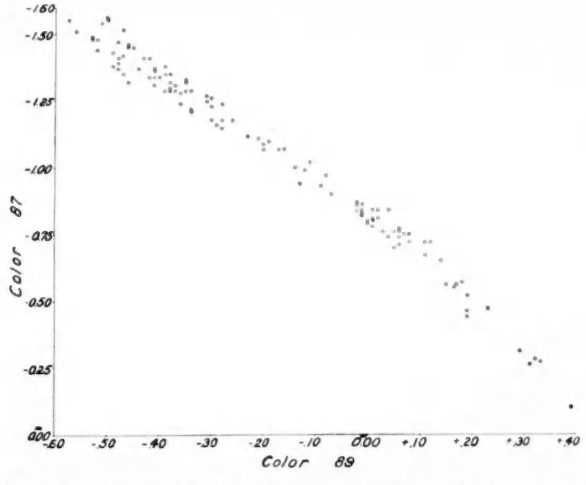

FIG. 5.—Colors 87 plotted against colors 89. This graph shows one-third of the entire material.

mag. for colors 89 on scale 89. The corresponding probable error of one observation for colors 87 is ±0.028 mag. on scale 87. A fair approximation to the ratio of the two scales is easily found from Figure 5. The average probable error of 89 on scale 87 becomes ±0.026 mag.

If the errors are reduced to the same scale (87 in this case), and if the scattering is due entirely to the errors of observation, the probable error of a single point representing one observation on a graph similar to Figure 5 would be

$$\sqrt{0.026^2+0.028^2}=\pm 0.038 \text{ mag. on scale 87 .}$$

But each point on Figure 5, exclusive of variable stars, averages 3.32 observations. Therefore the computed internal probable devia-

tion of a single point from a mean straight line is ± 0.021 mag. The actual probable deviation comes out practically the same, ± 0.022 mag.

Colors 89 and 87 are not entirely independent since each set contains the same readings with no color filter. The deflection was usually more rapid for these readings than for the others, and therefore one would expect the errors to be small compared with the errors of the readings made with the color filters in place.

The residuals $(89-\overline{89})$ were then plotted against the corresponding residuals $(87-\overline{87})$. If the two sets of colors were entirely independent, the points would be symmetrically scattered about the origin. A graph of 398 observations of 118 stars indicated some correlation. Approximately 14 per cent of the residuals would have to be displaced from one pair of quadrants to the other in order to make the diagram symmetrical with respect to the origin. This fact tends to *decrease* slightly the observed probable error, ± 0.022 mag. On the other hand, since the two sets of colors are reduced entirely independently of each other, a small systematic difference (previously referred to) exists between colors 89 and 87. This may signify that an insufficient number of observations were made to connect the colors of these stars with those of the standard night. These relative systematic errors tend to *increase* this probable error.

There is no definite evidence of a deviation of individual stars within this range of colors from a linear relationship between colors 87 and 89. And if the stars under consideration are arranged in order of colors 89, barring errors of observation, the order would be the same as if they were arranged in order of colors 87. In what is to follow, therefore, any conclusions drawn from a discussion of colors 89 should in general be true for colors 87 also. It is interesting to note that the colors of each set are determined with very nearly the same accuracy.

3. Colors 89 are plotted against the Harvard spectral type in Figure 6. The filled circles represent the mean color for that spectral type. It so happens that a very nearly linear relationship exists between the two co-ordinates. King[19] similarly found a linear relation between color index and spectral type.

There is a group of eight early-type stars that appear too red for

[19] *Harvard Annals*, **59**, 180, 1912.

their spectral types. Table IV compares various other determinations of color temperature of these stars with the Yale color excesses (89). Column 4 shows the galactic latitude. Columns 6 and 7 give the temperatures of these stars derived by Wilsing and Scheiner and at Greenwich, respectively. These temperatures were derived from spectro-photometric measurements and therefore should be free from the influence of absorption lines or bands. Under "Hz" the differences $(c_2/T - \overline{c_2/T})$ are given, where $\overline{c_2/T}$ is its mean value for the particular spectral type, these data being taken from Hertzsprung's compilation. The next column gives the photoelectric color excesses observed by Bottlinger[20] in the blue region of the spectrum. The Yale color excesses (Y) were computed from the best straight line through the points of Figure 6, stars earlier than B5 being excluded. A positive sign in any of the last three columns indicates that the observed color of the star is redder than was to be expected for stars of that spectral class.

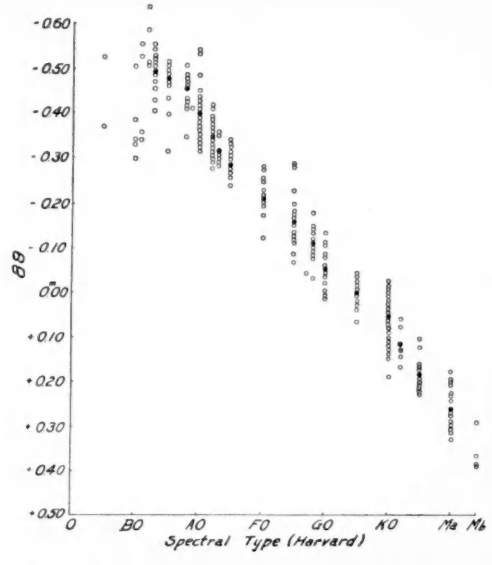

FIG. 6.—Colors 89 plotted against spectral type. The filled circles represent the mean color for each spectral type.

With the possible exception of BS 264, these data show that these eight stars have peculiarly reddish colors regardless of whether their energy-curves are measured in the blue, the yellow, or the infra-red region of the spectrum. Bottlinger's color excesses, though usually positive, are small. BS 264, γ Cassiopeiae, was observed only once at Yale, consequently its color excess should not be given too much

[20] *Veröffentlichungen, Berlin-Babelsberg*, **3**, Heft 4, 1923.

weight, even though an accidental error half as large as its color excess is quite improbable. H. H. Plaskett[21] made a special study of this star. He derived a temperature of 6800° from the position of the maximum of a spectro-photometric curve. The spectrum of this star consists principally of a series of bright Balmer lines superimposed on hazy, wide, and dark bands.

Four other stars that have spectra similar to that of BS 264 all show positive color excesses in the Yale observations. One of these (β Lyrae) has much the largest excess, +0.14 mag., provided its com-

TABLE IV

BS	PGC	Star	b	Sp.	WS	Gw	Hz (Mag.)	B (Mag.)	Y (Mag.)
					T	T	c_2/T	CE	CE
130.....	103	15 κ Cass	0°	Bo	.....	.....	+0.62	+0.17	+0.24
264.....	199	γ Cass	− 2	Boe	9600°	13,100°	− .02	− .01	.16
496.....	384	ϕ Pers	−11	Bo	.....	.....	+ .04	+ .00	.21
1131.....	844	38 o Pers	−16	B1	6800	.....	+ .10	+ .03	.16
1203.....	894	44 ζ Pers	−15	B1	7600	10,100	+ .16	+ .05	.18
1228.....	913	46 ξ Pers	−13	oe5	.....	.....	+ .36	+ .04	.25
1542.....	1139	9 Caml	+15	Bo	.....	11,700	+ .27	+0.05	.20
6714.....	4548	67 Ophi	+10	B5	12,100	.....	+0.18	.....	+0.16

posite spectrum is equivalent to that of a B2 star. This star is not shown in Figure 6 because of this uncertainty; but even if it be rated B5, the excess would still be +0.10 mag.

The galactic latitudes of these eight stars are all small and their parallaxes are all less than 0".037. Half of them (130, 1131, 1228, and 1542) have spectra that indicate the presence of interstellar calcium. Rayleigh's[22] formula tells us that if light passes through an intervening cloud of atoms or molecules, the scattering varies as the reciprocal of the fourth power of the wave-length. The two effective wave-lengths used by Bottlinger are near 4400 and 4600 A, while my own (for colors 89) are near 7400 and 7950 A for a Go star. Therefore, even though the difference between the two effective wave-lengths in the blue is roughly one-third that in the infra-red, this does not

[21] *Monthly Notices of the Royal Astronomical Society*, **80**, 771, 1920.

[22] Strutt, *Philosophical Magazine*, **41**, 107, 1871.

compensate for the large difference in the scattering coefficient for such a widely separated pair of wave-lengths. The presence of matter in interstellar space should therefore affect the colors observed with the blue-sensitive cell more than my own, if Rayleigh's formula is applicable. Table IV shows that the reverse is the case for these four stars.

BS 6714 is a *c* star. Table V shows that the colors of all the observed *c* stars are slightly redder than normal for their spectral types. These are supergiants having unusually strong and sharp lines. Similar stars having the same characteristics less pronounced are de-

TABLE V

COLOR EXCESSES OF THE OBSERVED *c* STARS

BS	PGC	COLOR EXCESS (MAG.)		SP.	STAR
		89	87		
1605	1187	+0.09	+0.16	cF5	7 ϵ Aur (var.)
3975	2694	.07	.05	cA0	30 η Leo
6714	4548	.16	.26	cB5	67 Oph
7796	5229	.03	.01	cF8	37 γ Cyg
7924	5320	.00	.01	cA2	50 α Cyg
8143	5469	+0.08	+0.08	cA0	67 σ Cyg

noted as *ac* stars; their colors are not noticeably abnormal for their spectral class.

For these six stars the average probable error of the mean for colors 89 is $\pm$0.012 mag. and for colors 87, $\pm$0.016 mag. The color excesses contain an error due to the fact that the normal color for a given spectral class is not exactly known, and also there is a possibility that the spectral classification is slightly in error.

In contrast to photo-electric observations[20] in the blue end of the spectrum, Figure 6 shows that the scatter within any given spectral class does not vary appreciably from one end of the spectral sequence to the other, if we disregard the eight early-type stars that have abnormal colors.

4. The relation between Bottlinger's[20] colors and my own is shown in Figure 7. The filled circles represent seven of the eight stars listed in Table IV. In view of the fact that we were measuring

the energy in two entirely different regions of the spectrum, the general agreement seems remarkably good. The average probable error for a single star computed from a smoothed curve is ± 0.033 mag., no stars being excluded. This is somewhat larger than would be expected from the errors in the two co-ordinates if the measurements were made in the same region of the spectrum. It is quite possible that some of the deviations shown in this figure are due to the presence of faint companions of different spectral type which have not been previously detected by other methods.

When Bottlinger's observations are plotted against spectral type, the late-type stars are more scattered about a mean curve than those

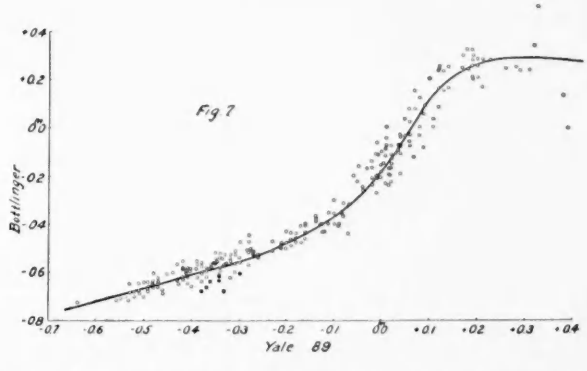

FIG. 7.—The colors observed by Bottlinger with a blue-sensitive cell compared with those for the same stars observed at Yale. The mean curve is arbitrarily drawn.

of early type. The star μ Cephei has a positive excess of 0.25 mag. on his scale and an excess of +0.08 mag. on the scale of colors 89. The variability of these red giants makes comparison a little risky. It appears that the colors of stars of very early type and also those of very late type depend much more on the region used in measuring them than do the colors of other stars. The colors measured in a particular region of the spectrum are influenced by absorption lines or bands peculiar to the region under consideration. In connection with the Yale observations, it should be mentioned that the head of the Paschen series of hydrogen is at 8205 A. This wave-length is well beyond both filter cut-offs.

As would be expected from the data already given on the relation

of spectral type to color, the average deviation about the mean curve in Figure 7 is less on Bottlinger's scale for stars of early spectral classes than for late-type stars. The probable errors of each set of colors for such bright stars are practically independent of spectral type. If interstellar atoms or molecules were present, one would expect that the stars of early type would show more scattering, provided the stars radiate as black or gray bodies and provided their colors are uninfluenced by line and band absorptions. The color excesses of colors 89 show no dependence on galactic latitude, regardless of the spectral type. The apparent magnitudes of the observed early-type stars may be used as a rough measure of their distances. If the color excesses of these stars are plotted against their absolute magnitudes, no correlation is evident. It seems highly probable that the colors of these stars, measured in the infra-red, are not noticeably influenced by matter in interstellar space.

Elvey[23] attributes the reddening of the light from the bright stars of early spectral type, which he observed with a blue-sensitive cell, to at least two causes; namely, interstellar scattering and hydrogen line absorption in the violet end of the spectrum. His list contains 153 stars, one-quarter of which are fainter than 4.4 mag. His conclusion concerning interstellar scattering is based primarily on the large color excesses of the fainter stars. My observations do not contradict Elvey's on this point, if the difference in wave-lengths in which we have worked is taken into consideration. Further observations on much fainter stars would be necessary in order to detect the presence of an interstellar gas with a *CsO* photo-electric cell. Something more concerning the nature of interstellar scattering might be learned if the globular clusters observed by Stebbins[24] were reobserved with a cell sensitive in the infra-red.

5. Bottlinger's color observations suggest that it may be possible to distinguish between giants and supergiants from accurate color excesses, and in this way to find parallaxes that may serve for statistical purposes. In order to do this the stars must of course be accurately classified in the spectral sequence.

The Yale color excesses 87 were multiplied by 0.78 in order to re-

[23] *Astrophysical Journal*, **74**, 311, 1931.

[24] *Proceedings of the National Academy of Sciences*, **19**, 222, 1933.

duce them approximately to scale 89. The means of these reduced excesses and excesses 89 are plotted in Figure 8 against the corresponding absolute magnitudes. The parallaxes used to determine these magnitudes were taken from the card catalogue of parallaxes being compiled at Yale. No spectroscopic or dynamic parallaxes were used. The eight stars whose parallaxes were either negative or zero are not shown in Figure 8. The filled circles represent stars whose given parallaxes are greater than 0".029.

The diagram shows that the colors of these stars become redder as the luminosity increases. With a single exception, the stars plotted in the lower half of the diagram would be classed as giants. The color excesses of stars earlier than Go show no correlation with absolute magnitude. There is also no relation between color excess and apparent magnitude, regardless of the spectral class.

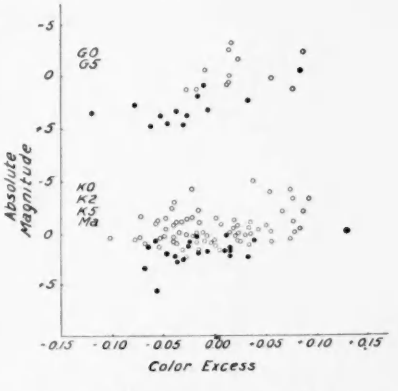

FIG. 8.—The color excesses of late-type stars plotted against their absolute magnitudes. The filled circles are for stars whose parallaxes exceed 0".029.

Since the spectroscope can be used to distinguish giants from dwarfs, color observations may be of use where the spectroscope is weak; namely, in distinguishing giants from supergiants. And since this concerns stars that are Go and later, other things being equal, the *CsO* cell should have a decided advantage over the blue-sensitive *KH* cell, as well as the spectrograph. I hope to have an opportunity to investigate this possibility in a quantitative way in the near future.

ACKNOWLEDGMENTS

I wish to express my sincere thanks to Dr. Schlesinger for suggesting this problem and for his constant interest and advice. I am also grateful to Dr. Schilt for many helpful suggestions when the development of the apparatus was in progress. I wish to thank the other members of the Yale Observatory staff for their general interest and encouragement. The co-operation of the Bell Laboratory of New

York, and of Dr. Prescott in particular, was most helpful. Mr. A. Klocker very skilfully constructed the more delicate parts of the apparatus. My brother, N. C. Hall, Jr., very kindly made the graphs.

A grant from the Draper Fund enabled me to make a substantial share of the observations given in this paper.

YALE UNIVERSITY OBSERVATORY
June 1933

PHOTOGRAPHY OF THE NEAR INFRA-RED REGION OF STELLAR SPECTRA[1]

By PAUL W. MERRILL

ABSTRACT

This paper describes the chief features shown by a photographic reconnaissance of stellar spectra in the region λλ 7000–9000 A, made with a plane-grating spectrograph attached to the 100-inch telescope. Most of the spectrograms are of dispersion 33 A/mm and show the region λλ 8320–8900, which is free from serious interference by terrestrial lines and includes a number of stellar lines of special interest.

Results.—Radial velocities from infra-red lines (Table VII) agree well with each other and with previous determinations from lines in the blue-violet region.

The chief lines in the infra-red spectrum of α Cygni (Table II) are due to *H*, *N* I, *O* I, *Mg* II, *Ca* II. The Paschen series of hydrogen lines is conspicuous in A-type spectra, especially those having the "c" characteristic, e.g., α Cygni, β Orionis. The lines of *Ca* II λλ 8498, 8542, 8662 are prominent in types A–M and may have an interesting relationship to absolute magnitude. They were found to be bright in the spectrum of R Hydrae. The *O* I lines λλ 7772, 7774, 7775, and 8446 are important in types A and F. They appear very sensitive to absolute magnitude, being more intense in the brighter stars.

Lines of neutral *Ca*, *Ti*, and *Fe* dominate spectra of classes K and M in the region λλ 8320–8840. Many band heads were measured in spectra of class M. Most of them, especially in the λ 7000 region, are due to *TiO*. A comparison of N-type spectra with furnace spectra taken by King shows that a large part of the complex structure between λ 6910 and λ 8780 is due to absorption by cyanogen.

Before 1930, photographic emulsions for the extreme red and near infra-red were relatively insensitive, and considerable difficulty was experienced in obtaining useful stellar spectrograms beyond about λ 7000A. A few photographs, however, were made by V. M. Slipher,[2] J. Bosler,[3] W. H. Wright,[4] and the writer[5] on plates sensitized with dicyanin, kryptocyanin, or neocyanin.

The recent discovery and systematic testing of new dyes, particularly by the Research Laboratory of the Eastman Kodak Company,[6] have resulted in greatly improved emulsions for the longer

[1] *Contributions from the Mount Wilson Observatory, Carnegie Institution of Washington*, No. 486.

[2] *Astrophysical Journal*, **25**, 235, 1907; *Encyclopaedia Britannica* (11th ed.), **21**, 717, 1910–1911; *Lowell Observatory Bulletins*, **1**, 231, 1903–1911; *Popular Astronomy*, **37**, 140, 1929.

[3] *Comptes rendus*, **160**, 124, 1915.

[4] *Publications of the Astronomical Society of the Pacific*, **32**, 63, 1920.

[5] *Scientific Papers of the Bureau of Standards*, **14** (No. 318), 487, 1918; *Publications of the Astronomical Society of the Pacific*, **37**, 272, 1925; *ibid.*, **40**, 254, 1928; *Mt. Wilson Contr.*, No. 432; *Astrophysical Journal*, **74**, 188, 1931.

[6] Brooker, Hamer, and Mees, *Journal of the Optical Society of America*, **23**, 216, 1933.

wave-lengths, and it is now possible to obtain, with moderate exposure times, satisfactory stellar spectrograms extending into the infra-red as far as λ 9000A. The chief features shown by a recent reconnaissance of stellar spectra in the region λλ 7000–9000 may therefore be of interest.

In this region, lines of the earth's atmosphere (Fig. 1) are numerous and intense and interfere considerably with the observation of stellar lines. Most of the photographs include the clear region λλ 8320–8900; a smaller number are of the region λλ 6800–8320. No effort was made to penetrate the dense group of atmospheric lines beginning about λ 8950, for although feasible to do so, the study of stellar features would be handicapped by the intense and closely

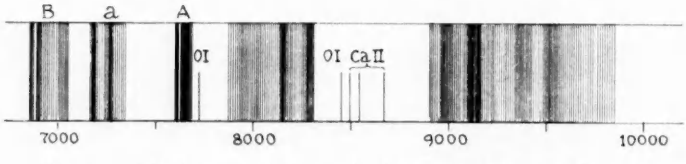

FIG. 1.—Chief groups of atmospheric lines in the near infra-red

packed telluric lines. With zenocyanin plates it does not appear out of the question to extend stellar observations beyond the end of this group at λ 9800, but this has not yet been attempted.

The spectrograms, listed in Table I, were obtained with the 100-inch reflector. The first of α Cygni, G 11, taken with a concave grating spectrograph, is on celluloid film. All other photographs are on glass plates; nearly all were made with the plane-grating spectrograph described in *Mount Wilson Contribution* No. 432.[7] A 10-inch camera lens giving a dispersion of 64.8 A/mm was used for most of the earlier observations. The later plates were taken with an 18-inch camera,[8] dispersion 33.4 A/mm, most of the spectra being widened to 0.3 mm by allowing the star to drift along the slit.

Early observations were on plates sensitized with dicyanin, kryptocyanin, or neocyanin; the later ones, on the R or P plates

[7] *Astrophysical Journal*, **74**, 188, 1931. The exceptions were taken in 1925 with a plane grating in a preliminary mounting. The plate numbers are α Lyrae, G 62; α Cygni, G 65, 70; R Leonis, G 60; R Hydrae, G 64, 69.

[8] So called; actual equivalent focal length about 19½ inches.

obtained from the Research Laboratory of the Eastman Kodak Company,[9] with the greatest sensitivity in the regions λλ 7600–8400 and λλ 8200–8900, respectively. The numbers 3 or 4 preceding the symbols R and P in Table I indicate characteristics of the basic emulsions, described as follows by Dr. C. E. K. Mees: 3, medium speed, high contrast, low graininess; 4, low speed, very high contrast, very low graininess.

The spectral region under discussion is so far from that to which the eye is most sensitive that a star's visual magnitude is no longer even an approximate measure of the proper exposure time. For example, on the assumption of black-body radiation, a long-period variable, temperature say 2300°, has about nineteen times as much energy at λ 8600 as a B-type star, temperature 20,000°, of the same visual magnitude. The exposure times in Table I, given as a guide to future investigations and because photometric measurements are to be made on some of the plates, are not in all instances those in the observing record, but are the times as judged by the appearance of the developed negatives which would have yielded the optimum density. Times unduly long because of poor conditions are inclosed in parentheses.

Argon furnishes a fairly suitable comparison spectrum for the region λλ 6965–8425, although the lines are not so numerous as might be desired. A Hilger 220-volt discharge tube is a convenient source. For the region λλ 8300–8700, titanium and iron lines have been used, but no entirely satisfactory method of obtaining these lines from a single source has yet been devised. Two forms of arc have been used: (1) one electrode of iron, the other a cored carbon loaded with titanium oxide;[10] (2) both electrodes of an alloy of 25 per cent titanium, 75 per cent iron. The latter arc yields the titanium lines in fair intensity, together with a few iron lines, but it is troublesome because it is inclined to burn in an irregular manner, at times giving considerable continuous spectrum. An alloy of lower titanium content might perform better.

[9] Three plates taken in July, 1931, on a special Eastman emulsion sensitive from λ 7600 to λ 8300 are designated λ 8100.

[10] Powdered rutile will serve.

TABLE I

JOURNAL OF OBSERVATIONS

Star	Sp.	Mag.	R.A. 1900	Plate	Date	Em.†	Corr. Exp.	Remarks
							Minutes	
NGC 6572	P	.....	$18^h\ 7^m.2$	G 157*	1928 June 29	Kr	600	For λ 7325
NGC 7027	P	.....	21 3.3	160*	1928 June 30	Kr	600	For λ 7325
α Vir	B2n	1.2	13 19.9	152*	1928 June 7	Ne	(200)	Narrow
				569	1932 June 18	3P	120	
				735	1933 Feb. 15	3P	180	
γ Cas	Bone	2.2	0 50.7	578	1932 July 18	3P	(220)	Narrow
				583	July 20	4R	100	
P Cyg	Beq	5.0	20 14.1	158*	1928 June 29	Kr	100	Poor
				346*	1930 Mar. 20	Kr	300	Underexposed
				581	1932 July 19	3P	400	Narrow
α Leo	B8n	1.3	10 3.0	734	1933 Feb. 15	3P	(300)	
				741	Mar. 8	3P	80	Narrow; overexposed
				744	Mar. 9	3P	120	
β Ori	cB8	0.3	5 9.7	732	1933 Feb. 15	3P	(130)	Narrow
				742	Mar. 9	3P	60	
α C Ma	Ao	−1.6	6 40.7	59*	1925 Apr. 10	Di	(4)	
				225*	1929 Jan. 26	Ne	(60)	
				339*	1930 Mar. 20	Kr	(2)	
				347	Mar. 21	Kr	(8)	
				450*	1931 Apr. 2	Ne	(80)	
				733	1933 Feb. 15	3P	(30)	
				736	Mar. 7	3P	20	
				737	Mar. 7	3P	(40)	
				743	Mar. 9	3P	15	
α Lyr	Ao	0.1	18 33.6	62*	1925 Apr. 10	Di	40?	Trial mounting
				151*	1928 June 6	Ne	(180)	
				353	1930 Mar. 21	Kr	25	
				561	1932 June 16	4R	(30)	
				565	June 17	3P	15	Overexposed
				566	June 17	3P	50	Narrow slit
				567	June 17	4R	(20)	
				757	1933 Apr. 2	3P	60	
				768	Apr. 3	3R	(50)	
α Cyg	cA2	1.3	20 38.0	11	1922 July 10	Di	150	Concave grating; film poor
				65*	1925 Apr. 11	Di	(60)	Trial mounting
				70*	June 8	Di	?	Trial mounting
				506*	1931 July 27	‡	(70)	
				568	1932 June 17	4R	80	
				572	June 18	3P	80	
				577	July 18	3P	(120)	
				750	1933 Apr. 1	3P	140	
				776	May 13	3P	(150)	
				778	June 10	3P	(200)	Underexposed
				779	June 10	3P	(250)	
α Aql	A5	0.9	19 45.9	509*	1931 July 28	‡	34	
α C Mi	dF5	0.5	7 34.1	739	1933 Mar. 8	3P	50	
				740	Mar. 8	3P	(60)	
				746	Apr. 1	3P	80	
				751	Apr. 2	3P	90	
				763	Apr. 3	3R	30	Overexposed
γ Cyg	cF8	2.3	20 18.6	573	1932 June 18	3P	120	

* Dispersion 65 A/mm. Plates not starred, dispersion 33 A/mm.

† Di, dicyanin; Kr, kryptocyanin; Ne, neocyanin; 3P, 3R, 4R, special emulsions made by the Research Laboratory of the Eastman Kodak Co.

‡ Special emulsion labeled λ 8100.

TABLE I—*Continued*

Star	Sp.	Mag.	R.A. 1900	Plate	Date	Em.†	Corr. Exp.	Remarks
							Minutes	
α Boo	K0	0.2	14^h11^m1	G 133	1928 May 4	Ne	30	Overexposed
				149*	June 6	Ne	60	Poor
				350	1930 Mar. 21	Kr	4	
				452*	1931 Apr. 2	Ne	90	
				507*	July 28	‡	10	
				560	1932 June 16	3R	8	Narrow slit
				570	June 18	3P	6	
				574	July 18	3P	15	
				579	July 19	3P	8	
				749	1933 Apr. 1	3P	12	
				754	Apr. 2	3P	14	
α Sco	gM1	1.2	16 23.3	150*	1928 June 6	Ne	(120)	
				352	1930 Mar. 21	Kr	18	
				453*	1931 Apr. 2	Ne	(150)	
				564	1932 June 17	3P	(15)	Overexposed
				571	June 18	3P	10	
				575	July 18	3P	18	
				755	1933 Apr. 2	3P	(24)	
α Ori	gM2	0.5– 1.1	5 49.8	728	1933 Feb. 14	3P	4	Overexposed
				729	Feb. 14	3P	5	
				738	Mar. 8	3P	6	
α Her	M5	3.1– 3.9	19 10.1	153*	1928 June 7	Ne	((240))	
				345*	1930 Mar. 20	Kr	3	
				351	Mar. 21	Kr	30	
				576	1932 July 18	3P	40	
				580	July 19	3P	30	
				756	1933 Apr. 2	3P	50	Overexposed
				767	Apr. 3	3R	(12)	
R Lyr	M5	4.2– 5.1	18 52.3	775	1933 May 13	3P	70	
o Cet	M6e	3.4– 9.2	2 14.3	201*	1928 Aug. 31	Ne	70	Overexposed
				208*	Sept. 1	Ne	100	
R Hya	M7e	4.2– 9.5	13 24.2	64*	1925 Apr. 11	Di	160	Trial mounting
				69*	June 8	Di	(150)	Trial mounting
				748	1933 Apr. 1	3P	90	Overexposed
				753	Apr. 2	3P	(140)	
				766	Apr. 3	3R	(60)	
				774	May 13	3P	(200)	
				777	June 10	3P	(140)	
R Leo	M8e	5.9–10.1	9 42.2	60*	1925 Apr. 10	Di	120	Trial mounting
Y C Vn	Nb	4.8– 6.0	12 40.4	159*	1928 June 30	Kr	120	
				745	1933 Mar. 9	3P	200?	Narrow
				752	Apr. 2	3P	200	Narrow
				765	Apr. 3	3R	90	
U Hya	Nb	4.5– 6.3	10 32.6	747	1933 Apr. 1	3P	300?	Underexposed
				764	Apr. 3	3R	(150)	

CLASS P. GASEOUS NEBULAE

The plates of NGC 6572 and 7027, listed in Table I, were taken to determine the structure of the line λ 7325, previously observed by W. H. Wright.[11] The results, reported elsewhere,[12] confirmed I. S. Bowen's identification of it as a forbidden line of singly ionized

[11] *Publications of the Lick Observatory*, **13**, 193, 1918.

[12] *Publications of the Astronomical Society of the Pacific*, **40**, 254, 1928.

oxygen.[13] A five-hour exposure on NGC 6572 made on July 20, 1932, with the grating spectrograph and 6-inch camera, on emulsion 4R, showed nothing. This negative result probably means that no very strong lines exist in the region λλ 7700–8300. An adequate survey of the infra-red spectra of gaseous nebulae remains to be made.

CLASS B

α *Virginis*, *B2n*.—The spectrograms are not of the highest quality, but show the absence of strong lines between λ 7600 and λ 8800. The Paschen lines are not conspicuous, but several, wide and ill defined, may be recognized with a low-power eyepiece.

γ *Cassiopeiae*, *Bone*.—The spectrum of this well-known bright-line star shows in emission the Paschen series and also the oxygen lines near λ 7774 and λ 8446. The triplet λλ 7772–7774–7775 appears as a wide blur, but λ 8446, the strongest line in this part of the spectrum, has two well-marked bright components about 4.4 A apart.

P Cygni, *Beq*.—The Paschen lines have both bright and dark components. *O* λ 8446 is bright and more intense than any other line in this part of the spectrum. Plates G 158 and G 346 show *Hα* and the helium lines λλ 6678 (trace), 7065, and 7281 in emission.

α *Leonis*, *B8n*.—The Paschen lines are fairly strong, but also extremely broad and diffuse. *O* λ 8446 and the calcium triplet λλ 8498, 8542, 8662 (Pl. II) are weak or absent.

β *Orionis*, *cB8*.—The Paschen lines are very conspicuous. *O* λ 8446 also is outstanding; it is narrower than the Paschen lines and its edges are much sharper. The calcium triplet is not certainly seen but may be faintly present. It is decidedly less intense than in α Canis Majoris, α Lyrae, or α Cygni. A few nitrogen lines are visible, but are much less intense than in α Cygni.

CLASS A

α *Canis Majoris*, *Ao*.—The Paschen lines and *O* λ 8446 are strong, and the calcium triplet is distinct. A few nitrogen lines are seen. Among the earlier plates, G 59, 225, and 450 show the oxygen lines, while a trace of the Paschen series may be surmised on G 225.

α *Lyrae*, *Ao*.—The Paschen series is strongly developed. *O*

[13] *Astrophysical Journal*, **57**, 1, 1928.

PLATE II

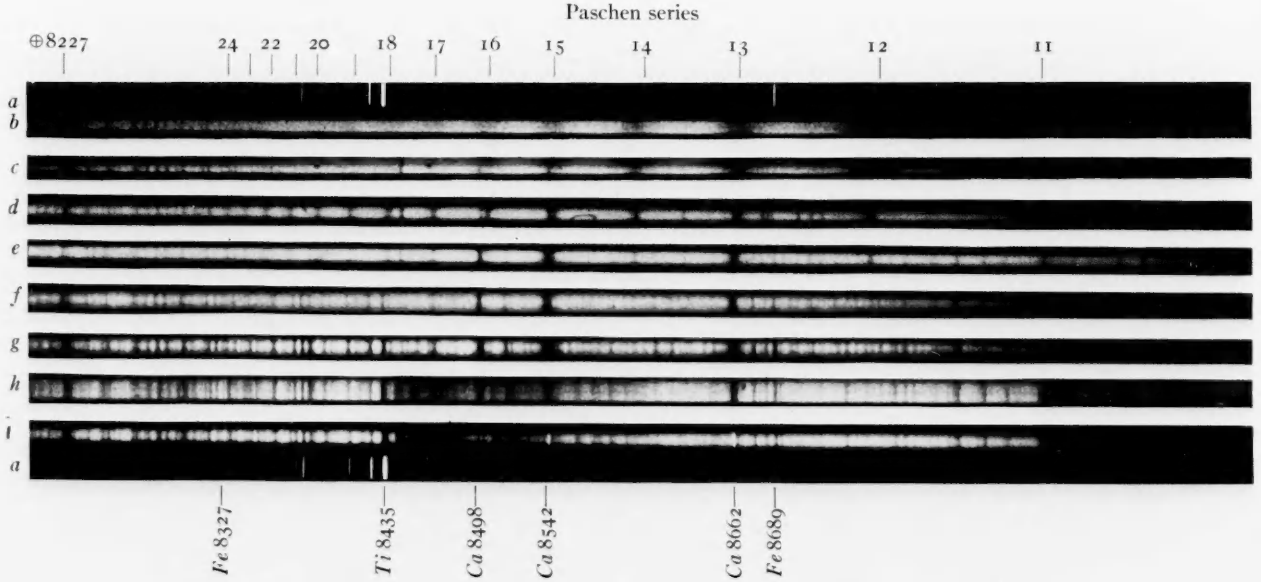

STELLAR SPECTRA IN THE REGION λλ 8300–8900

a) Comp. spectrum *Ti*, *Fe*
b) α Leonis, B8n, G 744
c) α Lyrae, Ao, G 757
d) α Cygni, cA2, G 776
e) γ Cygni, cF8, G 573
f) α Boötis, Ko, G 754
g) α Scorpii, gM1, G 755
h) α Herculis, M5, G 756
i) R Hydrae, M6e, G 774
a) Comp. spectrum *Ti*, *Fe*

YERKES OBS.

λλ 7772–7774–7775 and λ 8446 are intense and sharp. The calcium lines are weak and narrow, and the nitrogen lines are very weak. *Mg* II λ 7877 and λ 7896 are present but are much weaker than in α Cygni. The oxygen lines may be seen on the early plates, G 62 and G 151. The spectrum is very similar to that of α Canis Majoris (see Pl. II).

α Cygni, cA2.—The infra-red spectrum of this remarkable high-luminosity star is especially interesting (see Pl. II). The Paschen series and the oxygen lines are outstanding; the calcium triplet is well marked, while lines of neutral nitrogen are much stronger and more numerous than in any other spectrum observed. *Mg* II λ 7877 and λ 7896 also are fairly strong. The chief lines measured, with their approximate relative intensities, are listed in Table II. The wave-lengths of the Paschen lines are those calculated from the frequency differences of Balmer lines as given by A. Fowler.[14] C. C. Kiess's measurements in the nitrogen spectrum[15] are used, while other data are from Miss C. E. Moore's convenient compilation, "A Multiplet Table of Astrophysical Interest." The oxygen lines are of high intensity with well-defined edges. The triplet λλ 7772–7774–7775 is shown on G 11, although this negative is very poor; it is outstanding on G 506, which shows also *Mg* II λ 7877 and λ 7896. The best plate of this region is G 568. Compared with the oxygen lines, the hydrogen lines are wider and their edges less sharp, but their centers are fairly definite. The tabulated intensities are estimates based on the appearance of the lines and may perhaps represent the central absorption more closely than the total intensity. Thus a hydrogen line estimated of intensity 9 may have a greater total intensity than *O* λ 8446, also estimated 9. The calcium lines appear to be intermediate in sharpness between the oxygen lines and those of hydrogen. The nitrogen lines are fairly sharp. Table III gives the atomic transitions corresponding to the observed lines with the excitation potentials of the lower levels, and the ionization potentials of the atoms concerned. Hydrogen, nitrogen, and oxygen, whose first ionization potentials are 13.5 volts or higher, are represented by lines of the neutral atom; but iron, magnesium, and calcium, whose

[14] *Report on Series in Line Spectra*, p. 90, London, 1922.

[15] *Journal of the Optical Society of America*, 11, 1, 1925.

first ionization potentials are not over 7.8 volts, exhibit lines of the first stage of ionization. Some atoms of calcium must be doubly ionized because the second ionization potential is 11.8 volts and great numbers of hydrogen atoms are lifted to a level of excitation

TABLE II

LINES IN THE SPECTRUM OF α CYGNI
(Laboratory or Calculated Wave-Lengths)

I.A.	Ident.	Int.	I.A.	Ident.	Int.
7423.88	*N* I	0	8413.33	*P* 19	6
42.56	*N* I	1	37.96	*P* 18	7
62.34	*Fe* II?	0	46.35	*O* I	9
68.74	*N* I	2	46.73	*O* I	
			67.27	*P* 17	7
7515.89	*Fe* II?	0	98.06	*Ca* II	3
7711.94	*Fe* II	2	8502.50	*P* 16	7
71.95	*O* I	8	42.13	*Ca* II	8
74.18	*O* I	14	45.39	*P* 15	7
75.39	*O* I		68.04	*N* I	1
			94.34	*N* I	1
7877.13	*Mg* II	2	98.40	*P* 14	8
96.37	*Mg* II	4			
			8629.61	*N* I	2
8185.05	*N* I	0	56.32	*N* I	1
88.16	*N* I	?	62.17	*Ca* II	9
			65.03	*P* 13	9
8200.33	*N* I	1	80.35	*N* I	4
10.94	*N* I	1	83.61	*N* I	2
16.46	*N* I	2	86.38	*N* I	1
23.28	*N* I	1?			
42.47	*N* I	1	8703.42	*N* I	3
			11.84	*N* I	3
8333.79	*P* 24	1?	18.99	*N* I	3
45.55	*P* 23	2	29.07	*N* I	1
59.01	*P* 22	3	50.47	*P* 12	11
74.49	*P* 21	4			
92.41	*P* 20	5	8862.79	*P* 11	12±

potential 12.0 volts, but I am not aware that lines of *Ca* III have been recognized in the spectrum of α Cygni.[16]

The measured displacements of lines of various elements are shown in Table IV. The smaller discrepancies are doubtless due to errors of measurement, but the larger ones are probably intrinsic. The nitrogen lines are apparently systematically displaced toward

[16] O. Struve (*Astrophysical Journal*, **74**, 225, 1931) has suggested that two inconspicuous lines in the spectrum of β Cephei, B1, are due to *Ca* III.

shorter wave-lengths, relative to the other lines, by about 0.23 A. The mean velocities in the last column of Table IV include those

TABLE III

ATOMIC TRANSITIONS REPRESENTED IN THE INFRA-RED SPECTRUM OF α CYGNI

ELEMENT	I.P.		TRANSITION	E.P. LOWER LEVEL
	I	II		
	volts	volts		volts
H	13.5	.....	Paschen 11–24	12.0
N I	14.5	.....	$^4P - {}^4S^o$	10.3
			$^4P - {}^4P^o$	10.3
			$^4P - {}^4D^o$	10.3
			$^2P - {}^2P^o$	.....
Fe II	7.8	16.5	$^4D - {}^4D^o$	3.9
Mg II	7.6	15.0	$^2P^o - {}^2D$	10.0
O I	13.6	.....	$^5S^o - {}^5P$	9.1
			$^3S^o - {}^3P$	9.5
Ca II	6.1	11.8	$^2D - {}^2P^o$	1.7

TABLE IV

MEASURED DISPLACEMENTS IN THE SPECTRUM OF α CYGNI
(km/sec.)

PLATE	HYDROGEN		NITROGEN		CALCIUM		OXYGEN		MAGNESIUM		ALL
	Vel.	No.	Vel.	No.	Vel.	No.	Vel.	No.	Vel.	No.	
G 568	−10.9	6	−10.0	9	.....	.....	−3.6	3	−4.4	2	− 8.4
572	− 6.9	13	21.1	11	−8.5	3	−4.2	1	.....	.....	12.8
577	+ 2.2	9	8.3	9	−8.5	3	+2.5	1	.....	.....	3.8
750	− 0.1	12	11.0	7	−9.1	3	−1.4	1	.....	.....	4.6
776	− 0.1	14	8.4	13	+3.4	3	+1.1	1	.....	.....	3.2
779	0.0	10	−13.0	11	−6.2	3	−2.8	1	.....	.....	− 6.6
Mean	− 2.6	.....	−12.0	.....	−5.8	.....	−1.4	.....	−4.4	.....	− 6.6

from *all* lines, but in forming the values in Table VII the displacements derived from the nitrogen lines were omitted. Dr. G. F. Paddock kindly informs me that the change in velocity between June 18

and July 17, 1932 (pls. G 572 and G 577), has the same sign as that found by him at Lick Observatory from three-prism spectrograms of the λ 4500 region.

α *Aquilae, A5.*—*O* λλ 7772–7774–7775 is visible but has only a fraction of its intensity in α Cygni.

CLASS F

α *Canis Minoris, dF5.*—The Paschen series is not conspicuous, but six or eight lines may be recognized. *O* λ 8446 is much more intense than in the solar spectrum, while the calcium triplet, the titanium lines, and certain iron lines—for example, λ 8688—are less intense.

TABLE V

MEASURED DISPLACEMENTS IN THE SPECTRUM OF γ CYGNI, PLATE G 573

Element	No. of Lines	Rad. Vel.
Fe I	8	− 3.9 km/sec.
H	7	7.6
Ca II	3	9.7
Mg I	1	10.6
N I	3	11.4
O I	1	13.1
Unidentified solar lines	10	−15.8
All	33	−10.0
Omitting unidentified lines	23	− 7.4

γ *Cygni, cF8.*—The Paschen lines are more intense than in α Canis Minoris. The calcium triplet and *O* λ 8446 may be slightly more intense. Several lines, including two of considerable intensity, λ 8912 and λ 8927, apparently correspond to unidentified solar lines (see Pl. II).[17] Displacements of various groups of lines, measured on plate G 573, are in Table V. The discrepancy between the velocities from the first and last groups of lines is large compared with the internal probable errors, which are ±1.2 and ±1.3 km/sec., respectively. The effect, however, requires confirmation; if real, it should

[17] C. E. St. John and Others, *Revision of Rowland's Preliminary Table of Solar Spectrum Wave-Lengths: Carnegie Institution of Washington Publication*, No. 396.

be thoroughly studied. As several of the unidentified lines are considerably stronger in γ Cygni than in the sun, they may be either high-excitation lines or lines of an ionized atom. A comparison of the intensities in sun-spots, however, seems not to confirm this suggestion. The mean velocity from all lines is -10.0 km/sec.; omitting the unidentified lines, it becomes -7.4 km/sec.

CLASS K

α *Boötis, Ko.*—This spectrum differs from that of the sun in the greatly increased absorption of many metallic lines, especially those of titanium. The calcium triplet is somewhat more intense than in the solar spectrum (see Pl. II).

CLASS M

α *Scorpii, gM1.*—The metallic lines are generally more intense than in α Boötis, the difference in the titanium lines being especially marked. Several titanium lines near λ 8400 are outstanding. The calcium triplet also is decidedly more intense (see Pl. II).

α *Orionis, gM2.*—The spectrum in the region $\lambda\lambda$ 8300–8800 closely resembles that of α Scorpii.

α *Herculis, M5.*—The high intensity of the (unresolved) double line *Ti* λ 8434.9 and λ 8435.6 is striking. It is stronger than any member of the calcium triplet, which is considerably less intense than in the spectrum of α Scorpii. Several facts suggest that the double titanium line may be reinforced by the head of an absorption band degraded toward longer wave-lengths (see Pl. II). On plate G 767 (two exposures), the potassium lines λ 7665 and λ 7699 appear to be displaced about 0.25 A (10 km/sec.) toward shorter wave-lengths with respect to other lines. This relative displacement may be a matter of importance and should have a thorough investigation, preferably with higher dispersion.[18]

R Lyrae, M5.—The spectrum resembles that of α Herculis, but several features indicate that the type is slightly less advanced.

o *Ceti, M6e.*—The lines measured are listed in *Contribution* No. 432; *Astrophysical Journal*, **74**, 188, 1931. The double titanium line

[18] Mr. Adams kindly permits me to mention the fact that on a coudé spectrogram taken by him on March 13, 1933, the yellow sodium lines show a relative displacement of the same sign as that of the potassium line but of smaller magnitude (*ca.* 0.1 A).

at λ 8435 appears remarkably intense. No spectrograms have been obtained since 1928.

R Hydrae, M7e.—The band heads measured in α Herculis and R Lyrae are accentuated, and numerous weaker heads are visible (see Table VIII). The behavior of the calcium lines is remarkable. On plates G 748 and G 753, phases (counted from maximum light) −34 and −33 days, respectively, the dark lines have bright borders on their short wave-length edges, no portion being of high intensity. On G 774 (see Pl. II) and G 777, phases +8 and +36 days, respectively, the bright components have greatly increased intensities and are conspicuous features.[19] It thus appears probable that their time

TABLE VI

DISPLACEMENTS OF BRIGHT CALCIUM LINES IN THE SPECTRUM OF R HYDRAE

(km/sec.)

	G 748	G 753	G 774	G 777
λ 8498	.....	.....	−20	−22
8542	.....	−47	−34	−34
8662	−37	−36	−33	−30
Absorption lines	− 7.5	− 6.9	−10.6	−13.9
Phase (days)	−34	−33	+ 8	+36
Magnitude	4.9	4.9	4.1	5.4

of maximum intensity follows that of maximum light, although perhaps by a few days only. The photometric data in Table VI were supplied through the kindness of Mr. Leon Campbell of the Harvard College Observatory.

The apparent radial velocities derived from the bright calcium lines are in Table VI. These lines are displaced toward shorter wave-lengths with respect to the absorption lines as are the bright lines in the blue-violet portion of the spectrum,[20] but the shift (expressed in radial velocity) appears to be numerically greater.

CLASS N

Y Canum Venaticorum, Nb.—Plate G 159, taken on June 30, 1928, showing the spectrum from λ 6800 to λ 7650, is reproduced in

[19] They may be slightly stronger on G 774.

[20] *Mt. Wilson Contr.*, No. 264; *Astrophysical Journal*, **58**, 215, 1923.

UNIV. OF MICH.

PLATE III

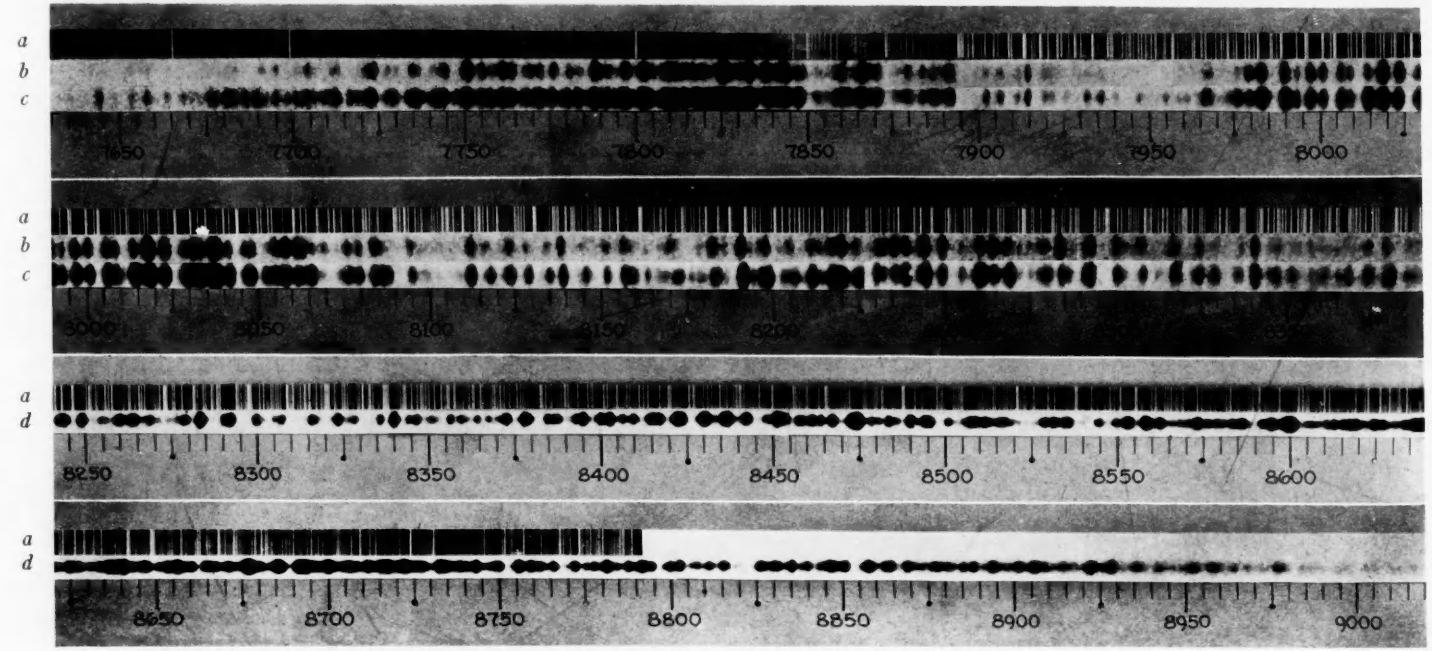

N-Type Spectra Compared with the Furnace Spectrum of Cyanogen

a) Furnace spectrum of carbon tube (positive)
b) Y Canum Venaticorum, G 765 (negative)
c) U Hydrae, G 764 (negative)
d) Y Canum Venaticorum, G 745 (negative)

Contribution No. 432.[21] On G 765 the spectrum extends from λ 7700 past λ 8400; on G 745, from λ 8200 to about λ 8900 (see Pl. III). G 752 is of the same region as G 745 but is less strongly exposed; it shows the chief features from λ 8400 to about λ 8800.

U Hydrae, Nb.—Plate G 764 (Pl. III) records the spectrum from λ 7600 to λ 8450. G 747 is underexposed but shows many of the stronger features between λ 8400 and λ 8700.

The spectrum corresponds closely to that of Y Canum Venaticorum, although there are differences in the relative intensities of numerous features. The spectrum of Y Canum Venaticorum has somewhat higher general contrast, and at certain wave-lengths there is evidence of absorption which in U Hydrae is either absent or weaker. Examples are found on the short wave-length side of the band heads λ 7850 and λ 7873, also in narrow maxima near λλ 7976, 8014, 8029, 8041, 8052, 8065, 8086, 8206, 8211, 8217, 8230, 8260, 8269; at these points the spectrum of Y Canum Venaticorum is noticeably less intense. On the other hand, a few narrow maxima, notably one near λ 8284, are more pronounced in Y Canum Venaticorum than in U Hydrae. This effect may possibly be caused by relatively stronger absorption in adjacent portions of the spectrum.

DISCUSSION

Radial velocities.—About twenty-five of the infra-red spectrograms have been measured with a micrometer wire in the usual way by Miss Burwell and the writer. The definition is fairly good,[22] and the comparison spectra, although not all that could be desired, serve reasonably well. In the region λλ 7600–8300, lines due to the earth's atmosphere have been used to some extent along with the comparison lines to determine corrections to the dispersion formula.

The radial velocities derived from lines of known wave-length are in Table VII. While the general accuracy of measurement is not especially high, the relatively large linear displacement at these

[21] *Astrophysical Journal*, **74**, 188, 1931.

[22] The spectrograms were obtained with camera lenses designed for the blue-violet, and narrow lines in the infra-red seem slightly less sharp than those at shorter wave-lengths. This may be due in part to the decreased resolving power yielded, of necessity, by longer waves, but I am inclined to believe that somewhat better definition could be obtained with lenses designed particularly for the near infra-red.

wave-lengths for a given velocity is a favorable feature, and the results agree well with each other and with previous determinations from lines in the blue-violet region.

TABLE VII

RADIAL VELOCITIES FROM LINES IN THE INFRA-RED

Star	Plate	Date	Velocity	General Cat.*	Lines
			km/sec.	km/sec.	
α Lyr....	G 757	1933 Apr. 2	−13.7	−13.8	*H* 3, *Ca* II 3, *O* I 1
α Cyg†...	568	1932 June 17	− 6.8	.....	*H* 6, *O* I 3, *Mg* II 2
	572	June 18	− 7.5	.....	*H* 13, *Ca* II 3, *O* I 1
	577	July 18	− 0.3		*H* 9, *Ca* II 3, *O* I 1
	750	1933 Apr. 1	− 1.9		*H* 12, *Ca* II 3, *O* I 1
	776	May 13	+ 0.6	.....	*H* 14, *Ca* II 3, *O* I 1
	779	June 10	− 1.6	.....	*H* 10, *Ca* II 3, *O* I 1
α C Mi....	740	1933 Mar. 8	− 3.4	− 3.0	*Ca* II 3, *Fe* I 2, *O* I 1, *Si?* 1, ⊙ 4
	751	Apr. 2	− 3.9	.....	*Ca* II 3, *Fe* I 4, *O* I 1, *Mg* I 1, *Si?* 1, ⊙ 5
γ Cyg‡...	573	1932 June 18	− 7.4	− 7.6	*H* 7, *Ca* II 3, *Fe* I 8, *N* I 3, *O* I 1, *Mg* I 1
α Boo....	560	1932 June 16	− 6.8	− 5.1	*Fe* 12, *Ti* 6, *Ni* 5, Misc. 4
	754	1933 Apr. 1	− 4.7	.....	*Fe* 11, *Ti* 8, *Ca* II 3, Misc. 2
α Sco....	575	1932 July 18	− 4.1	− 3.2	*Fe* 14, *Ti* 12, *Ca* II 3, Misc. 2
	755*a*	1933 Apr. 2	+ 0.3	.....	*Fe* 10, *Ti* 13, *Ca* II 3
	755*b*	Apr. 2	+ 1.8	.....	*Fe* 9, *Ti* 11, *Ca* II 1
α Ori....	738*a*	1933 Mar. 8	+19.6	+21.0	*Fe* 6, *Ti* 8, *Ca* II 3, *Mg* 1
	738*b*	Mar. 8	+20.3	.....	*Fe* 9, *Ti* 11, *Ca* II 3
α Her....	580	1932 July 19	−36.4	−32.5	*Fe* 6, *Ti* 8, *Ca* II 3, *Na* 1, *Mg* 1
	756	1933 Apr. 2	−34.1	.....	*Fe* 8, *Ti* 8, *Ca* II 3, *Mg* 1
	767*a*	Apr. 3	−34.8	.....	*Fe* 4, *Ti* 7, *Ca* II 1
	767*b*	Apr. 3	−36.2	.....	*Fe* 3, *Ti* 7 *Na* 1
R Lyr....	775	1933 May 13	−28.1	−28.3	*Fe* 10, *Ti* 12, *Ca* II 3, Misc. 4
R Hya...	748	1933 Apr. 1	− 7.5	− 5.4	*Fe* 4, *Ti* 9, *Mg* 1
	753	Apr. 2	− 6.9	.....	*Fe* 3, *Ti* 10, Misc. 2
	766	Apr. 3	− 6.8	.....	*Fe* 1, *Ti* 7, Misc. 3
	774	May 13	−10.6	.....	*Fe* 4, *Ti* 10, Misc. 2
	777	June 10	−13.9	.....	*Fe* 5, *Ti* 7, *Mg* 1

* J. H. Moore, "A General Catalogue of the Radial Velocities of Stars, Nebulae and Clusters," *Publications of the Lick Observatory*, **18**, 1932.

† See Table III. ‡ See Table V.

The *Paschen lines* of *hydrogen* will be discussed in another *Contribution.*

The *ionized calcium lines*, λλ 8498.06, 8542.13, and 8662.17, like the related lines H and K in the violet, are prominent through a range of spectral type from A to M. In the early-type stars the infra-red lines are narrow and well defined; even in the later types, in which the lines become very intense, the wings are narrow and inconspicuous. As illustrated by a partial Grotrian diagram in Figure 2, the infra-red lines arise from a metastable D-term and thus tend to exhibit, in absorption, the properties of ultimate lines. The general behavior of the infra-red triplet in stellar spectra is therefore much like that of H and K, but some interesting exceptions occur. In the spectrum of β Orionis, cB8, for example, H and K are well marked, while the infra-red triplet is scarcely detectable; they are slightly more intense than in the spectrum of α Lyrae, while the triplet is decidedly less intense. In the red supergiant stars α Scorpii and α Orionis, on the other hand, the triplet is much stronger than H and K. Moreover, in these stars the triplet is stronger than in α Boötis and α Herculis, while H and K are weaker. The facts suggest that among the hotter stars high luminosity enhances H and K with respect to the infra-red lines, while among red stars the reverse relationship holds. It is hoped later to make a photometric comparison of the two sets of ionized calcium lines in various stars.

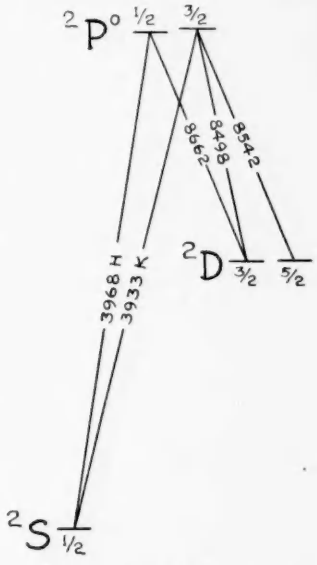

FIG. 2.—Partial Grotrian diagram of *Ca* II.

Attention was called several years ago to the high intensity of the *neutral oxygen triplet*, λλ 7771.95, 7774.18, 7775.39, in the spectrum of α Cygni, cA2, and to its presence in α Canis Majoris, Ao, and α Lyrae, Ao.[23] On a plate of α Aquilae, A5, taken in 1931, the lines are

[23] *Publications of the Astronomical Society of the Pacific*, **37**, 272, 1925.

visible but have only a fraction of their intensity in α Cygni. On the higher-dispersion photographs more recently obtained, these lines are well marked in the spectrum of α Lyrae, while in α Cygni they are of outstanding intensity. The two components of longer wave-length are not quite resolved. Under favorable conditions, however, the spectrograph is probably capable of showing them as separate lines. The component of shortest wave-length, λ 7771.95, is, of course, well separated from the others. The strong oxygen line λ 8446.46[24] has been photographed in a somewhat larger number of stars. The interval of spectral type throughout which it has considerable intensity is about Ao–Go, but it appears to be very sensitive to absolute magnitude. For example, the line is not seen in α Leonis, B8n, but in β Orionis, cB8, is outstanding, being considerably more intense than in the Ao stars α Canis Majoris and α Lyrae. Similarly, it is stronger in γ Cygni, cF8, than in the sun, dGo. It is considerably more intense in α Cygni than in any other object photographed.

In A-type spectra its appearance is strikingly different from that of the broad Paschen lines in that it is narrow, with well-defined edges and without wings. To explain the breadth of the hydrogen lines, one must therefore look not to stellar rotation but to some atomic cause such as Stark effect.

The presence of the infra-red oxygen lines in emission in the spectra of γ Cassiopeiae and P Cygni strengthens the correspondence between the atmospheres of Be stars[25] and the solar chromosphere.[26]

Lines accentuated in the infra-red spectrum of α Cygni, possibly in consequence of the star's high absolute magnitude, are those of *H*, *O* I, *N* I, and *Mg* II (Table II). These lines should prove valuable in the problems of high-luminosity stars of types B–G.

The probable correspondence of important lines in the infra-red spectra of certain stars, particularly those of class F, with measured but unidentified lines in the solar spectrum, emphasizes the need for more complete laboratory and solar data in this region.

The region from λ 8320 to λ 8840 in spectra of classes K and M is dominated by the lines of three elements, calcium, titanium, and

[24] A blend of two components, λ 8446.35 and λ 8446.73.

[25] P. W. Merrill, *Lick Observatory Bulletins*, **7**, 97, 1912.

[26] H. W. Babcock, *Publications of the Astronomical Society of the Pacific*, **44**, 323, 1932.

iron. Calcium is represented by the triplet of ionized lines, titanium and iron by numerous lines of the neutral atom. The only notable line not due to one of these three elements is λ 8806.78 of neutral magnesium.

Plate G 60 of R Leonis records a considerable portion of the region of the $^3P - {}^3S$ system of titanium oxide bands classified by Andrew Christy.[27] The following band heads seem to be present:

0–0	3–1?
0–1	3–2
1–0	3–4
2–0	4–2
2–1	4–3
2–3	4–5?
	5–4

In the region beyond λ 8000 several new bands, all of which degrade toward longer wave-lengths, have been observed in the spectra

TABLE VIII

MEASUREMENTS OF BAND HEADS IN SPECTRA OF CLASS M; MEAN WAVE-LENGTHS AND INDIVIDUAL PLATES *minus* MEANS

MEAN I.A.	R HYDRAE				α HERCULIS		R LYRAE
	G 777	G 748	G 774	G 753	G 580	G 756	G 795
(8433)							
8441.42*	+0.2	+0.2	−0.2	−0.3	0.0	+0.1	+0.1
8451.26†	+0.1	.0	− .1	.....	+ .2	− .3	− .2
8504.1	+0.5	− .1	+ .7	− .4	− .2	.....	.....
8514.2	+1.2	+ .3	+ .4	.....	− .7	.....	− .9
8558.2	+0.2	− .1	− .1	.....	.....	.....	.....
8568.7	+0.4	− .1	+ .7	− .9	.....	.....	.....
8580.1	+0.1	− .4	− .2	.....	.....	.....	+ .9
8623.9	+0.2	− .2	+ .1	− .3	.....	.....	.....
8858.78*	−0.1	.0	0.0	− .3	+ .2	0.0	− .1
8868.3†	+0.8	−0.1	.....	+0.3	−0.2	.....	−0.7
(8937)							

* Outstanding. † Strong.

of R Hydrae, α Herculis, and R Lyrae. Measurements of their heads are in Table VIII. The head measured at λ 8858.78 is probably due to titanium oxide, since Mr. A. S. King informs me that a correspond-

[27] *Astrophysical Journal*, **70**, 1, 1929.

ing feature appears near this wave-length on his photographs of the titanium spectrum. The heads near λ 8440 also may be due to titanium oxide since numerous weak lines, probably of molecular origin, occur in this region on the laboratory plates. Band heads are not clearly distinguished, however, on the laboratory photographs now available.

The characteristic bands in N-type spectra have, for many years, been ascribed to carbon or cyanogen. Additional identifications in the extreme red and infra-red have been brought out by recent photographs at Mount Wilson. A spectrogram of Y Canum Venaticorum taken in 1928[28] showed the cyanogen band heads at λλ 6910, 6926, 6943[29] and possibly those at λ 7259 and λ 7435;[30] and observations of Y Canum Venaticorum and U Hydrae in 1933 revealed the heads at λλ 7850, 7873, 7894 (Pl. III).[29]

In view of these facts, it seemed desirable to ascertain whether details of the complex stellar spectra, almost wholly unidentified except for the band heads, correspond to those of groups of individual band lines. For this purpose Mr. King very kindly offered his photographs of the furnace spectra of carbon, dispersion 3.7 A/mm, from which Mr. Ellerman prepared positive copies with the scale reduced to that of the stellar photographs, 66 A/mm for the region λλ 6800–7650, 33 A/mm for longer wave-lengths. A direct comparison was then made of the stellar negatives and the laboratory positives by viewing them side by side in the comparator with the following results:

Y Canum Venaticorum.—G 159 (*Contr.* No. 432, Pl. X). The band heads λλ 6910, 6926, 6943 and the alternating maxima and minima from λ 7020 to λ 7080 clearly correspond to features in the furnace spectrum. Narrow maxima at λ 6973 and λ 6990 and some of the structure from λ 7160 to λ 7200 may coincide, but the agreement is better from λ 7210 to λ 7330, especially from λ 7210 to λ 7260. Beyond λ 7330 the laboratory spectrum is unsuitable.

G 745. The correspondence is fair from λ 8200 to λ 8300, good

[28] *Mt. Wilson Contr.*, No. 432; *Astrophysical Journal*, **74**, 188, 1931.

[29] A. S. King, *Publications of the Astronomical Society of the Pacific*, **38**, 173, 1926.

[30] A. Fowler and H. Shaw, *Proceedings of the Royal Society of London*, A, **86**, 118, 1912.

from λ 8300 to λ 8400, and even better from there to λ 8780, the end of the laboratory spectrogram.

U Hydrae.—G 764. The band heads λλ 7850, 7873, 7894 clearly correspond, as do some of the details between them and λ 7970, but considerable additional absorption appears to be present in the stellar spectrum. The correspondence is somewhat closer from λ 7970 to λ 8260, and is even better from there to λ 8480, beyond which the stellar spectrum is underexposed.

In order to see the individual lines in the furnace spectra while making the comparison with the stellar plates, both spectra were enlarged on paper prints to a scale of 0.9 A/mm, the laboratory spectra appearing as positives, the stellar as negatives. When the same wave-lengths are brought together (Pl. III), it is seen that, with very few exceptions, well-marked groups of furnace lines correspond to absorption spaces in the stellar spectra. Moreover, nearly all narrow maxima in the stellar spectra (many of which look like emission lines) fall at places free from furnace lines. At certain points stellar absorption apparently not connected with any features in the furnace spectrum may be detected, but these places are scarcely as numerous or as prominent as might be expected. Instances of different relative intensities of features in stellar and laboratory spectra may, when analyzed, yield valuable information.

Broad flat minima, each embracing many narrow details, occur near λλ 7940, 8130, and 8300 (not so well marked). The first is undoubtedly connected with the cyanogen bands having heads at λλ 7850, 7873, 7894. A possible connection between the other minima and cyanogen absorption is supported by the following facts: Narrow spaces near λλ 8041, 8065, 8086, 8269 are weaker in Y Canum Venaticorum than in U Hydrae,[31] indicating additional absorption in the first star. The general appearance of the spectrum near these points and the relative behavior in the two stars is somewhat like that near the cyanogen band heads λλ 7850, 7873. On the assumption that band heads degraded toward longer wave-lengths lie near the spaces mentioned, their approximate positions are λλ 8043, 8066,

[31] See. p. 16.

8090, 8270, which may correspond to cyanogen band heads (see Pl. III).[32]

The comparisons offer convincing evidence that a very large part of the extraordinary structure in N-type spectra between λ 6910 and λ 8780 is to be attributed to absorption by carbon or cyanogen molecules.[33] Many, and perhaps all, of the apparently bright lines in this region are only bits of continuous spectrum emerging through narrow interstices in the complex network of absorption lines. If this explanation is true also of the regions of shorter wave-length, the difficulty experienced by previous observers in making chemical identifications of the narrow maxima as emission lines is understandable.

Effective wave-lengths of numerous well-defined features, both maxima and minima, in N-type spectra can be determined from King's photographs and used to obtain a desirable check on possible systematic errors in the stellar radial velocities.

It is the intention of Mr. Sanford, Mr. King, and the writer to compare in detail all observable portions of N-type spectra with the laboratory spectra of carbon and cyanogen.

CARNEGIE INSTITUTION OF WASHINGTON
MOUNT WILSON OBSERVATORY
August 1933

[32] Also R. K. Asundi and J. W. Ryde, *Nature*, **124**, 57, 1929.

[33] It seems to be generally agreed that the band heads λλ 6910, 6926, 6943, 7850, 7873, 7894 are due to cyanogen; and it seems probable that the numerous band lines in King's furnace spectra in the region under discussion are due to the same molecule.

SYSTEMATIC CORRECTIONS TO PHOTOGRAPHIC MAGNITUDES OF POLAR STARS[1]

By FREDERICK H. SEARES AND MARY C. JOYNER

ABSTRACT

Provisional systematic corrections for the reduction of six catalogues of photographic magnitude to the international system—*Greenwich* I, *Simeis*, *Harvard-Payne*, *Leiden-De Sitter*, *Göttingen Aktinometrie*, and *Yerkes Actinometry*—have been tested with the aid of a working list of magnitudes for 373 stars (WPg) based on these corrections.

WPg was compared with (*a*) *Harvard Catalogue of Photographic Magnitudes of Bright Stars North of* $+57^{\circ}.5$ (HPP) (Tables I, II), and (*b*) magnitudes from four plates of the polar region taken by F. E. Ross (RPg) (Tables III–V). Further, the RPg magnitudes of 21 NPS stars were compared directly with the international standards for these stars (Table VI).

These comparisons indicate a zero-point correction of 0.01 mag. in WPg, and hence in the systematic corrections underlying WPg; and also a change in certain extrapolated corrections to Greenwich and Simeis for stars fainter than magnitude 9.5. Otherwise the scale and color system remain unchanged. With these minor revisions included, the corrections for the six catalogues are as in Table VII. The consistency of the results is illustrated by Table VIII.

The corrections for Greenwich and Yerkes were independently determined with the aid of HPP, the results (Tables IX–XIV) confirming those of Table VII.

Mount Wilson Contribution No. 472[2] gives in Table I systematic corrections for the reduction of three catalogues of visual and photovisual magnitudes to the international system of scale and color—*Yerkes Actinometry* (YPv), Potsdam *Durchmusterung* (PD), and Potsdam *Catalogue of Polar Stars* (PDP). With the aid of the *Greenwich Effective Wave-Lengths*, the discussion also provides an indirect test of the systematic corrections to six catalogues of photographic magnitude—*Greenwich* (Gr I),[3] *Simeis* (S),[4] *Harvard-Payne* (HP),[5] *Leiden-De Sitter* (L),[6] *Göttingen Aktinometrie*, Polar Stars (GAP), and *Yerkes Actinometry* (YPg). With minor differences, the photographic corrections are those given in *Transactions of the International Astronomical Union*, **4**, 148, Table IV, 1932.

Direct tests of these corrections can now be made with the aid of

[1] *Contributions from the Mount Wilson Observatory, Carnegie Institution of Washington*, No. 489.

[2] *Astrophysical Journal*, **78**, 141, 1933.

[3] Dec. $+75^{\circ}$ to $+90^{\circ}$, 1913.

[4] *Bulletin, Poulkovo*, No. 72, 1915.

[5] *Harvard Bulletin*, No. 881, 1931.

[6] *Bulletin Astronomical Institutes of the Netherlands*, **6**, 65 (No. 210), 1930.

(*a*) *Harvard Catalogue of Photographic Magnitudes of Bright Stars North of* $+57°.5$ (HPP),[7] recently issued in typescript form by Miss Payne and Dr. Shapley, and (*b*) results from four photographs of the polar region (RPg) taken by Dr. F. E. Ross at the Yerkes Observatory with the 3-inch camera lens of his own design. Both (*a*) and (*b*), the latter being part of the material collected for an extension of the Polar Sequence,[8] are on the international system. The magnitudes from these sources were compared with a working list of mean magnitudes of 373 stars (WPg), based on the six catalogues after

TABLE I

COMPARISON OF HPP AND WPG

(Unit, 0.01 in magnitude differences and in color coefficients)

Pg	HPP − WPg*	Av. Diff.†	No. Stars
4.50	+3	±12	2
5.25	−2.6 −(6.5)	4.8	5
5.75	+0.7 (6.0)	6.1	10
6.25	−0.1 5.6	2.7	20
6.75	−1.9 5.0	2.0	34
7.25	−2.5 4.6	2.4	52
7.75	−0.9 4.0	3.3	55
8.25	−0.2 − 3.5	± 4.8	32
All	−1.2 − 5.0	.....	210

* The first number in each entry is the combined scale and zero-point difference; the second, the color coefficient. Thus for $Pg = 5.25$, in magnitudes, HPP − WPg = −0.026 − 0.065*C*, where *C* is the color index on the international system. Values of the color coefficient in parentheses are extrapolations.

† Corrected for zero-point difference of 0.01 mag.

reduction to the international system by applying the corrections now to be tested.

a) Two hundred and thirteen stars are common to HPP and WPg, of which 3 were rejected because of exceptional discordances. The mean scale differences and color coefficients for the stars in half-magnitude intervals are given in the second column of Table I. With allowance for 0.01 mag. in the zero point, the maximum scale difference below $Pg = 5.0$ is less than 0.02 mag. The significance of the color coefficient, about 0.05 in the mean, is discussed later; the change in the coefficient with magnitude, although small, is probably real.

The means of the differences for individual stars, corrected for

[7] Cf. *Harvard Bulletin*, No. 892, 1933.

[8] Cf. *Mt. Wilson Contr.*, No. 472; *Astrophysical Journal*, **78**, 141, 1933.

zero point and taken without regard to sign, are in the third column of Table I. Grouped according to the number of catalogues included in WPg, the means are as shown in Table II. In the favorable region of the scale (Table I), or for those stars whose WPg magnitudes are based on five or six catalogues (Table II), the average difference is only 0.02–0.03 mag.

The magnitudes compared are not, however, wholly independent, for data from HP, Gr1, YPg, and L enter into both HPP and WPg. The systematic reductions of these catalogues to the international system are, nevertheless, more or less independent, and each mean HPP magnitude also includes eight modern values derived from four

TABLE II

MEAN DIFFERENCE OF MAGNITUDES IN HPP AND WPG

(Corrected for zero-point difference; unit = 0.01 mag.)

No. Catalogues in WPg	Mean Diff.	Systematic Diff.	No. Stars
2	±7	−3	4
3	5.4	−1.9	28
4	4.0	+0.4	42
5	2.4	+1.4	17
6	±2.7	+0.5	119
Total			210

Harvard polar-comparison photographs connecting the individual stars with the Polar Sequence standards. WPg, on the other hand, includes magnitudes from S and GAP, which were not used in the preparation of HPP.

b) To eliminate any asymmetry in the distance correction, the four plates by Ross, all centered on BD+87°143, were taken in pairs, one plate with telescope east, one with telescope west.[9] Reduction-curves were derived from the NPS stars listed in Table III for each plate, but the mean magnitudes from the two plates of each pair have been used for the discussion. Corrections for the color of the stars and distance from the axis were determined and applied as usual. The differences between mean RPg and NPS magnitudes for the polar stars, Table III, third column, indicate close agreement of RPg with the international system in color, scale, and zero point.

[9] Pair I, pls. 1089, 1094; Pair II, pls. 1098, 1101.

Comparison of RPg with WPg should therefore show the relation of WPg to the international system. The means of RPg−WPg for 169 stars (1 rejected), grouped according to magnitude, are given in Table IV.

TABLE III

MEAN RPG MAGNITUDES OF NPS STARS COMPARED WITH INTERNATIONAL VALUES

(Unit=0.01 mag.)

NPS	RPg	IPg−RPg	Mean	NPS	RPg	IPg−RPg	Mean
5	6.54	−8		11	9.72	+5	
2S	6.45	+2	−0.2	12	10.06	+2	+0.5
3S	6.60	+4		5R	10.18	−2	
1R	6.68	+1		4S	10.34	−3	
6	7.16	−4		13	10.53	−1	
7	7.36	+2	+0.6	6R	10.48	+5	+0.5
2R	7.89	+4		14	10.94	−2	
8	8.33	−1		7R	10.96	0	
9	8.96	−3		15	11.24	+3	
3R	8.96	0	+0.6	6S	11.34	+2	+0.2
10	9.07	+4		8R	11.50	−6	
4R	9.21	+3		16	11.56	+2	
Mean						±2.9	+0.4

TABLE IV

SCALE DIFFERENCE FOR RPG AND WPG*

(Unit=0.01 mag.)

WPg	RPg−WPg	Av. Diff.	Av. Diff. Pr. I−Pr. II	No. Stars
< 6.0	+ 2		±1.6	3
6.50	− 3.2	±5.2	6.0	6
7.25	+ 0.3	5.5	5.3	10
7.75	− 2.3	4.5	4.8	12
8.25	+ 2.8	5.5	4.3	14
8.75	+ 1.4	5.2	4.0	21
9.25	− 1.3	5.2	4.6	27
9.75	+10.6	7.4	6.0	39
10.25	+14.2	±7.1	6.1	33
10.75	+32		±7.5	4
Total	+ 0.1†			169

* *Note added to proofs.*—Results from six additional plates (Nos. 1144, 1155, 1158, 1160, 1190, 1191) taken by Ross at Mount Wilson with the 5-inch Ross camera confirm, with minor exceptions, the correction to the scale of WPg given in this table. The revised zero-point correction is now −0.01 mag., in agreement with the value adopted on p. 209. The systematic corrections in Table VII are slightly affected below the eighth magnitude and have been modified (0.01–0.03 mag.) to include all the data now available.

† Zero-point difference from 90 stars between 6.0 and 9.5.

The corrections to the six catalogues used for WPg were originally determined to magnitude 8.0;[10] later they were slightly revised and extended another magnitude. From about 9.0 on, the corrections for Gr 1 and S, the only catalogues extending into this region of the scale, were smoothly extrapolated in a manner which would bring their magnitudes into systematic agreement and thus provide approximate mean values for the fainter stars in the working list. The last three differences in the second column of Table IV indicate the changes required by the extrapolated corrections for Gr 1 and S in order that the corrected magnitudes may be on the international system.

TABLE V*

DIFFERENCES GROUPED ACCORDING TO COLOR INDEX

(Unit = 0.01 mag.)

C	RPg − WPg	No. Stars
−0.07	+0.8	15
+0.10	+1.3	52
0.30	−2.4	42
0.64	+1.3	18
0.98	+0.5	23
1.50	−1.7	12
Total		162

* First and last groups of Table IV omitted.

Grouped according to color index, with allowance for the difference in scale, the magnitude differences included in Table IV (magnitudes 6.0–10.5) give the results shown in Table V.

The inferences to be drawn from comparisons (*a*) and (*b*) are: (1) The zero-point error of WPg does not exceed 0.01 mag. (2) From magnitude 4.5 to 9.5 the scale of WPg agrees with that of NPS; below 9.5 the original corrections for Gr 1 and S must be increased (Tables I and IV). (3) The color equation of WPg relative to NPS is sensibly zero (Table V); relative to HPP, it is about −0.05 C (Table I).

The difference in color coefficients noted in (3) is probably as it

[10] *Transactions I.A.U.*, **4**, 148, Table IV, 1932.

should be. The number of NPS stars brighter than the limiting magnitude of HPP (about 8.5) is insufficient to establish with exactness the color system of a series of magnitudes determined by polar comparisons. To meet this difficulty Shapley and Miss Payne[11] seem to have based the color relations of the HPP on the provisional systematic corrections in *Transactions I.A.U.*, **4**, 148, Table IV, 1932. In deriving these corrections we also met the difficulty arising from the small number of bright NPS stars, and in the attempt to refer the corrections to the international color system we were obliged to use an indirect method which assumed the color system of the main catalogue of the PDP to be the same as that of appended zones of NPS stars. It is now clear, however, that these systems are not exactly the same and that the color coefficients in the previously adopted corrections should be increased by 0.05 throughout.[12] The coefficients used in deriving the WPg magnitudes include this change in color system, and apparently HPP should receive a similar correction, a conclusion consistent with the results of comparison (*a*).

As noted in *Contribution* No. 472, a change in color coefficient requires a compensating change in zero point (unless the zero point has been based on blue stars alone), the estimated amount in this case being −0.02 mag.; but since the systematic corrections were inherently uncertain by about 0.01 mag., no zero-point change was made when the WPg magnitudes were determined. Comparisons (*a*) and (*b*) now give −0.01 and 0.00, respectively, for this correction.

Additional evidence is afforded by the WPg magnitudes of the NPS stars listed in Table VI. The deviations from the IPg values, third column, show an excess of negative signs to about 9.2, where a divergence corresponding to that shown in Table IV makes its appearance. The eleven bright NPS stars whose mean WPg magnitudes depend on four to six catalogues indicate a correction of −0.015 mag., part of which, however, is attributable to the fact that the S magnitudes of the NPS stars are not representative of that catalogue as a whole. Since the zero value of the correction found by

[11] Cf. Introduction to the typescript catalogue.

[12] Cf. *Mt. Wilson Contr.*, Nos. 431, 472; *Astrophysical Journal*, **74**, 131, 1931; **78**, 141, 1933.

comparison (*b*) may be slightly affected by residual distance error, −0.01 mag. is provisionally adopted as the correction to the zero point of the WPg magnitudes.

Application of this correction and allowance for the revision of the systematic corrections to Gr 1 and S below 9.5 give finally for the NPS stars the residuals shown in the fourth column of Table VI.

TABLE VI

SCALE AND ZERO-POINT CORRECTIONS FOR WPG DERIVED FROM NPS STARS

(Unit = 0.01 mag.)

NPS	WPg	IPg − WPg	Corrected Diff.	No. Cat.	NPS	WPg	IPg − WPg	Corrected Diff.	No. Cat.
1	4.40	0	+1	4	8	8.34	− 2	− 1	2
2	5.20	+4	+5	6	9	8.95	− 2	− 1	2
3	5.75	+3	+4	5	3r	8.78	+18	+19	2
4	5.95	−4	−3	6	10	9.16	− 5	− 4	2
5	6.49	−3	−2	5	4r	9.19	− 1	0	2
2s	6.54	−7	−6	6	11	9.70	+ 7	− 1	2
3s	6.67	−3	−2	6	12	9.94	+14	+ 2	2
1r	6.66	+3	+4	6	5r	10.16	0	−12	2
6	7.19	−7	−6	5	4s	10.14	+17	+ 3	2
7	7.38	0	+1	5	6r	10.35	+18	+ 2	1
2r	7.95	−2	−1	4					
Zero point		−1.5*			Zero point			−0.2†	

* Zero-point correction derived from 11 NPS stars.

† Zero-point difference from 21 NPS stars after correction for zero point (−0.01 mag.) and for scale below 9.5.

The clustered signs for the bright stars arise mostly from Gr 1, for which, like S, the bright NPS stars are not representative of the other stars in the catalogue.[13]

With allowance for these minor changes, the systematic reductions to the international system for the six catalogues now have the values shown in Table VII. The consistency of these corrections is indicated by Table VIII, which shows for each catalogue the systematic deviations from the corrected WPg system, in scale above, and in zero point and color below.

[13] *Cf. Transactions I.A.U.*, **4**, 149, 1932. The lack of comparability appears again in the discussion on a later page.

Additional observations similar to those used in comparison (*b*) will diminish the accidental errors, but the systematic relations should remain substantially as they are. It must be noted, however, that the corrections in Table VII are established only for the stars actually used in the comparisons. The homogeneity of the various catalogues is therefore a pertinent question. For Gr the matter has

TABLE VII*

SYSTEMATIC CORRECTIONS FOR REDUCTION OF SIX CATALOGUES OF PHOTOGRAPHIC MAGNITUDE TO INTERNATIONAL SYSTEM

Pg	IPg−Gr I	IPg−S	IPg−HP	IPg−L	IPg−GAP	IPg−YPg
5.0	−13 +7	+ 5 −65	0 +5	0 +5	+8 −14	+14 −4
5.5	− 9 +6	+ 5 −48	0 5	0 6	8 −14	10 4
6.0	0 +6	+ 6 −33	+1 5	0 7	7 −13	6 4
6.5	+ 8 +5	+ 5 −20	+1 5	+ 1 7	7 −11	4 3
7.0	+16 +3	+ 2 − 7	+1 5	4 7	7 − 7	1 3
7.5	+20 0	− 1 + 3	−1 5	6 7	6 − 1	0 4
8.0	+23 −2	− 4 + 5	−4 +5	+10 +8	+5 + 8	1 5
8.5	+25 −5	− 2 + 5	.....	.....	.....	8 6
9.0	+29 −5	+ 1 + 5	.....	.....	.....	+22 −7
9.5	+40 −5	+ 6 + 5	.....	.....	.....	.....
10.0	+47 −5	+12 + 5	.....	.....	.....	.....
10.5	+53 −5	+16 + 5	.....	.....	.....	.....

* *Pg* in the first column refers in succession to the magnitudes of each catalogue. The first term in each entry is the combined scale and zero-point correction; the second, the color coefficient. In both cases the unit is 0.01. Thus for Gr I = 5.0, the total correction, in magnitudes, is IPg−Gr I = −0.13+0.07*C*, where *C* is the international color index.

been investigated as far as possible by detailed comparisons of Gr I and Gr II[14] with HPP.

Gr I.—The differences in magnitude for 669 stars occurring in both Gr I and HPP (3 were rejected) were grouped according to HPP magnitude and HD spectrum for each four hours of right ascension. Since the A0 stars indicated similar scale corrections for all right-ascension groups, the color coefficients were determined from all data combined.[15] Examination of the differences for all stars, after correction for color, confirmed the constancy of the scale; hence only the mean results for all right ascensions need be given. The differ-

[14] *Photographic Magnitudes, Declinations +65° to 75°*, 1914. Similar in plan and execution to Gr I, although not used for the WPg magnitudes, which, with very few exceptions, are for stars north of +80°.

[15] The color equivalents used for HD spectra are the MW values in Table I, *Transactions I.A.U.*, **4**, 137, 1932.

ences in Table IX are for the argument HPP; values referred to the argument Gr I are in the second column of Table X. In order to compare the results with the adopted systematic corrections for

TABLE VIII

DEVIATIONS FROM THE IPG SYSTEM IN SCALE, ZERO POINT, AND COLOR OF CORRECTED MAGNITUDES FOR SIX CATALOGUES

(Unit = 0.01 mag.)

IPG AND C	IPG − CATALOGUE											
	Gr I		S		HP		L		GAP		YPg	
4.4	+9	2*	.....		.....		+2	1	−2	1	−8	2
5.5	−0.1	17	−0.8	16	+0.6	14	+0.2	15	−0.8	13	+0.6	17
6.25	−0.2	18	+0.9	18	−2.5	17	+0.6	18	+1.0	18	0.0	18
6.62	−0.8	18	−3.2	18	+2.4	17	−0.3	17	+2.3	15	0.0	17
6.88	+2.1	18	−0.8	18	+0.1	17	+0.6	17	−2.9	15	−0.2	18
7.12	+1.4	19	+2.2	19	+0.7	16	+0.1	18	−3.6	17	−1.4	18
7.38	0.0	30	+0.1	30	+0.3	29	−1.4	30	+1.2	22	+0.1	27
7.62	+0.2	37	−0.8	36	−0.6	34	−0.1	34	0.0	22	+2.2	28
7.88	+3.4	23	+0.4	23	−3.9	11	0.0	11	−3.2	13	−0.1	18
8.12	−0.6	22	−1.0	22	.....		.....		+4.7	11	−0.9	21
8.38	−2.7	18	+2.2	18	.....		.....		.....		+0.7	12
8.62	−1.8	19	−1.1	18	.....		.....		.....		+4.1	13
8.88	+0.1	17	+1.2	17	.....		.....		.....		−4.0	4
9.24	−0.8	26	+0.2	26	.....		.....		.....		.....	
9.75	+0.6	27	−0.5	27	.....		.....		.....		.....	
10.15	+0.4	7	−0.2	7	.....		.....		.....		.....	
Totals...		318		313		155		161		147		213
−0.07	+1.3†	50	−1.6	47	+1.0	32	−0.2	35	0.0	25	−0.6	34
+0.11	−0.7	43	+1.4	43	+0.6	40	+0.1	42	−0.2	32	−1.4	37
0.30	+0.9	62	−0.7	61	−1.4	40	−1.2	40	−0.5	35	+2.3	47
0.78	−0.3	37	−1.2	36	−2.7	15	+1.0	15	+1.3	22	+1.4	33
1.12	+1.1	46	+1.4	46	+0.3	23	+0.4	23	−3.0	23	−1.0	42
1.51	−3.8	20	+1.0	20	−0.4	5	+0.2	6	+3.8	10	+0.8	20
Zero point	+0.2	258	−0.1	253	−0.2	155	−0.2	161	−0.2	147	+0.3	213

* Number of stars in the mean magnitude difference at the left on the same line.

† The differences grouped according to color index (C in the first column) and the zero point depend on stars brighter than magnitude 9.0.

Gr I (Table VII), these differences must be referred to the IPg system by applying the correction

$$\text{IPg} - \text{HPP} = -(\text{HPP} - \text{WPg}) - 0.01 ,$$

in which the values of the parenthesis may be taken from Table I The values of the total correction for the argument Gr I are in the

third column of Table X. Applied to the differences in the preceding column, they give the reduction of Gr I to the IPg system shown in the fourth column of the table. These results from 666 stars common to Gr I and HPP and the 210 stars in both HPP and WPg agree closely (last column, Table X) with the adopted corrections for Gr I in Table VII. Incidentally, this agreement also confirms the variable color coefficient of HPP relative to WPg (Table I).

TABLE IX

SCALE DIFFERENCE FOR GR I AND HPP

HPP	No. Stars	Gr I − HPP*	HPP	No. Stars	Gr I − HPP
4.35	3	+10	7.75	176	−20.3 +4
5.25	11	+14.3	8.25	224	21.0 5
5.75	20	+ 3.0 0	8.6	28	−24.1 +8
6.25	37	− 5.6			
6.75	70	− 9.8 +1	Total	666	
7.25	97	−16.8 +2			

* See first note to Table I.

TABLE X

SYSTEMATIC CORRECTIONS FOR GR I OBTAINED FROM TABLE IX AND COMPARED WITH THOSE IN TABLE VII

Gr I	HPP − Gr I	IPg − HPP	IPg − Gr I	Table VII − Table X
4.5	−14 0			
5.0	−12 0	−1 +7	−13 +7	0 0
5.5	−10 0	+1 6	− 9 6	0 0
6.0	+ 1 0	−1 6	0 6	0 0
6.5	+ 9 −1	0 5	+ 9 4	−1 +1
7.0	+15 2	+1 5	+16 +3	0 0
7.5	+20 4	0 4	+20 0	0 0
8.0	+22 5	−1 3^5	+21 -1^5	+2 -0^5
8.5	+24 −8	−1 +3	+23 −5	+2 0

Gr II.—Of the 1373 stars common to Gr II and HPP, 41 were rejected, mostly because the HPP magnitude is marked as uncertain. The magnitude differences were grouped as for Gr I, except that 2^h intervals in right ascension were used. Owing to a change in scale, the stars in the interval $22^h - 24^h$ were omitted in deriving the color

coefficient. The remaining stars give, for all magnitudes, the constant color correction

$$\text{HPP} - \text{Gr II} = -0.02\,C\ .$$

After correction for color, the differences, for all stars together, give the mean scale correction shown in the last column of Table XI,

TABLE XI

SCALE DIFFERENCE FOR GR II AND HPP

(Unit = 0.01 mag.)

HPP	Gr II − HPP for Group *minus* Mean												Mean Gr II − HPP
	1h	3h	5h	7h	9h	11h	13h	15h	17h	19h	21h	23h	
4.25	− 8	−4	+ 7	+ 6	....	+18	+ 4	+ 9	+ 3	+7	−34	−24	+ 9.0
5.25	−12	....	+13	− 1	+10	....	....	....	+ 9	....	− 8	− 7	+ 3.6
5.75	−18	+3	+ 1	....	0	+23	+ 3	+15	+36	7	+ 8	−10	+ 5.4
6.25	− 8	−3	+ 6	+ 2	0	+18	−17	+10	0	4	+ 1	− 4	− 1.7
6.75	− 6	+4	+ 3	− 2	− 3	0	− 2	− 1	+ 2	5	− 4	+ 1	− 9.3
7.25	− 1	+1	+ 2	− 1	+ 1	+ 1	− 2	− 1	0	3	0	− 1	−14.7
7.75	− 2	−2	− 2	− 1	− 2	− 4	− 8	− 3	− 1	3	+ 2	+ 7	−19.1
8.25	+ 3	−4	− 3	− 4	− 1	− 2	−10	− 6	0	2	+ 7	+11	−20.2
8.75	+16	−2	− 3	− 4	+ 2	+ 1	+ 4	− 4	−10	+7	+ 4	+16	−21.6
9.10	....	....	− 1	−10	+ 8	+ 8	....	....	....	....	....	....	−24.3
	Number of Stars												
4.25	3	3	1	1	....	1	1	2	2	5	1	1	21
5.25	3	....	1	2	2	....	....	....	4	....	2	3	17
5.75	3	1	1	....	2	1	2	1	1	4	3	7	26
6.25	10	6	4	4	9	6	4	4	3	3	8	5	66
6.75	15	6	9	6	6	3	9	3	9	11	11	17	105
7.25	21	14	20	12	16	10	7	11	6	12	23	22	174
7.75	27	38	28	20	11	14	15	24	23	26	27	47	300
8.25	30	47	41	31	29	23	39	25	40	47	40	49	441
8.75	7	12	21	20	32	27	10	13	11	8	2	6	169
9.10	....	....	4	4	2	3	....	....	....	....	....	....	13
Total	119	127	130	100	109	88	87	83	99	116	117	157	1332

while the preceding columns indicate the deviations of the corrections for the individual right-ascension groups from the mean in the last column, all referred to the argument HPP. The number of stars included in each scale difference appears in the lower half of the table. The color coefficient is that just found, or with regard to the order of subtraction, +0.02, which applies to the whole table.

On the assumption that the scale and color relations for HPP are the same in declinations $+65^\circ$ to $+75^\circ$ as from $+75^\circ$ to the pole, the reduction of Gr II to the international system, for argument Gr II, is that shown in Table XII. The color coefficients included with the mean scale correction in the last column apply to all right ascensions. The greatest uniformity of scale occurs near magnitude 7.0. For both brighter and fainter stars the systematic variation with the right ascension is more pronounced.

TABLE XII

SYSTEMATIC CORRECTIONS FOR GR II OBTAINED FROM TABLE XI

(Unit = 0.01 mag.)

GR II	IPG − GR II												MEAN IPG − GR II	
	1^h	3^h	5^h	7^h	9^h	11^h	13^h	15^h	17^h	19^h	21^h	23^h		
5.0	+ 7	− 5	−16	−10	....	....	....	....	−13	−15	....	+ 5	− 7	+5*
5.5	12	− 5	−15	− 4	−12	....	....	....	−13	−13	− 8	5	− 6	4
6.0	11	− 2	− 5	− 1	− 2	....	+10	....	−11	− 9	− 2	6	− 2	4
6.5	14	+ 5	+ 1	+ 7	+ 8	− 7	12	+ 1	+ 1	+ 1	+10	8	+ 6	3
7.0	16	+12	+11	+15	+14	+12	15	15	+14	+10	+15	13	+13	3
7.5	21	+20	+20	+20	+20	+22	27	21	+19	+15	+16	12	+19	2
8.0	17	+24	+23	+24	+20	+21	30	26	+20	+18	+14	10	+20	1[5]
8.5	+ 9	+24	+25	+26	+20	+20	+20	+26	+27	+15	+14	+ 6	+22	+1

* The color coefficients (unit = 0.01) apply to all right ascensions.

Table XIII summarizes the relations of various corrections to the Gr scale. The Polar Sequence standards of *Harvard Circular* No. 170 were used as the basis for both Gr I and Gr II; the corrections to these standards, which have been adopted by Miss Payne as the proper reduction for the two catalogues, are in the second column. Both the adopted systematic correction for Gr I in Table VII (fourth column, Table XIII) and that found in the preceding comparison with HPP (third column) diverge systematically from the corrections that reduce HC 170 to the international system. The Gr I magnitudes of the NPS (fifth column), on the other hand, are at least approximately on the scale of HC 170. Gr II (sixth column) occupies an intermediate position. These results are instructive as an illustration of the ease with which systematic errors may enter into so simple an operation as a polar comparison. Apparently such errors

are not unusual, the cause presumably being some lack of comparability in the images of the polar standards and of the stars whose magnitudes are to be determined.

One other matter bearing on the corrections in Table VII requires comment. *Harvard Bulletin*, No. 892, p. 4, states: "Parkhurst's catalogue [YPg] . . . . was directly compared with the Harvard catalogue [HPP]. The scales and zero points of the systems are sensibly coincident, ..."

TABLE XIII

SUMMARY FOR SCALE CORRECTIONS TO GR I AND GR II

(Unit = 0.01 mag.)

Gr	IPg − HC 170 (HB 892)	IPg − Gr I			IPg − Gr II Mean 1332 Stars	Gr I − Gr II
		HPP 666 Stars	MW 318 Stars	NPS 15 Stars		
5.0	− 3	−13	−13	− 3	− 7	+6
5.5	+ 1	− 9	− 9	0	− 6	+3
6.0	+ 4	0	0	+ 4	− 2	−2
6.5	+ 9	+ 9	+ 8	+ 7	+ 6	−3
7.0	+13	+16	+16	+11	+13	−3
7.5	+16	+20	+20	+14	+19	−1
8.0	+20	+21	+22	+18	+20	−1
8.5	+23	+23	+23	+21	+22	−1

The results in Table I and in the last column of Table VII (in which IPg is really WPg −0.01) are inconsistent with this conclusion.

The matter was examined at first hand by forming the differences HPP − YPg for stars in the WPg list and for about one hundred additional stars in declinations +73° to +80° having magnitudes < 6.0 or > 8.0, a selection which utilizes practically all the data relating to those parts of the scale for which there are discordances. The corrections used for difference in color system were in the main those of HB 892, Table III, diminished by 0.05 mag. throughout in order to reduce the correction for Ao stars to zero. The corrected mean scale differences are in the second column of Table XIV. Since HPP agrees with the international scale, these differences may be compared directly with the adopted systematic corrections for YPg given

in Table VII. The residual differences in the fourth column of Table XIV may be regarded as a satisfactory confirmation of the corrections in Table VII.

TABLE XIV

SCALE DIFFERENCE FOR HPP AND YPG

(Unit=0.01 mag.)

YPg	HPP −YPg	No. Stars	Diff. in Corrs.*	YPg	HPP −YPg	No. Stars	Diff. in Corrs.
4.34.....	+28	5	(−7)	8.10.....	+2	45	0
5.25.....	+13	19	−1	8.30.....	4	34	0
5.75.....	+ 7	21	+1	8.50.....	8	23	0
6.25.....	+ 5	20	0	8.70.....	+9	3	+4
6.75.....	0	31	+2				
7.25.....	− 1	45	+2	Total...	.....	292	.....
7.75.....	+ 1	46	0				

* (IPg−YPg) from Table VII *minus* (HPP−YPg) from the second column of this table.

CARNEGIE INSTITUTION OF WASHINGTON
MOUNT WILSON OBSERVATORY
October 1933

THE ABSOLUTE INTENSITY OF THE NEBULAR LINES[1]

By E. U. CONDON

ABSTRACT

The quantum mechanical theory of the transition probability for transitions due to magnetic dipole and electric quadrupole radiation in atomic spectra is briefly developed and applied to the calculation of transition probabilities in p^2, p^3, p^4 configurations. It is found that the nebular lines N_1 and N_2 are essentially due to magnetic dipole radiation, the quadrupole being but 0.1 per cent as intense. Numerical values of the transition probability for all possible combinations in the $2p^2$ configuration in *C* I, *N* II, and *O* III are given, also for $2p^4$ in *O* I and $2p^3$ in *O* II and for the transauroral pair in $2p3p^3$ *S* II.

Thanks to the discovery of Bowen,[2] we know that many lines of astrophysical interest[3] are due to transitions between levels belonging to the normal configuration of various atoms (and ions). The atoms involved have p^2, p^3, and p^4 for their normal configuration. Such transitions are forbidden in the approximation which considers only the electric dipole radiation. It is necessary, therefore, to consider the next higher approximation for the interaction between matter and the radiation field to account for them. This second approximation brings in two types of radiation, measured respectively by the magnetic dipole and the electric quadrupole moments of the atom.

Although the theory of quadrupole radiation is quite well worked out,[4] the magnetic dipole radiation has not received much attention. Bartlett[5] has made a calculation of the quadrupole transition proba-

[1] Just as this paper was ready for publication I received a letter from Professor Menzel calling my attention to the paper on this same subject by Professor A. F. Stevenson (*Proceedings of the Royal Society*, A, **137**, 298, 1932) which I had overlooked. His method of calculation is somewhat different in that he treats the second approximation as a unit instead of separating the magnetic dipole and electric quadrupole parts as is done here. Our results, where comparable, are in substantial agreement; the differences perhaps serve to indicate the limitations of the method. This paper goes beyond Stevenson's in that it also treats the p^3 and p^4 configurations.

[2] *Astrophysical Journal*, **67**, 1, 1928.

[3] Boyce, Menzel, and Payne (*Proceedings of the National Academy of Science*, **19**, 581, 1933) have given an excellent up-to-date summary of the data with new cases discovered by them.

[4] See the review by Rubinowicz, *Ergebnisse der exakten Naturwissenschaften*, **11**, 170, 1932.

[5] *Physical Review*, **34**, 1247, 1929.

bilities for the nebular lines of *O* III, but owing to the approximations involved he did not obtain accord with observation. It therefore seemed desirable to go into the whole question carefully. The result (this paper) is that fairly good theoretical values of the absolute transition probabilities have been obtained. These should be useful in discussions of the physical conditions in nebulae and novae which emit the "forbidden" lines. From the physicist's point of view an interesting result is that the magnetic dipole radiation is much more important than the electric quadrupole in many cases.

The plan of the calculation is as follows: in § 1 we develop the formulae giving transition probabilities in terms of matrix components, in § 2 we calculate the transition probabilities in the p^2 configuration, in § 3 we give results of similar calculations for the p^4 configuration, and in § 4 we give the results for the p^3 configuration.

1. TRANSITION PROBABILITIES FOR MAGNETIC DIPOLE AND ELECTRIC QUADRUPOLE RADIATION

First we consider the magnetic dipole field. This is the radiation field produced by an oscillating magnetic dipole (sometimes called a FitzGerald oscillator). It is exactly like that for the electric dipole (Hertz oscillator) where the magnetic moment, $\boldsymbol{M}$, replaces the electric moment, $\boldsymbol{P}$, and $\boldsymbol{E}$ replaces $\boldsymbol{H}$ and $\boldsymbol{H}$ replaces $-\boldsymbol{E}$, where $\boldsymbol{E}$ and $\boldsymbol{H}$ are the electric and magnetic vectors, respectively. The theory goes through exactly as for the electric dipole, so we may write that the Einstein transition probability from state[6] a to state b is

$$A(a, b) = \frac{64\pi^4\sigma^3}{3h} |(a|\boldsymbol{M}|b)|^2 , \tag{1}$$

where σ is the wave number (cm^{-1}) of the line and $(a|\boldsymbol{M}|b)$ is the matrix component of the magnetic moment connecting the two states in question.

From the close analogy between electric dipole and magnetic dipole radiation it follows that much of the ordinary radiation theory is applicable to the latter. Thus the selection rules $\Delta J = 0, \pm 1$ (except $0 \to 0$) and $\Delta M = 0, \pm 1$ and the formulae for the relative in-

[6] We use the word "state" to mean one non-degenerate state of the atom such as is produced when the degeneracy is removed by putting the atom in a magnetic field.

tensity of the Zeeman components of a line may be derived by using no other property of $\boldsymbol{P}$ than its law of commutation with the resultant angular momentum, $\boldsymbol{J}$ of the atom.[7] The magnetic moment of an atom is, as in the theory of the anomalous Zeeman effect,

$$\boldsymbol{M} = -\frac{e\hbar}{2\mu c}(\boldsymbol{L}+2\boldsymbol{S}) , \tag{2}$$

where $\boldsymbol{L}$ and $\boldsymbol{S}$ are the resultant orbital and spin angular momenta measured in terms of the Bohr units, $\hbar = h/2\pi$. This is readily seen to obey the same law of commutation with $\boldsymbol{J}$ as does the electric moment $\boldsymbol{P}$, hence the selection rule on J and M and the Zeeman intensity formulae are the same.

As to the numerical magnitude of (1), let us agree to measure σ in terms of the Rydberg constant as unit; then (1) can be written

$$A(a, b) = \frac{\alpha^5\tau^{-1}}{24}\sigma^3 |(a|\boldsymbol{L}+2\boldsymbol{S}|b)|^2 , \tag{3}$$

where α is the fine structure constant ($\sim 1/137$) and τ is the Hartree[8] unit of time, $\tau = \hbar^3/\mu e^4$. We have

$$\frac{\alpha^5\tau^{-1}}{24} = 35{,}300 \text{ sec.}^{-1} , \tag{4}$$

so the absolute value of A is known as soon as we have calculated the matrix component $(a|\boldsymbol{L}+2\boldsymbol{S}|b)$. For a complete line, $A \to B$, the ensemble of all the components $a \to b$ connecting the different states a of A to the states b of B, we have

$$A(A, B) = \frac{\alpha^5\tau^{-1}}{24}\frac{\sigma^3}{2J_A+1}S(A, B) , \tag{5}$$

where $S(A, B)$ is called the strength of the line and is defined by

$$S(A, B) = \sum_{a, b}(a|\boldsymbol{L}+2\boldsymbol{S}|b)^2 \tag{6}$$

for the magnetic dipole case. Note that the strength is symmetric in A and B, so $S(B, A) = S(A, B)$.

[7] Dirac, *Quantum Mechanics*, p. 147.

[8] *Proceedings of the Cambridge Philosophical Society*, **24**, 89, 1928.

The electric quadrupole radiation may be handled in a similar way. The quadrupole moment is a symmetric tensor or a self-conjugate dyadic in Gibbs's terminology. We denote it by $\mathbf{N}$. In terms of the position vectors, $\boldsymbol{r}_i$ of the electrons, it is a sum of dyads, $\boldsymbol{r}_i\boldsymbol{r}_i$:

$$\mathbf{N} = -e\sum_i \boldsymbol{r}_i\boldsymbol{r}_i \,, \tag{7}$$

the sum extending over all the electrons of the atom. If we look over Rubinowicz' formulae[9] for the relative intensity of the Zeeman components of a quadrupole line, we see that they may be written conveniently as numerical multiples of certain unit dyadics which depend only on ΔM. These are

$$\left.\begin{aligned} \boldsymbol{\Phi}(\pm 2) &= \tfrac{1}{2}[\boldsymbol{ii} - \boldsymbol{jj} + i(\boldsymbol{ij} + \boldsymbol{ji})] \,, \\ \boldsymbol{\Phi}(\pm 1) &= \tfrac{1}{2}[\boldsymbol{ki} + \boldsymbol{ik} \pm i(\boldsymbol{kj} + \boldsymbol{jk})] \,, \\ \boldsymbol{\Phi}(0) &= \sqrt{\tfrac{2}{3}}[\boldsymbol{kk} - \tfrac{1}{2}\boldsymbol{ii} - \tfrac{1}{2}\boldsymbol{jj}] \,, \\ \boldsymbol{I} &= \boldsymbol{ii} + \boldsymbol{jj} + \boldsymbol{kk} \,. \end{aligned}\right\} \tag{8}$$

If αJM and $\alpha' J' M'$ are the quantum numbers of the states a and b, then we may find the dependence of the matrix component $(\alpha JM|\mathbf{N}|\alpha' J' M')$ on M and M' from Rubinowicz' formulae, which we reprint here for convenience:

$J' = J$: (9)

$$(\alpha JM|\mathbf{N}|\alpha' JM \pm 2) = A[(J \mp M)(J \mp M - 1)(J \mp M + 1)(J \mp M + 2)]^{\frac{1}{2}}\boldsymbol{\Phi}(\pm 2)$$

$$(\alpha JM|\mathbf{N}|\alpha' JM \pm 1) = A(2M \pm 1)[(J \mp M)(J \pm M + 1)]^{\frac{1}{2}}\boldsymbol{\Phi}(\pm 1)$$

$$(\alpha JM|\mathbf{N}|\alpha' JM) = A\sqrt{\tfrac{2}{3}}[3M^2 - J(J+1)]\boldsymbol{\Phi}(0) + \tfrac{1}{3}N\boldsymbol{I}$$

$J' = J - 1$:

$$(\alpha JM|\mathbf{N}|\alpha' J-1 \;\; M \pm 2) = \pm B[(J \mp M)(J \mp M - 1)(J \mp M - 2)(J \pm M - 1)]^{\frac{1}{2}}\boldsymbol{\Phi}(\pm 2)$$

$$(\alpha JM|\mathbf{N}|\alpha' J-1 \;\; M \pm 1) = \tfrac{1}{2}B(J \pm 2M + 1)[(J \mp M)(J \mp M - 1)]^{\frac{1}{2}}\boldsymbol{\Phi}(\pm 1)$$

$$(\alpha JM|\mathbf{N}|\alpha' J-1 \;\; M) = \sqrt{\tfrac{3}{2}}BM[J^2 - M^2]^{\frac{1}{2}}\boldsymbol{\Phi}(0)$$

[9] *Zeitschrift für Physik*, **61**, 338, 1930.

$J'=J-2$:

$$(\alpha JM\,|\,\mathbf{N}\,|\,\alpha' J-2\;\; M\pm 2)=\tfrac{1}{2}C[(J\mp M)(J\mp M-1)(J\mp M-2)(J\mp M-3)]^{\frac{1}{2}}\Phi(\pm 2)$$

$$(\alpha JM\,|\,\mathbf{N}\,|\,\alpha' J-2\;\; M\pm 1)=\pm C[(J^2-M^2)(J\mp M-1)(J\mp M-2)]^{\frac{1}{2}}\Phi(\pm 1)$$

$$(\alpha JM\,|\,\mathbf{N}\,|\,\alpha' J-2\;\; M)=\sqrt{\tfrac{3}{2}}C[(J^2-M^2)\{(J-1)^2-M^2\}]^{\frac{1}{2}}\Phi(0)$$

These contain within themselves the selection rules:

$\Delta J=0,\ \pm 1,\ \pm 2$ (except $0\to 0$, $\tfrac{1}{2}\to\tfrac{1}{2}$, $1\not\gtrless 0$) and $\Delta M=0,\ \pm 1,\ \pm 2$.

The electric and magnetic vectors of the spherical radiation wave due to the quadrupole moment are

$$\left.\begin{aligned}\mathbf{E}&=\frac{i(2\pi\sigma)^3}{2}\,\frac{e^{2\pi i(\nu t-\sigma r)}}{r}\,(\boldsymbol{I}-\boldsymbol{r}_0\boldsymbol{r}_0)\cdot(\mathbf{N}\cdot\boldsymbol{r}_0)\ ,\\ \mathbf{H}&=\frac{i(2\pi\sigma)^3}{2}\,\frac{e^{2\pi i(\nu t-\sigma r)}}{r}\,\boldsymbol{r}_0\times(\mathbf{N}\cdot\boldsymbol{r}_0)\ ,\end{aligned}\right\}\qquad(10)$$

where $\boldsymbol{r}_0$ is the unit vector toward the point for which $\mathbf{E}$ and $\mathbf{H}$ are computed. From these, the angular intensity distribution and polarization of Zeeman components readily follows. Integrating the Poynting vector over all directions and using the connection between the classical radiation rate and the Einstein transition probability, we may obtain

$$A(a,\,b)=\frac{32\pi^6\sigma^5}{5h}\,|\,(a\,|\,\mathbf{N}\,|\,b)\,|^2\qquad(11)$$

for the quadrupole radiation. Measuring $\mathbf{N}$ in the Hartree unit, ea^2, and σ in the Rydberg unit, this is

$$A(a,\,b)=\frac{3}{40}\,\frac{\alpha^5\tau^{-1}}{24}\,\sigma^5\,|\,(a\,|\,\mathbf{N}\,|\,b)\,|^2\ .\qquad(12)$$

For a whole line we may introduce the quadrupole strength

$$S(A,\,B)=\sum_{a,\,b}|\,(a\,|\,\mathbf{N}\,|\,b)\,|^2\qquad(13)$$

in analogy with (6); the transition probability for the whole line is obtained by writing $S(A,B)/(2J_A+1)$ for $|\,(a\,|\,\mathbf{N}\,|\,b)\,|^2$ in (11) or (12).

By evaluating the sums, one may express the strength in terms of the A, B, and C of (9), the results being

$$\left.\begin{aligned} S(A_J, B_J) &= \tfrac{2}{3}J(J+1)(2J+1)(2J-1)(2J+3)A^2 , \\ S(A_J B_{J-1}) &= \tfrac{1}{2}J(J+1)(J-1)(2J+1)(2J-1)B^2 , \\ S(A_J, B_{J-2}) &= J(J-1)(2J+1)(2J-1)(2J-3)C^2 . \end{aligned}\right\} \tag{14}$$

Thus for corresponding values of $S(A, B)$, the quadrupole radiation is weaker than the dipole, by the factor $\frac{3}{4}\sigma^2$, *weaker* because $\sigma \sim 0.2$ for the nebular lines.

2. APPLICATION TO THE p^2 CONFIGURATION

We consider first the p^2 configuration since it is this one in *O* III which gives rise to the nebulium lines N_1 and N_2 in Bowen's interpretation. The energy-levels in Russell-Saunders coupling (with the usual designations at the right) are shown in Figure 1. The lines N_1 and N_2 owe their existence to the slight departure from Russell-Saunders coupling, as they are intersystem combinations. We therefore need a notation (at the left in Fig. 1) for the actual eigenfunctions of the atom obtained by perturbation theory from the pure states of the Russell-Saunders scheme. Owing to the magnetic spin-orbit interaction, the levels A_2 and B_2 (corresponding to $J=2$) interact, as do also the levels C_0 and D_0. We may write for the eigenfunctions,

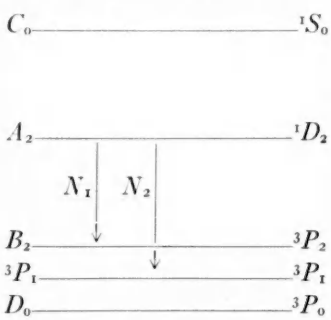

FIG. 1

$$\left.\begin{aligned} \Psi(A_2) &= a\Psi(^1D_2) + b\Psi(^3P_2) , \\ \Psi(B_2) &= -b\Psi(^1D_2) + a\Psi(^3P_2) , \end{aligned}\right\} \tag{15}$$

and a similar pair,

$$\left.\begin{aligned} \Psi(C_0) &= c\Psi(^1S_0) + d\Psi(^3P_0) , \\ \Psi(D_0) &= -d\Psi(^1S_0) + c\Psi(^3P_0) . \end{aligned}\right\} \tag{16}$$

The coefficients a and b, and c and d, are related:

$$a^2+b^2=1; \qquad c^2+d^2=1 .$$

If we write for the spin-orbit interaction

$$V = \sum_i \xi(r_i) \boldsymbol{L}_i \cdot \boldsymbol{S}_i \,, \tag{17}$$

it is found[10] that the pertinent matrix components of V are (the values are diagonal in M and independent of M):

$$\left.\begin{aligned} (^1D_2|\,V\,|^1D_2) &= 0 & (^3P_2|\,V\,|^3P_2) &= \frac{\zeta}{2} \\ (^1D_2|\,V\,|^3P_2) &= \frac{\zeta}{\sqrt{2}} & (^3P_1|\,V\,|^3P_1) &= -\frac{\zeta}{2} \\ (^3P_0|\,V\,|^3P_0) &= -\zeta & (^1S_0|\,V\,|^1S_0) &= 0 \\ (^1S_0|\,V\,|^3P_0) &= -\sqrt{2}\zeta \end{aligned}\right\} \tag{18}$$

where ζ is the radial integral

$$\zeta = \int_0^\infty \xi(r) R^2(np)\, dr \,,$$

$R(np)/r$ being the radial factor of the eigenfunction of the np electron. We shall treat ζ as an adjustable parameter.

The breakdown of Russell-Saunders coupling is so small that we may use the ordinary perturbation theory to the first order, which gives

$$E(^3P_2) - E(^3P_1) = \zeta\,; \qquad E(^3P_1) - E(^3P_0) = \tfrac{1}{2}\zeta \,,$$

the ratio of these being a simple case of the Landé interval rule. The rule is imperfectly satisfied in O III, the values of ζ inferred from the two intervals being 193 and 232 cm^{-1}. We adopt the mean, $\zeta = 210$ cm^{-1}, for O III. The first-order values of b and d are given by

$$b = \frac{(^1D_2|\,V\,|^3P_2)}{E(^1D) - E(^3P)}\,; \qquad d = \frac{(^1S|\,V\,|^3P_0)}{E(^1S) - E(^3P)} \,, \tag{19}$$

hence with our value of ζ, we have for O III,

$$b = 0.0074; \qquad d = -0.0069 \,. \tag{20}$$

It is the small departure from Russell-Saunders coupling measured by b and d which makes the singlet-triplet combinations possible.

[10] Bartlett, *loc. cit.*

Now we consider the matrix components for the lines N_1 and N_2. For any quantity α we have

$$\left.\begin{aligned}(A_2^2|\,\alpha\,|B_2^2) = a^2\bar{\Psi}(^1D_2^2)\alpha\Psi(^3P_2^2)\\ -b^2\bar{\Psi}(^3P_2^2)\alpha\Psi(^1D_2^2)\\ +ab\bar{\Psi}(^3P_2^2)\alpha\Psi(^3P_2^2)\\ -ab\bar{\Psi}(^1D_2^2)\alpha\Psi(^1D_2^2)\ ,\end{aligned}\right\} \tag{21}$$

where the superscript gives the value of M. To calculate the values we need the formulae giving the eigenfunctions of the Russell-Saunders states in terms of the zero-order states. The zero-order states are characterized by quantum numbers nlm_lm_s and $n'l'm_l'm_s'$ for individual electrons and were used by Slater[11] to calculate the separation between terms of the same configuration. If $u(nlm_lm_s)$ is the eigenfunction for one electron in a central field, we adopt the notation

$$\Phi(m_l^{\pm}m_l'^{\pm}) = \frac{1}{\sqrt{2}}\begin{vmatrix} u_1(nlm_lm_s) & u_2(nlm_lm_s)\\ u_1(n'l'm_l'm_s') & u_2(n'l'm_l'm_s')\end{vmatrix} \tag{22}$$

where the $\pm$ signs written as superscripts on the m_l's show the value of m_s, which is restricted to $m_s = \pm\frac{1}{2}$. The connections between these states and the Russell-Saunders states which we need are[12]

$$\left.\begin{aligned}\Psi(^1D_2^2) &= \Phi(1^+1^-)\ ,\\ \Psi(^3P_2^2) &= \Phi(1^+0^+)\ ,\\ \Psi(^3P_1^1) &= \tfrac{1}{2}\Phi(1^+0^-)+\tfrac{1}{2}\Phi(1^-0^+)-\frac{1}{\sqrt{2}}\Phi(1^+-1^+)\ ,\\ \Psi(^3P_0^0) &= \frac{1}{\sqrt{3}}\left[\Phi(0^+-1^+)-\frac{1}{\sqrt{2}}\Phi(1^--1^+)-\frac{1}{\sqrt{2}}\Phi(1^+-1^-)\right.\\ &\qquad\left.+\Phi(1^-0^-)\right]\ ,\\ \Psi(^1S_0^0) &= \frac{1}{\sqrt{3}}\left(\Phi(1^+-1^-)-\Phi(1^--1^+)-\Phi(0^+0^-)\right]\ .\end{aligned}\right\} \tag{23}$$

For the magnetic moment $\boldsymbol{M}$ we have

$$\boldsymbol{L}+2\boldsymbol{S}=\boldsymbol{J}+\boldsymbol{S}\ ,$$

[11] Slater, *Physical Review*, **34**, 1293, 1929.

[12] There are several methods available for finding these. One is due to Gray and Wills, *ibid.*, **38**, 248, 1931.

and J is a diagonal matrix with respect to all quantum numbers other than J, so only S contributes to the radiation. Pauli's[13] one electron matrix components of S_i are

$$\begin{aligned}(+|S_i|+)&=\tfrac{1}{2}k\ ,\\ (+|S_i|-)&=\overline{(-|S_i|+)}=\tfrac{1}{2}(i-ij)\ ,\\ (-|S_i|-)&=-\tfrac{1}{2}k\ .\end{aligned}\qquad(24)$$

Since $S=S_1+S_2$, where S_1 and S_2 belong to the two electrons, we may reduce these to the one-electron matrix components.[14] In this way we find

$$\left.\begin{aligned}(A_2^2|S|B_2^2)&=ab\ k\\ (A_2^2|S|{}^3P_1^1)&=\tfrac{1}{2}b(i+ij)\ ,\end{aligned}\right\}\qquad(25)$$

the connections of A_2 with C_0 and D_0 vanishing on account of the selection rule on J. With these we may calculate the transition probability for the particular Zeeman component involved and pass to the total transition probability for the line by use of the standard formulae.[15] These give us

$$S(A_2B_2)=\tfrac{1}{2}^5\ a^2b^2\ ,\qquad S(A_2,\ {}^3P_1)=\tfrac{5}{2}b^2\ .\qquad(26)$$

Hence, since $a\sim 1$, the intensity ratio of N_1 to N_2 is $3:1$ so far as magnetic dipole radiation is concerned.

The quadrupole moment for a particular Zeeman component can be evaluated in terms of the zero-order states in the same way. All the matrix components involve the integral

$$r(2p)=\int_0^\infty r^2R^2(2p)dr\ .$$

The numerical value of this for oxygen should be given quite accurately by using the eigenfunctions of Hartree and Black.[16] The values which we find by numerical integration are

	O I	O II	O III
$r(2p)$:	2.44	1.75	1.24

[13] *Zeitschrift für Physik*, **43**, 601, 1927.

[14] Condon, *Physical Review*, **36**, 1121, 1930. See Shortley, *ibid.*, **40**, 195, 1932, for proper signs of matrix components.

[15] See, e.g., Pauli, *Handbuch der Physik*, **24**, 238, 1926.

[16] *Proceedings of the Royal Society*, A, **139**, 311, 1933.

We shall not give further details concerning the calculation of the strengths. For $A_2 \rightarrow {}^3P$ we find

$$\left.\begin{aligned} S(A_2B_2) &= \tfrac{2}{15}\tfrac{8}{5}\ a^2b^2r(2p)^2\ , \\ S(A_2{}^3P_1) &= \tfrac{9}{15}b^2r(2p)^2\ , \\ S(A_2D_0) &= 0 \end{aligned}\right\} \tag{27}$$

The last result is rather odd. The transition seems not to be forbidden by any general rule; it is therefore an allowed transition whose transition probability is zero! The quadrupole strengths are in the ratio 28:9, quite close to the ratio 27:9 found for the magnetic dipole strengths.

If we put the numerical values for the strengths in the formulae of § 1, we obtain finally the absolute value of the transition probabilities for the nebular lines N_1 and N_2:

$$\left.\begin{aligned} N_1\text{:}\quad A(A_2B_2) &= a^2b^2[\tfrac{1}{2}\tfrac{5}{2} + \tfrac{3}{4}\tfrac{0}{0}]\frac{\alpha^5\tau^{-1}}{24} = 0.018\ \text{sec.}^{-1}\ , \\ N_2\text{:}\quad A(A_2{}^3P_1) &= b^2\left[\tfrac{5}{2} + \frac{0.97}{400}\right]\frac{\alpha^5\tau^{-1}}{24} = 0.006\ \text{sec.}^{-1} \end{aligned}\right\} \tag{28}$$

The quantities in brackets represent the magnetic dipole and electric quadrupole contributions, respectively. The quadrupole turns out to be 0.1 per cent of the dipole.

The total transition probability out of the A_2 level is the sum of these, hence the absolute value of the mean life (reciprocal of the sum) of the metastable ${}^1D_2$ state of *O* III is 42 seconds.

We may calculate the absolute strengths of the auroral and transauroral[17] lines in the same way. For the auroral line, $C_0 \rightarrow A_2$, we find the quadrupole strength

$$S(C_0A_2) = \tfrac{1}{15}\tfrac{6}{5}\ a^2c^2r(2p)^2\ . \tag{29}$$

Since a and c are nearly unity, this leads to

$$A(C_0A_2) = 1.8\ \text{sec.}^{-1} \tag{30}$$

[17] Boyce, Menzel, and Payne, *loc. cit.*

This is larger than for the nebular lines because the gain through not being an intersystem combination is greater than the loss occasioned by the absence of the magnetic dipole radiation.

Finally, for the transauroral triplet $C_0 \rightarrow B_2$ and $C_0 \rightarrow {}^3P_1$ and $C_0 \rightarrow B_0$, we note that the latter is forbidden in all approximations as it is a $0 \rightarrow 0$ transition in J. Similarly, $C_0 \rightarrow {}^3P_1$ is forbidden in quadrupole radiation by (14). Also $C_0 \rightarrow B_2$ is forbidden in magnetic dipole radiation by the selection rule on J. The quadrupole strength of $C_0 \rightarrow B_2$ is calculated as above to be

$$S(C_0B_2) = \tfrac{4}{15}\, r(2p)^2(bc+\tfrac{1}{2}ad)^2 , \tag{31}$$

and the magnetic dipole strength of $C_0 \rightarrow {}^3P_1$ is

$$S(C_0{}^3P_1) = \tfrac{9}{2}\, d^2 . \tag{32}$$

From these the absolute values of the transition probabilities are

$$\left.\begin{aligned} A(C_0B_2) &= 1.5 \times 10^{-4} \text{ sec.}^{-1} \\ A(C_0{}^3P_1) &= 0.102 \text{ sec.}^{-1} \end{aligned}\right\} \tag{33}$$

Hence the ratio of the intensity of the auroral to the transauroral lines is 5:1 and one of the transauroral lines is 680 times as intense as the other. This makes the weak one practically not observable. The mean life of the metastable C_0 or ${}^1S_0$ level is 0.83 sec. Unfortunately, it appears from Table I of Boyce, Menzel, and Payne that there is no case in which both the auroral and the transauroral lines of the same element can be observed in the p^2 configuration.

In the same way the results for *C* I and *N* II have been calculated. For *C* I the 2p eigenfunction was taken from a paper by Brown, Bartlett, and Dunn.[18] This was obtained by an interpolation process and is not as accurate as the Hartree-Black 2p function for *O* III. The integral is $r(2p) = 5.35$ for *C* I. For *N* II no eigenfunction is available; the value $r(2p) = 2.5$ was adopted from a rough interpolation based on the values for *O* I, *O* II, *O* III, *C* I, and *N* I calculated from the Brown, Bartlett, and Dunn functions. The value for *N* I is $r(2p) = 3.45$. Although these values are rather uncertain, there can be little doubt that the transition probabilities involving them

[18] *Physical Review*, **44**, 296, 1933.

are correct to within 20 per cent. The results are summarized in Table I, where the ordinary notation for the levels is used.

TABLE I*

$2p^2$ CONFIGURATION

	C I	N II	O III
Nebular:			
$A(^1D\,^3P_2)$	1.5×10^{-4}	24×10^{-4}	180×10^{-4} sec.$^{-1}$ (d)
$A(^1D_2\,^3P_1)$	0.5×10^{-4}	8.1×10^{-4}	60×10^{-4} sec.$^{-1}$ (d)
Auroral:			
$A(^1S_0\,^1D_2)$	1.0	1.7	1.8 sec.$^{-1}$ (q)
Transauroral:			
$A(^1S_0\,^3P_1)$	41×10^{-4}	660×10^{-4}	1020×10^{-4} sec.$^{-1}$ (d)
$A(^1S_0\,^3P_2)$	0.06×10^{-4}	0.50×10^{-4}	1.5×10^{-4} sec.$^{-1}$ (q)

* The magnetic dipole lines are marked d; the quadrupole, q.

3. APPLICATION TO THE p^4 CONFIGURATION

The formulae for the p^4 configuration are in all respects those of the preceding section except that $-\zeta$ is to be written for ζ in (18). This follows from the work of Shortley.[19] The only case of astrophysical interest for which the data are known with accuracy is *O* I. For this we have from (18) and (19),

$$b = -6.7 \times 10^{-3}\ ; \qquad d = +6.3 \times 10^{-3}\ , \tag{34}$$

the values being based on $\zeta = 150$ cm^{-1}. Hence for the nebular lines we have

$$A(^1D_2,\ ^3P_2) = 75 \times 10^{-4} \text{ sec.}^{-1}\ ,$$
$$A(^1D_2,\ ^3P_1) = 25 \times 10^{-4} \text{ sec.}^{-1}\ ;$$

for the auroral line,

$$A(^1S_0,\ ^1D_2) = 2.0 \text{ sec.}^{-1}\ ;$$

and for the transauroral lines,

$$A(^1S_0\ ^3P_2) = 1.6 \times 10^{-4} \text{ sec.}^{-1}\ ,$$
$$A(^1S_0\ ^3P_1) = 0.18 \text{ sec.}^{-1}$$

Accordingly, the second of the transauroral lines should have an intensity about one-sixth of the auroral green line.

[19] *Op. cit.*, p. 185.

4. APPLICATION TO THE p^3 CONFIGURATION

The energy-levels for p^3 in Russell-Saunders coupling are shown in Figure 2, with the usual designations on the right. There is one level each with $J=\frac{1}{2}$ and $J=\frac{5}{2}$, and three levels with $J=\frac{3}{2}$. These interact when the spin-orbit energy is taken into account and produce the doublet separations. This configuration has been studied by Inglis.[20] For the matrix components of spin-orbit interaction he found the only non-vanishing components for the $J=\frac{3}{2}$ levels to be

$$(^2P|\,V\,|^4S)=\zeta \text{ and } (^2P|\,V\,|^2D)=\sqrt{5}\zeta/2\,. \qquad (35)$$

The vanishing of the diagonal matrix elements is due to p^3 being in the middle of the shell, so to the first order the doublet interval equals its own negative and therefore vanishes.

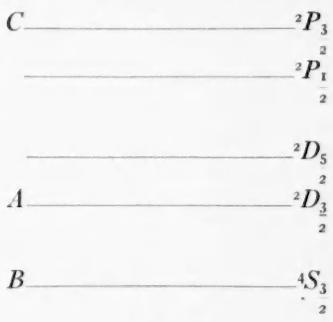

FIG. 2

The observed doublet intervals are therefore due to the second-order effect and are of the order of the departures from the Landé interval rule observed in p^2 and p^4. These departures as well as the whole effect in p^3 are due partly to configuration interaction and partly to the mutual interactions of the levels in the same configuration. This is evident when we consider the $2p^3$ configuration in *O* II. It is a well-known property of the perturbation theory that interacting terms tend to move apart on the energy scale. With spin-orbit interaction neglected the doublet intervals vanish. Bringing it in, $^2P_{3/2}$ moves up, pushed by both ^4S and ^2D below; ^2D moves down since it is not pushed by ^4S below but only by ^2P above; and ^4S moves down, but as this term has but a single level, its small change is not noticeable. Thus both doublets should be normal, with the low J-value level lower in energy. Inglis finds that this is the case in several instances, but for *O* II the data show that ^2D is inverted with an interval of -19.8 cm^{-1} while ^2P is normal with an interval of $+4.5$ cm^{-1}.

[20] *Physical Review*, **38**, 872, 1932.

The ^{2}P interval is of the right order of magnitude for ζ, for O II must lie between the values 150 and 210 for O I and O III. This puts the theoretical interval for the ^{2}P interval by the second-order formula between the limits 4.6 and 9.1 cm^{-1}. The inversion of the ^{2}D must be due to pushing by the levels above in the $2p^2np$ series. This disturbance by the higher members of the series is of course reflected in the eigenfunctions and hence affects the calculation of the transition probabilities. There seems to be no definite way of allowing for it at present. The effect on the transition probabilities is probably no more serious than in p^2 and p^4 and is probably quite small in all cases, but it seems more striking here because the first-order term intervals are zero. Therefore we shall go ahead with p^3 as in the previous sections and use the value $\zeta = 150$ cm^{-1} for O II in getting numerical results.

The quadrupole part of the auroral multiplet, ^{2}P$\rightarrow{}^2$D, can be calculated without taking account of the small departure from Russell-Saunders coupling by using the quadrupole multiplet formulae of Rubinowicz.[21] According to these, the strengths are proportional to the numbers in the following:

	$^2P_{3/2}$	$^2P_{1/2}$
$^2D_{5/2}$	7	2
$^2D_{3/2}$	3	3

(36)

The nebular pair ^{2}D$\rightarrow{}^4$S, the transauroral pair ^{2}P$\rightarrow{}^4$S, and the magnetic dipole part of the auroral multiplet come into existence because of the departure from Russell-Saunders coupling. To calculate their transition probabilities we need the Russell-Saunders eigenfunctions in terms of the zero-order states. Confining ourselves to the particular value $M_J = \frac{1}{2}$, there are five zero-order states:

$$\begin{aligned} &\alpha\colon (1^-\ 0^+\quad 0^-) \qquad \gamma\colon (1^+\ 0^+\ -1^-) \\ &\beta\colon (1^+\ 1^-\ -1^-) \qquad \delta\colon (1^+\ 0^-\ -1^+) \\ &\qquad\qquad \epsilon\colon (1^-\ 0^+\ -1^+) \end{aligned} \tag{37}$$

[21] *Zeitschrift für Physik*, **65**, 662, 1930.

and in terms of these the Russell-Saunders eigenfunctions for $M_J=\frac{1}{2}$ are

$$\left.\begin{aligned}
\Psi(^2P_1)_{\frac{1}{2}} &= -\frac{1}{\sqrt{3}}\Phi(\alpha)-\frac{1}{\sqrt{3}}\Phi(\beta)+\frac{1}{\sqrt{6}}\Phi(\gamma)-\frac{1}{\sqrt{6}}\Phi(\epsilon)\,,\\
\Psi(^2P_3)_{\frac{1}{2}} &= \frac{1}{\sqrt{6}}\Phi(\alpha)+\frac{1}{\sqrt{6}}\Phi(\beta)+\frac{1}{\sqrt{3}}\Phi(\gamma)-\frac{1}{\sqrt{3}}\Phi(\epsilon)\,,\\
\Psi(^4S_1)_{\frac{1}{2}} &= \frac{1}{\sqrt{3}}[\Phi(\gamma)+\Phi(\delta)+\Phi(\epsilon)]\,,\\
\Psi(^2D_3)_{\frac{1}{2}} &= -\sqrt{\frac{3}{10}}\Phi(\alpha)+\sqrt{\frac{3}{10}}\Phi(\beta)+\frac{1}{\sqrt{15}}\Phi(\gamma)-\frac{2}{\sqrt{15}}\Phi(\delta)\\
&\qquad +\frac{1}{\sqrt{15}}\Phi(\epsilon)\,,\\
\Psi(^2D_5)_{\frac{1}{2}} &= \frac{1}{\sqrt{5}}\Phi(\alpha)-\frac{1}{\sqrt{5}}\Phi(\beta)+\frac{1}{\sqrt{10}}\Phi(\gamma)-\frac{2}{\sqrt{10}}\Phi(\delta)\\
&\qquad +\frac{1}{\sqrt{10}}\Phi(\epsilon)\,.
\end{aligned}\right\} \tag{38}$$

For the $M_J=\frac{1}{2}$ state of the perturbed levels A, B, and C, we have, using the first-order perturbation theory,

$$\left.\begin{aligned}
\Psi(A) &= \Psi(^2D_3)_{\frac{1}{2}}-a\Psi(^2P_3)_{\frac{1}{2}}\,,\\
\Psi(B) &= \Psi(^4S_3)_{\frac{1}{2}}-b\Psi(^2P_3)_{\frac{1}{2}}\,,\\
\Psi(C) &= \Psi(^2P_3)_{\frac{1}{2}}+a\Psi(^2D_3)_{\frac{1}{2}}+b\Psi(^4S_3)_{\frac{1}{2}}\,,
\end{aligned}\right\} \tag{39}$$

in which

$$a=\frac{\sqrt{5}\zeta/2}{E(^2P)-E(^2D)} \qquad b=\frac{\zeta}{E(^2P)-E(^4S)}\,. \tag{40}$$

The values for O II with $\zeta=150$ are

$$a=0.0123; \qquad b=0.00371\,.$$

Let us first consider the auroral multiplet $^2P \rightarrow {}^2D$. Using the eigenfunctions and proceeding exactly as in § 2, we find that the magnetic dipole strengths are

$$\left.\begin{array}{lll} & {}^2P_{\frac{3}{2}} & {}^2P_{\frac{1}{2}} \\ {}^2D_{\frac{5}{2}} & \frac{36}{15}\,a^2 & 0 \\ {}^2D_{\frac{3}{2}} & \frac{64}{15}\,a^2 & \frac{60}{15}\,a^2 \end{array}\right\} \tag{41}$$

These do not satisfy the Ornstein-Burger-Dorgelo sum rule, of course, since they are only part of the supermultiplet to which the rule applies in intermediate coupling. Similarly, we find that the quadrupole strengths are given by (36) when multiplied by $\frac{8}{25}r(2p)^2$. The transition probabilities have the values

$$\left.\begin{array}{llllllll} & \text{Quadrupole} & & \text{Dipole} & & \text{Sum} & \\ *A({}^2P_{\frac{3}{2}}, {}^2D_{\frac{5}{2}}) & = & 1.8 & + & 0.50 & = & 2.3 \text{ sec.}^{-1} \\ *A({}^2P_{\frac{3}{2}}, {}^2D_{\frac{3}{2}}) & = & 0.78 & + & 0.90 & = & 1.7 \\ A({}^2P_{\frac{1}{2}}, {}^2D_{\frac{5}{2}}) & = & 1.0 & + & 0.0 & = & 1.0 \\ A({}^2P_{\frac{1}{2}}, {}^2D_{\frac{3}{2}}) & = & 1.6 & + & 1.7 & = & 3.3 \end{array}\right\} \tag{42}$$

The relative intensities implied by these results do not check very well with the astrophysical identification reported by Merrill.[22] He found the two lines marked with an asterisk in (42) but not the other two, although the intensities are all nearly equal theoretically.

The nebular pair is principally due to the quadrupole radiation, for here the magnetic dipole is of the second order in the parameters a and b which measure the coupling breakdown. The quadrupole strengths are

$$\left.\begin{array}{l} S(A_{\frac{3}{2}}B_{\frac{3}{2}}) = b^2 S({}^2D_{\frac{3}{2}}\,{}^2P_{\frac{3}{2}}) \,, \\ S({}^2D_{\frac{5}{2}}B_{\frac{3}{2}}) = b^2 S({}^2D_{\frac{5}{2}}\,{}^2P_{\frac{3}{2}}) \,, \end{array}\right\} \tag{43}$$

[22] *Publications of the Astronomical Society of the Pacific*, **40**, 254, 1928; see also Boyce, Menzel, and Payne, *op. cit.*, Table II.

while the magnetic dipole strengths are

$$\left.\begin{aligned} S(\,{}^2_2A_3\,{}^2_2B_3) &= \tfrac{5}{3}\,a^2b^2\,, \\ S({}^2_2D_5\,{}^2_2B_3) &= 0\,. \end{aligned}\right\} \tag{44}$$

Using the numerical values for *O* II, the transition probabilities are

$$\left.\begin{aligned} A({}^2_2D_5\,{}^2_2B_3) &= 37\ \times 10^{-6} + 0.0 \qquad = 37\ \times 10^{-6}\ \text{sec.}^{-1} \\ A(\,{}^2_2A_3\,{}^2_2B_3) &= 23.8\times 10^{-6} + 0.4\times 10^{-6} = 24.2\times 10^{-6}\ \text{sec.}^{-1} \end{aligned}\right\} \tag{45}$$

(Quadrupole, Dipole, Sum)

Therefore the intensity ratio of the two lines of the nebular pair is $(37\times 3):(24.2\times 2) = 2.3:1$. The observed values are about equal to the *reciprocal* of the theoretical ratio $1^+:3$, $7:15$, and $30:50$ in three instances.

For the transauroral pair ${}^2_2P_3 \rightarrow {}^4_2S_3$ and ${}^2_2P_1 \rightarrow {}^4_2S_3$, the magnetic dipole strengths are

$$S(\,{}^2_2C_3\,{}^2_2B_3) = \tfrac{20}{3}b^2; \quad S({}^2_2P_1\,{}^2_2B_3) = \tfrac{12}{3}b^2\,, \tag{46}$$

and the quadrupole strengths vanish. This gives an intensity ratio for the pair of $5:3$ and the absolute transition probabilities in *O* II become

$$\left.\begin{aligned} A({}^2_2P_3\ {}^4_2S_3) &= 0.041\ \text{sec.}^{-1}\,, \\ A({}^2_2P_1\ {}^4_2S_3) &= 0.049\ \text{sec.}^{-1} \end{aligned}\right\} \tag{47}$$

The observed intensity ratios are $6:3$, $60:20$, and $20:5$, according to Table III of Boyce, Menzel, and Payne, for *S* II. Since this pair is entirely magnetic dipole in character, we do not need a Hartree field to calculate the absolute values of the transition probabilities. From the term values as given in Bacher and Goudsmit, we find for *S* II

$$b = 0.0202\,,$$

and therefore

$$\left.\begin{aligned} A(^2P_{\frac{3}{2}}\ ^4S_{\frac{3}{2}}) &= 0.270 \text{ sec.}^{-1}, \\ A(^2P_{\frac{1}{2}}\ ^4S_{\frac{3}{2}}) &= 0.324 \text{ sec.}^{-1} \end{aligned}\right\} \tag{48}$$

In conclusion it may be said that the ratios of related transition probabilities are quite accurate wherever they are entirely magnetic dipole or entirely quadrupole, the absolute values and the ratios where the radiation is of mixed character are probably within 10 per cent of the true values for this formulation of the theory.

PALMER PHYSICAL LABORATORY
PRINCETON UNIVERSITY

SOME SPECTROSCOPIC PHENOMENA OF THE ECLIPSE OF ϵ AURIGAE

By DEAN B. McLAUGHLIN

ABSTRACT

Radial velocities of ϵ Aurigae during eclipse, observed at Ann Arbor, differ systematically from the Yerkes velocities, probably because of the asymmetries of the spectral lines.

The intrinsic variations of light are synchronous with the velocity variations, with a period of a few months. The relation of light- and velocity-curves is somewhat like that of a Mira star of short period, velocity maximum slightly preceding light maximum.

Systematic residuals of several lines are discussed. The largest were those of the hydrogen lines, positive before mid-eclipse and negative afterward, with a range of about 25 km/sec. The *Mg* II line 4481 shows a residual curve almost the inverse of the velocity-curve. These residuals are readily explained as due to differing amounts of asymmetry of the lines, 4481 showing no asymmetry and the hydrogen lines being most strongly affected.

Study of the edges of the hydrogen lines shows that their residuals are due to a flaring-out of the red edge before mid-eclipse and of the violet edge afterward, while the other edge in each case remains near its normal position. All the line residuals and asymmetries can be explained by the shifting of a strong line across a weaker one at mid-eclipse. A very similar phenomenon is known to occur in the spectrum of β Lyrae during primary eclipse.

It is suggested that these anomalous lines are produced in some way by the absorption of light of the bright star by the atmosphere of the fainter. The lack of similar effects in other eclipsing binaries is attributed to the smaller extent of the atmospheres of most stars as compared with those of supergiants.

Systematic spectrographic observations of Epsilon Aurigae at Ann Arbor were begun in 1927. Fourteen two-prism spectrograms were obtained before the beginning of the eclipse. Following these a long series of single-prism plates was taken: ninety-eight during eclipse (from July, 1928, to May, 1930), fifty-one during the next year, and additional plates in rather smaller number during the two succeeding years.

Results of the study of numerous spectrograms taken at the Yerkes Observatory over an interval of many years have been published by Frost, Struve, and Elvey.[1] The photometric observations made at the Washburn Observatory during about four years, including the eclipse, have been published by Huffer.[2] Preliminary

[1] *Publications of the Yerkes Observatory*, **7**, Part II, 1932.

[2] *Astrophysical Journal*, **76**, 1, 1932.

notes on the results presented in this paper have been published in abstract.[3]

1. THE RADIAL VELOCITIES

The Ann Arbor radial velocities are based on twenty strong lines. Apart from the systematic deviations of certain lines, discussed below, the results from the various lines are so consistent that it seems unlikely that an important change of velocity would result from the inclusion of more lines for the plate velocities. Struve and Elvey[4] pointed out a large systematic difference between the velocities indicated by strong and by weak lines, particularly during the latter half of eclipse. In what follows it is considered that the Ann Arbor velocities represent a fair sample of the strong lines. It should be borne in mind that the terms "velocity" and "velocity residual" are used as convenient modes of expression and are not intended to imply that the star, or even a part of its atmosphere, is actually moving with the velocity indicated.

Outside of eclipse the velocity of ϵ Aurigae is subject to variations with a range of about 15 km/sec. in an irregular period of a few months. These variations persist during the eclipse as well. Superimposed upon these changes a large shift of the lines toward the violet occurs during the latter half of eclipse, corresponding to a less conspicuous shift toward the red during the first half. The extreme value of this shift amounts to about 20 km/sec.

The changes just discussed are shown in Figure 1. At the top of the figure the Yerkes velocities are plotted for comparison with those observed at Ann Arbor, which are plotted just below them. At first glance the agreement appears satisfactory, when we consider the differences between the two sets of data. The Yerkes plates were taken partly with one and partly with three prisms, while all the Ann Arbor plates obtained during eclipse are of one-prism dispersion. There is a definite tendency for the Ann Arbor velocities to be systematically lower than those from Yerkes during the first half of eclipse, and higher during the latter half. When we recall that the change of direction of the line asymmetries studied at

[3] McLaughlin, *Popular Astronomy*, **38**, 29, 1930; *ibid.*, p. 601.

[4] *Astrophysical Journal*, **71**, 144, 1930.

the Yerkes Observatory occurred about the time of mid-eclipse, it appears plausible that the asymmetries are the cause of these systematic differences. Undoubtedly, the unsymmetrical lines would be measured differently on plates of different dispersion, and might even be measured differently by different measurers on the same

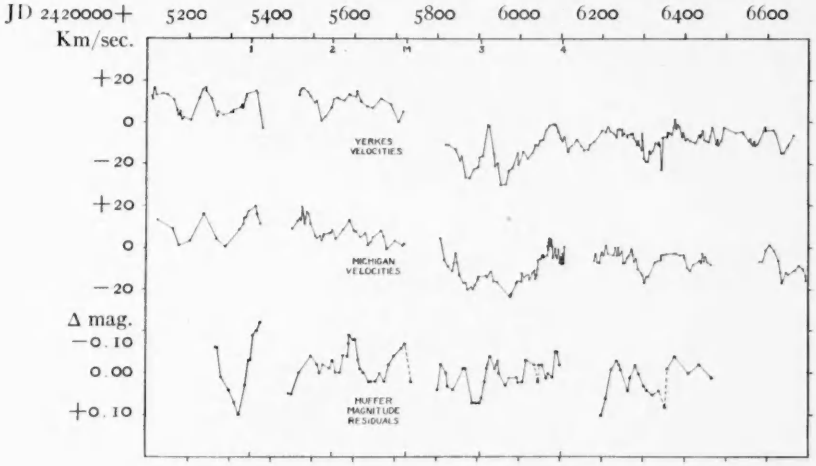

FIG. 1.—Yerkes and Ann Arbor radial velocities of ε Aurigae, and Huffer's magnitude residuals, showing correlation of velocities and intrinsic light variations. Symbols 1, 2, *M*, 3, and 4 indicate dates of first and second contact, mid-eclipse, third and fourth contact, based on Huffer's observations.

plates. The smaller amplitude of the Ann Arbor velocities during eclipse is probably to be ascribed to the same cause.

2. CORRELATION OF LIGHT AND VELOCITY VARIATIONS

Synchronous variations of light and velocity outside of eclipse were suggested by the writer,[5] and Struve and Elvey[6] found them related during the eclipse as well. With the publication of the photoelectric observations by Huffer,[7] a more definite comparison is now possible.

Huffer has given a plot of the residuals of his observations from a constant maximum and a smooth symmetrical curve of eclipse. The data from that plot are shown in the lower portion of Figure 1. With due allowance for the large shift of the lines during the second

[5] *Op. cit.*, p. 29. [6] *Op. cit.*, p. 147. [7] *Loc. cit.*

half of the eclipse, we can trace a rather definite correspondence of light maxima with velocity maxima. The pause on the ascending velocity-curve from J.D. 6000–6040 may be properly regarded as a maximum and a minimum of velocity, since we are dealing with fluctuations superimposed upon the rising curve of recovery from the asymmetry effect during eclipse. More definitely, most of the maxima or minima of light occur later than the maxima or minima of velocity. In some cases this difference amounts to as much as a month; more frequently it is one to two weeks. The correlation of light and velocity is thus very different from that of a Cepheid, but is not unlike that of a Mira variable of short period, such as SX Herculis.[8]

Although the variation is obviously not simply periodic, the length of cycle is comparable to that of a short-period Mira star. Individual cycles have been as long as 120 and as short as 60 days. There is some suspicion that the shorter cycles are only half-cycles, and that we are dealing with a type of variation allied to that of the more irregular members of the RV Tauri class, in which the secondary minima are sometimes omitted. Thus, in its intrinsic variations, ϵ Aurigae does not fall conspicuously out of line with other variable stars.

3. SYSTEMATIC DEVIATIONS OF LINES

Struve and Elvey noted that the line λ 4481, *Mg* II, was the only strong line which was not unsymmetrical during the eclipse. Its residuals are therefore of peculiar interest. In Figure 2 the curve of plate velocity during eclipse is plotted at the top, and beneath it are plotted the residuals of λ 4481 in the sense of line *minus* plate. These residuals are mostly negative during the first half of eclipse and positive during the second half. These results confirm those obtained at the Yerkes Observatory.[9] It is particularly interesting to note that during the latter part of eclipse, when the asymmetries of most of the lines are the greatest, the residual curve for λ 4481 is almost a mirror image of the curve of plate velocity. This is a strong indication that the line asymmetries alone are the cause of the large negative shift of the lines at that time.

[8] Joy, *Astrophysical Journal*, **75**, 127, 1932.

[9] *Yerkes Observatory Publications*, **7**, Part II, 23, 1932.

The line λ 4227, *Ca* I, shows a residual curve of a different character, as plotted just below the curve for λ 4481 in Figure 2. During the first half of eclipse the residuals are negative and nearly constant. During the second half the curve is rather similar to that of the plate velocities, suggesting that this line is subject to a greater asymmetry than the average of those measured.

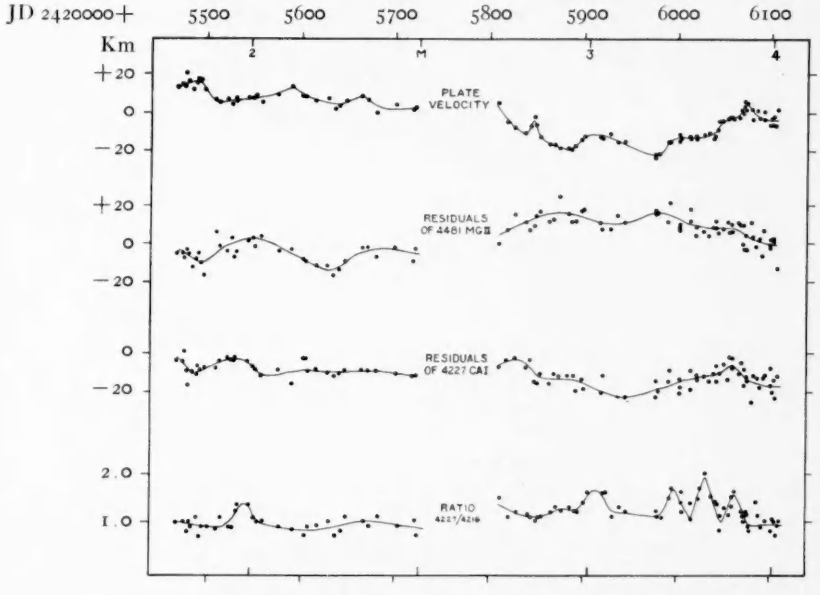

FIG. 2.—Curve of Ann Arbor plate velocities of ε Aurigae during eclipse. Residuals (line *minus* plate) for 4481 and 4227. Intensity ratio 4227/4215. Symbols 2, *M*, 3, and 4 indicate dates of second contact, mid-eclipse, third and fourth contact.

Systematic deviations of the velocities of the hydrogen lines were the first that were noted by the writer,[10] and were found independently at the Yerkes Observatory. The writer also noted that the largest residuals were associated with a conspicuous increase of width and intensity of the lines. We shall here discuss only the results for $H\delta$, noting that $H\gamma$ shows practically identical behavior.

The residual curve for $H\delta$ is plotted at the top of Figure 3. The deviations are positive during the first half of eclipse and negative during the second half. The trend reminds one somewhat of that of

[10] *Popular Astronomy*, **38**, 29, 1930.

the plate velocities, but there is a conspicuous difference in that the minimum of the $H\delta$ residual curve occurs a few months earlier and its rise to normal is slower and steadier. Some of the smaller irregularities (mostly smoothed out in the curve shown here) are probably real, as they are duplicated by $H\gamma$.

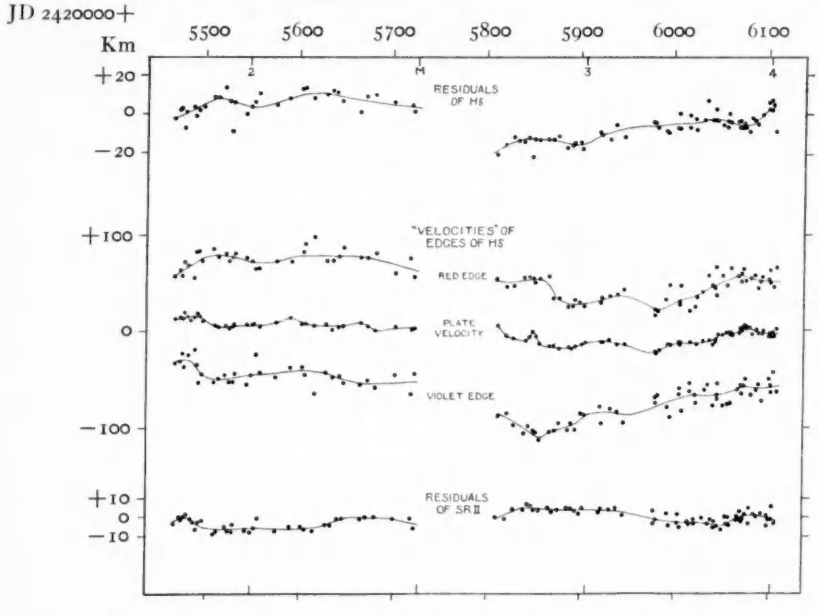

FIG. 3.—Residuals (line *minus* plate) of $H\delta$ in ϵ Aurigae during eclipse. "Velocity"-curves for edges of $H\delta$. Mean residuals of 4078, 4215, *Sr* II. Symbols 2, *M*, 3, and 4 indicate dates of second contact, mid-eclipse, third and fourth contact.

The doublet λλ 4215, 4078, *Sr* II, also shows systematic effects. The residuals of these lines are plotted at the bottom of Figure 3, where each point represents the mean for the two lines. The scatter is small and the curve appears well determined. It is sufficient to remark that it is essentially a vertically diminished mirror image of the curve of plate velocity, indicating that these lines are less affected by asymmetries than the average line measured. These results agree with those for λ 4215 found on the Yerkes plates.

4. CORRELATION OF WIDTHS AND ASYMMETRIES OF THE HYDROGEN LINES

The fact that the hydrogen lines showed simultaneously two abnormalities, viz., increased width and large residuals, suggested the investigation of the positions of the edges of these lines. These are undoubtedly affected by exposure, development, and contrast, but with a large number of plates these effects should be smoothed out. For convenience of discussion the positions of the edges are here expressed as velocities, although it should be borne in mind that this is merely used as the equivalent of a difference in wave-length.

In the middle of Figure 3 the "velocities" of the edges of $H\delta$ are plotted with the curve of plate velocity between them. Displayed in this manner, the changes of width and of position of the line with reference to the others measured are strikingly evident. The broader features of the residual curve at the top of Figure 3 find a ready explanation in the shifts of the edges of the line as shown below it. During the first half of eclipse the violet edge of $H\delta$ remained nearly in its normal position, but the red edge, beginning about J.D. 5490, flared far out and thus caused the positive residuals of the line. During that time the red edge was definitely sharper than the violet edge. Just before mid-eclipse the red edge began to return toward normal.

About J.D. 5810, when the star was first observed after conjunction with the sun, a conspicuous increase of intensity of the hydrogen lines was noted, and they showed simultaneously negative residuals of the order of 20 km/sec. The edge velocity-curves of Figure 3 make it clear that this was due to a great flaring-out of the violet edge of the line, the red edge having returned to its normal position. During this latter interval the violet edge was also the sharper. As it returned toward its normal position near the end of the eclipse, the residuals of the line became smaller and were practically zero when the eclipse ended.

Two dates of greatest width, J.D. 5520 and 5860, are very roughly symmetrical about the time of mid-eclipse (J.D. 5725, according to Huffer). The line was very wide also about J.D. 6080, but the symmetrical phase near the beginning of eclipse occurred near the time of conjunction with the sun and was not observed.

5. THE RATIO OF INTENSITY, λ 4227:λ 4215

On each plate the intensity ratio λ 4227:λ 4215 was estimated. The data were not examined or plotted until all the estimates were completed. It can hardly be a mere coincidence that the curve of this ratio, shown at the bottom of Figure 2, exhibits maxima almost precisely at the dates of beginning and ending of the total phase of the eclipse. Large fluctuations appear to have occurred during the later partial phases, but the symmetrical phases near the beginning of eclipse passed unobserved, owing to the proximity of the star to the sun.

6. INTERPRETATION OF LINE RESIDUALS AND ASYMMETRIES

From the data presented one result stands out rather clearly: the asymmetries of the lines, as pointed out by the Yerkes observers, are undoubtedly the major cause of the larger systematic displacements of lines during the eclipse. The line λ 4481, which shows no visible asymmetry, shows a residual curve which is nearly a mirror image of the curve of plate velocity during eclipse, indicating that the shifts of the strong lines are due to the asymmetry. The weak lines probably behave like λ 4481, according to Struve and Elvey. The large residuals of the hydrogen lines are due to their especially strong asymmetry, which is noticeable even on the one-prism Ann Arbor plates. The behavior of the edges of the hydrogen lines accounts fairly well for their residuals. The fact that the edge which flares out is the stronger and sharper suggests that the displacements and asymmetries of lines are to be interpreted as due to a strong sharp line which moves from the red to the violet side of a weaker, more diffuse line at the time of mid-eclipse.

The observations made by Adams and Sanford[11] give support to this interpretation. Soon after the beginning of the total phase they found many enhanced lines slightly displaced toward the red with reference to the neutral lines. They attributed this to a faint component on the red side of each enhanced line. In the light of other observations, chiefly the contours of lines on the Yerkes plates, the writer considers this effect as due to the positive shift of the strong components of the enhanced lines, while the neutral lines had no

[11] *Publications of the Astronomical Society of the Pacific*, **42**, 203, 1930.

such components. Two Mount Wilson plates taken during the latter half of the eclipse showed the enhanced lines and a few of the neutral lines clearly double; a strong component appeared displaced −35 km/sec., while a weak one showed a small positive displacement. On the Yerkes spectrograms these components are unresolved, and the blend appears as a single line, sharp on the violet side and more diffuse on the red edge.

7. COMPARISON WITH β LYRAE

The spurious shifting components of the lines of ε Aurigae find a rather close parallel in the spectrum of β Lyrae. During entrance into primary eclipse, this spectrum shows a set of absorption lines flanking the principal lines and displaced about 200 km/sec. toward the red,[12] and during the latter portion of the eclipse Miss Maury[13] remarked the presence of a "third set of lines" which "belong to neither of the two stars," and which are displaced toward the violet. The writer has examined a number of spectrograms taken at Ann Arbor and is able to confirm these observations. It appears plausible to regard these additional lines, which we may refer to as the "anomalous absorption," as due to the same causes as the strong shifting spurious components in the spectrum of ε Aurigae. The chief differences between the two cases lie in the smaller displacement and greater intensity of the spurious lines in ε Aurigae as compared with β Lyrae.

8. SUGGESTIONS AS TO THE ORIGIN OF THE ADDITIONAL LINES

The origin of the anomalous absorption lines in both these eclipsing systems remains a matter for further investigation. In the present state of the observational data a little speculation seems permissible. We may explain the phenomenon in a general way by supposing the faint star to have an atmosphere of very great extent which is rotating directly with an equatorial velocity of the order of 40 km/sec. in the system of ε Aurigae. A model of this type has been proposed by Struve and Elvey, who also point out some objections to it, and remark further: "It is possible that we are dealing here with a completely new physical phenomenon."

[12] Baxandall, *Annals of the Solar Physics Observatory, Cambridge*, **2**, Part I, 21, 1930.
[13] *Harvard Annals*, **28**, 103, 1897.

However well such a model may explain the anomalous lines in ϵ Aurigae, it fails in the case of β Lyrae. The tremendous tidal distortion of the two bodies appears to rule out completely a rotation of the faint star at a rate more rapid than that of orbital motion, and the shift observed appears entirely too great to be due to the rotation of the star. We may be forced to admit "a completely new physical phenomenon," and as a possibility in this direction it is suggested that something allied to anomalous dispersion may be operative. In any case the writer finds it difficult to escape the conviction that the anomalous lines are produced in some way by the passage of the light of the bright star through the atmosphere of the fainter. To elaborate upon this view, the fact that some lines show stronger asymmetries than others may be regarded as due to the greater extent of certain gases than of others in the atmosphere of the faint star. In particular, the especially strong asymmetries of the hydrogen lines may be due to the fact that the hydrogen has the greatest extent, and the lack of asymmetry of λ 4481 may indicate that ionized magnesium is present only in small amount, or at any rate does not extend far above the photosphere of the faint star. The fact that enhanced lines generally occur higher in the chromosphere than neutral lines may be directly related to the strong asymmetries of the enhanced lines in ϵ Aurigae.

Why should such effects not be observed in every eclipsing binary system? The answer is probably to be found in the fact that very few binary systems are composed of such tenuous stars as β Lyrae and ϵ Aurigae. The hypothesis suggested requires that the atmosphere of the faint star be comparable in extent with the photosphere of the brighter. Such a condition certainly does not obtain in the case of the sun (limiting the atmosphere to the chromosphere) and probably does not occur in any of the main sequence, but the tenuous giants and supergiants may have much more extensive atmospheres than has generally been supposed.

CONCLUSION

That the decrease of light of ϵ Aurigae every twenty-seven years is actually due to an eclipse can now be regarded as established beyond reasonable doubt, even though the nature of the eclipsing

body is as yet only vaguely suggested. The shape of the light-curve, the punctuality of the minima, and their occurrence at the correct phase of the twenty-seven-year velocity variation all point to an eclipse as the cause. Even the line asymmetries, apparently regarded as unique, find a parallel in the spectrum of the undoubted eclipsing binary, β Lyrae. The fact that the star is subject to intrinsic variations does not vitiate these conclusions.

The systematic deviations of individual lines during eclipse are satisfactorily accounted for by differing amounts of asymmetry. Observations of the edges of the hydrogen lines indicate that the asymmetries are caused by the shifting of a strong "anomalous" absorption line across the normal lines. That this phenomenon is due to absorption of light by the atmosphere of the fainter star appears to be the most hopeful working hypothesis. The precise manner of origin of the anomalous lines is by no means clear, and the cause of their displacements is likewise unknown.

THE OBSERVATORY
UNIVERSITY OF MICHIGAN
August 1933

β CEPHEI

By CLIFFORD C. CRUMP

ABSTRACT

The elements of nineteen new and separate determinations of the orbit of β Cephei are here given with a list of seventeen other determinations which have been made at different times by other observers. The material presented for study covers a period of twenty-six years and more than fifty thousand complete ranges of the variation of the radial velocity of this star.

The present investigation of β Cephei was undertaken with the thought of making available to those who are interested in the problem presented by this star a considerable amount of material which has been collected at the Yerkes Observatory, together with data which the writer obtained at the Observatory of the University of Michigan. Many series of spectrograms had been made at Yerkes covering the entire period of the variation of the radial velocity of the star. Some of these series had been measured and the reductions made but the results had not been published. In these reductions old determinations of wave-lengths had been used which could now be replaced by more recent and accurate values. Other series remained to be measured, and during the investigation further data were obtained with the Bruce spectrograph. In all, nineteen new and separate determinations of the elements of the orbit of this star are here presented, covering a period which extends from May 28, 1906, to September 5, 1932. In addition, the elements of seventeen orbits, published by various observers (including two by the writer), have been listed. The mass of data represents the study of at least 1120 spectrograms. The material presented for study covers a period of twenty-six years and more than fifty thousand complete ranges of the variation of the radial velocity.

The data obtained at the Yerkes Observatory can be divided into two parts: that obtained up to and including June 1, 1914, and that secured during the years 1929–1932. The early spectrograms were made with the two-prism arrangement of the Bruce spectrograph attached to the 40-inch refractor, which gave a dispersion of 22 A

per millimeter at λ 4500. These spectrograms were made on Seed N.H. and Seed 30 plates. While they are not as good as those secured later, they are satisfactory and the lines are well defined. The spectrograms made in 1929–1932 were secured with the one-prism spectrograph. Those made in 1929 were taken on Eastman 40 and Imperial Eclipse Ortho plates. For the series of October 19, 1930; September 11, 1931; and September 5, 1932, Eastman Process plates were used. The lines on these plates are excellent for the most part, and were used as a basis of an investigation of width and of intensity of the

TABLE I

λ	Element	λ	Element
3964.727	*He* I	4143.759	*He* I
3970.075	*H* (ε)	4253.79	*O* II, *S* III
3973.266	*O* II	4267.16	*C* II
3994.995	*N* II	4340.467	*H* (γ)
4009.267	*He* I	4387.928	*He* I
4026.189	*He* I, *N* II	4414.888	*O* II
4035.05	*N* II	4416.974	*O* II
4069.788	*O* II	4471.477	*He* I
4072.156	*O* II	4552.611	*Si* III, *N* II
4075.869	*O* II	4567.824	*Si* III
4089.07	*Si* IV, *O* II	4574.737	*Si* III
4101.738	*H* (δ)	4650.75	*C* III
4116.104	*Si* IV	4861.326	*Hβ*
4120.812	*He* I, *O* II	4921.929	*He* I
4132.82	*O* II		

lines in the spectrum of the star. The plates secured at Ann Arbor in 1919 with the one-prism spectrograph attached to the $37\frac{1}{2}$-inch reflector have the advantage of short exposure. Good spectrograms were obtained in five to ten minutes, the difference in time between exposures being about six or seven minutes.

The wave-lengths adopted for the stellar lines are given in Table I. Identification of the absorbing atom for each of the lines is given. The measures of the two-prism plates and those of the 1919 series were reduced by means of the Hartmann-Cornu formula. The 1929–1932 series were reduced by means of standard tables used for the reduction of one-prism plates at the Yerkes Observatory. Table II gives a list of the observations. It will be noted that Professor E. B.

TABLE II

Date	Julian Day	Phase	No. Lines	Length of Exp.	V	$V_{ob}-V_c$	Meas. By
1906	241+						
May 28.....	7359.661	.002	15	37^m	− 0.94	+6.77	C
	.684	.024	16	16	+ 7.28	+2.80	C
	.715	.055	13	12	+ 8.60	−2.57	C
	.735	.075	13	15	+ 2.63	−4.39	C
	.755	.095	16	16	− 2.62	+0.14	C
	.771	.111	17	13	−11.72	−0.22	C
	.785	.125	18	13	−13.68	+4.75	C
	.799	.139	14	11	−22.52	−0.15	C
	.812	.152	16	12	−18.80	+4.65	C
	.825	.166	16	11	−14.69	+5.68	C
	.836	.177	18	10	−17.09	−1.16	C
	.850	.000	17	12	−11.74	−3.18	C
	.862	.012	17	10	− 1.09	+0.46	C
	.874	.024	18	11	+ 0.32	−3 66	C
	.885	.035	16	11	+ 6.62	−1.61	C
	7359.909	.059	14	10	+ 6.35	−5.58	C
June 22.....	7384.715	.186	10	31	− 8.75	−2.92	C
	.742	.022	20	27	−21.91	+1.38	C
	.764	.044	21	27	−29.74	−1.25	C
	.788	.068	18	28	−21.25	+3.65	C
	.812	.092	15	31	− 8.22	+3.03	C
	.840	.122	18	27	+ 2.72	−2.36	C
	.865	.145	18	28	+ 8.67	−0.79	C
	7384.887	.167	11	20	+ 6.33	+0.78	C
July 6.....	7398.644	.014	9	24	−17.82	+4.57	F
	.662	.032	10	24	−25.73	+1.13	F
	.687	.057	10	24	−20.81	+3.37	F
	.727	.097	8	20	− 9.22	−0.84	F
	.746	.116	5	20	+ 3.68	+2.15	F
	.767	.137	12	20	+ 7.64	+2.85	F
	.786	.156	9	20	+ 3.34	−0.47	F
	.807	.177	11	20	− 4.15	−4.71	F
	.826	.005	9	20	−10.05	−0.15	F
	.845	.025	7	20	−19.60	+0.54	F
	.865	.044	6	20	−23.55	−0.72	F
	7398.889	.068	9	20	−19.83	+0.53	F
Aug. 27.....	7450.5861	.157	6	20	+ 4.41	+3.79	D
	.6368	.017	12	30	−31.53	−5.15	D
	.6556	.036	12	18	−27.43	+6.23	D
	.6896	.070	12	18	−23.31	+3.74	D
	.7035	.084	10	18	−16.48	+3.44	D
	.7316	.112	13	18	− 3.17	+0.20	D
	.7458	.126	9	21	+ 6.07	+1.95	D
	.7653	.145	11	19	+ 6.18	−3.12	D
	.7799	.160	8	20	+ 6.69	−0.55	D
	.7986	.179	8	18	− 0.92	+2.72	D
	.8118	.002	10	18	−12.76	−2.64	D
	.8292	.019	8	18	−19.64	+7.60	D
	7450.8424	.032	8	18	−35.22	−2.50	D

TABLE II—*Continued*

Date	Julian Day	Phase	No. Lines	Length of Exp.	V	$V_{ob}-V_c$	Meas. By
1906	241+						
Aug. 27.....	7450.8604	.050	9	18^m	−26.73	+6.66	D
	.8729	.063	9	18	−33.46	−3.43	D
	.8965	.086	12	25	−19.30	−0.96	D
	.9132	.103	7	22	−13.33	+5.08	D
	7450.9340	.124	11	25	− 0.95	+2.95	D
1907							
May 20.....	7716.604	.000	8	36	−22.02	−0.49	C
	.634	.030	10	46	−10.04	−2.04	C
	.669	.065	8	44	+ 4.15	−2.79	C
	.705	.101	10	44	− 7.11	−6.27	C
	.737	.133	12	36	−15.33	+8.42	C
	.764	.160	10	28	−26.62	+2.37	C
	.787	.183	12	28	−21.21	+3.10	C
	.811	.016	15	33	−21.29	−6.79	C
	.835	.040	12	24	+ 0.18	+4.11	C
	.858	.064	12	24	+10.73	+4.03	C
	.878	.083	13	20	+ 6.97	−1.19	C
	.896	.101	12	20	+ 0.63	+2.36	C
	7716.911	.116	8	15	−14.75	−1.46	C
July 29.....	7786.603	.153	8	20	+ 0.96	−4.21	F
	.619	.170	13	20	− 5.11	−3.38	F
	.645	.005	10	16	−11.75	+6.50	F
	.659	.020	8	16	−18.37	+4.73	F
	.673	.033	11	14	−22.02	+3.36	F
	.686	.046	10	14	−22.26	+2.61	F
	.701	.061	11	14	−22.82	−1.43	F
	.718	.078	8	17	−15.16	−1.09	F
	.738	.098	8	15	− 6.91	−3.21	F
	.752	.113	8	15	+ 0.37	−3.08	F
	.769	.129	10	14	+10.31	+2.99	F
	.783	.143	7	15	+ 5.12	−2.09	F
	.798	.158	7	13	− 4.35	−7.92	F
	.817	.178	7	15	− 9.60	−3.76	F
	.831	.001	8	15	−15.38	+0.87	F
	.860	.029	11	17	−27.42	−2.32	F
	.874	.044	9	16	−19.82	+5.36	F
	.889	.058	12	17	−23.89	−1.73	F
	7786.906	.075	8	22	−13.05	+2.49	F
Aug. 2.....	7790.626	.006	15	18	− 7.17	+3.54	C
	.638	.018	8	7	−12.07	+6.08	C
	.663	.043	18	20	−29.22	−0.20	C
	.688	.068	19	18	−28.18	+0.21	C
	.711	.091	15	20	−18.55	−0.58	C
	.748	.128	16	22	+ 2.47	−1.48	C
	.769	.149	14	32	+ 8.67	−0.43	C
	7790.799	.179	16	16	− 4.14	−4.00	C

TABLE II—*Continued*

Date	Julian Day	Phase	No. Lines	Length of Exp.	V	$V_{ob}-V_c$	Meas. By
1907	241+						
Nov. 11.....	7891.670	.000	16	20^m	−17.81	−0.11	C
	.690	.020	16	22	−10.20	−6.51	C
	.710	.040	13	22	+ 4.54	+1.36	C
	.730	.060	16	22	+ 8.32	+1.07	C
	.750	.080	14	22	+ 2.38	−1.36	C
	.770	.100	16	22	− 7.33	−1.06	C
	.789	.118	17	22	−14.00	+3.77	C
	.809	.139	12	22	−28.10	−1.10	C
	.831	.161	18	25	−29.69	−0.82	C
	7891.858	.188	9	24	−14.41	+4.52	C
1908							
June 15.....	8108.615	.175	9	28	−18.64	+1.75	F
	.638	.008	6	28	− 9.55	+0.86	F
	.661	.031	11	28	− 1.82	−0.92	F
	.683	.053	9	26	+ 4.61	+0.22	F
	.749	.119	11	24	−19.31	+1.95	F
	.768	.138	9	22	−22.28	+2.99	F
	.789	.159	10	22	−23.77	−0.02	F
	.809	.179	8	22	−21.68	−3.56	F
	.831	.010	12	23	−11.35	−1.85	F
	.851	.031	10	23	+ 1.28	−2.16	F
	8108.872	.052	12	23	+ 3.84	−0.42	F
June 29.....	8122.685	.150	6	25	−27.11	−3.73	F
	.707	.173	5	27	−12.37	+2.62	F
	.729	.004	8	25	− 8.68	−4.62	F
	.752	.027	6	25	+11.55	+4.27	F
	.775	.050	5	32	+13.59	−0.70	F
	.797	.072	7	25	+ 3.81	−5.69	F
	.818	.093	9	25	− 2.68	+4.33	F
	.836	.112	8	22	−11.08	+9.78	F
	.855	.130	7	22	−21.40	+4.50	F
	8122.872	.148	6	22	−21.58	+2.54	F
1912							
April 29.....	9522.765	.175	16	30	−16.30	−3.00	
	.791	.011	17	30	− 0.94	−2.30	C
	.816	.036	14	30	+ 6.36	−0.31	C
	.842	.062	18	30	− 1.04	+1.04	C
	.866	.086	17	30	−14.58	+2.83	C
	.891	.111	18	30	−25.53	+3.50	C
	9522.915	.135	20	30	−27.87	+2.40	C
May 13.....	9536.728	.180	11	36	+ 1.57	−4.87	D
	.758	.019	11	36	−12.03	+4.06	D
	.781	.043	8	36	−32.11	+0.55	D
	.817	.078	12	36	−28.88	+2.78	D
	.845	.107	10	36	−18.94	+1.23	D
	.874	.135	12	35	− 6.90	−7.35	D
	9536.898	.159	7	25	+10.98	+0.54	D

TABLE II—*Continued*

Date	Julian Day	Phase	No. Lines	Length of Exp.	V	$V_{ob}-V_c$	Meas. By
1914	242+						
June 1.....	0285.622	.010	11	30^m	−17.60	+3.59	D
	.646	.034	7	30	−11.24	−2.50	D
	.669	.057	7	30	− 1.05	+0.16	D
	.692	.081	9	32	− 6.89	−3.55	D
	.717	.105	13	30	−16.84	+2.05	D
	.740	.128	10	30	−38.47	−2.17	D
	.762	.152	9	30	−42.82	−1.16	D
	.786	.175	12	30	−28.11	+5.61	D
	.811	.009	12	32	−23.04	−1.29	D
	.833	.031	10	24	−12.22	−3.90	D
	.851	.049	11	20	− 3.86	−0.73	D
	.869	.067	7	26	+ 0.50	+1.10	D
	0285.890	.088	8	26	− 9.80	−2.98	D
1919							
Sept. 1.....	2203.685	.136	19	10	−14.78	−3.41	C
	.714	.165	20	6	− 5.54	+5.19	C
	.733	.184	8	6	− 0.61	+4.51	A
	.740	.000	20	6	− 2.10	+0.17	C
	.745	.006	20	7	+ 0.03	−0.86	A
	.766	.026	16	6	+11.41	−2.46	A
	.772	.032	15	8	+14.28	−2.78	C
	.779	.040	11	8	+19.55	−0.62	C
	.785	.045	20	6	+20.73	−0.50	A
	.794	.054	13	6	+23.89	+3.36	C
	.799	.060	16	6	+21.33	+2.51	A
	.807	.066	20	6	+18.38	+2.35	C
	.818	.078	19	6	+12.83	+3.47	A
	2203.832	.092	16	6	+ 0.34	+1.52	C
Sept. 2.....	2204.675	.174	19	6	− 6.71	+2.09	C
	.680	.178	17	6	−11.14	−3.84	A
	.686	.184	14	7	− 4.46	+0.62	C
	.706	.014	18	6	+ 7.12	+1.09	A
	.748	.056	19	5	+20.43	+0.56	C
	.752	.060	15	5	+19.98	+1.43	C
	.757	.065	18	5	+21.50	+4.79	A
	.761	.069	11	5	+10.77	−3.46	A
	.766	.074	8	5	+ 7.54	−4.45	C
	.774	.082	13	5	+ 6.68	−0.63	A
	.795	.104	20	5	− 3.54	−0.45	C
	.804	.113	18	5	+ 4.44	+1.89	A
	.809	.117	16	5	− 7.50	+0.10	C
	.813	.121	16	5	− 6.78	+1.93	C
	.817	.125	12	5	− 6.60	+3.04	C
	.823	.131	11	7	−19.05	−8.37	C
	.841	.159	9	6	− 7.48	+4.16	C
	2204.854	.163	5	5	−10.77	+0.36	C

TABLE II—*Continued*

Date	Julian Day	Phase	No. Lines	Length of Exp.	V	$V_{ob}-V_c$	Meas. By
1929*	242+						
Oct. 26–27....	5912.990	.161	14	37^m	−20.41	+1.08	C
	3.015	.186	12	26	−19.36	−4.65	C
	.035	.015	17	25	− 5.53	−0.54	C
	.062	.042	10	32	+ 5.24	−2.30	C
	.083	.063	15	20	+14.08	+1.92	C
	.100	.080	16	20	+ 8.96	−1.48	C
	.116	.096	17	20	+ 1.70	−2.67	C
	.133	.113	15	20	− 5.00	+0.19	C
	.156	.136	12	20	−11.45	+5.68	C
	.169	.149	13	31	−21.09	−0.05	C
	.192	.172	10	30	−18.41	+0.96	C
	.215	.004	4	30	− 6.47	+4.17	C
	.240	.029	7	31	+ 1.26	−0.56	C
	.264	.053	6	30	+10.19	−0.45	C
	5913.288	.078	8	31	+ 7.71	−3.39	C
Nov. 15–16....	5931.980	.140	8	20	−21.19	−0.23	C
	.996	.156	15	20	−15.95	+4.07	C
	2.015	.176	15	20	−12.80	+0.31	C
	.031	.001	15	20	− 4.62	−0.56	C
	.048	.018	12	21	+ 3.24	−2.96	C
	.064	.034	12	20	+13.54	−0.34	C
	.081	.051	13	22	+15.85	−1.63	C
	.097	.067	11	21	+13.64	−1.71	C
	.132	.102	8	20	− 1.06	+3.31	C
	.150	.120	12	23	−16.66	−1.81	C
	.167	.137	11	21	−18.11	+2.32	C
	.183	.154	10	20	−16.27	+4.39	C
	5932.206	.176	7	22	− 9.63	+3.58	C
1930							
Oct. 19.....	6269.008	.008	23	23	− 0.35	−1.37	C
	.025	.025	23	21	+ 5.49	−3.29	C
	.043	.043	23	23	+13.93	+0.28	C
	.064	.064	21	30	+11.00	−1.58	C
	.092	.092	23	29	− 1.30	−0.25	C
	.112	.112	19	22	−13.02	+0.34	C
	.131	.131	23	26	−18.79	+1.07	C
	.152	.152	21	27	−17.17	+1.70	C
	6269.172	.172	24	25	−10.12	+1.91	C
1931							
Sept. 11.....	6596.042	.162	16	21	− 9.81	+2.65	C
	.060	.180	16	20	− 1.98	+0.68	C
	.076	.006	23	18	− 0.91	−8.06	C
	.093	.022	27	20	+14.18	−0.78	C
	.111	.041	26	22	+19.97	+0.98	C
	.131	.060	24	26	+14.57	−0.67	C
	.150	.080	21	20	+ 4.29	−0.42	C
	6596.169	.100	24	23	− 2.54	+5.07	C

* G.M.T. has been used throughout this work.

TABLE II—*Continued*

Date	Julian Day	Phase	No. Lines	Length of Exp.	V	$V_{ob}-V_c$	Meas. By
1931	242+						
	6596.195	.125	22	29^m	−19.02	−1.24	C
	.215	.145	20	20	−14.86	+2.95	C
	.233	.163	18	21	−15.86	−3.98	C
	6596.252	.183	25	25	− 3.68	−2.39	C
1932							
Sept. 5.....	6956.072	.172	16	20	−12.00	+4.18	C
	.090	.000	23	20	+ 8.17	+4.05	C
	.101	.010	27	22	+13.44	+2.49	C
	.126	.036	11	20	+20.84	−0.74	C
	.148	.057	28	20	+18.31	−1.29	C
	.167	.076	29	22	+ 8.63	−0.91	C
	.184	.094	25	10	− 1.24	+2.23	C
	.208	.119	30	22	−13.77	+4.32	C
	.226	.136	24	20	−15.56	+5.44	C
	.244	.154	25	25	−16.35	+0.87	C
	.265	.170	29	25	− 6.70	+2.34	C
	.287	.006	26	28	+ 8.67	+0.57	C
	.308	.028	17	25	+18.21	−1.21	C
	.332	.051	23	33	+19.79	−1.55	C
	.356	.076	18	28	+13.10	+3.39	C
	.378	.097	18	25	− 2.04	+4.07	C
	.399	.118	14	26	−13.38	+4.32	C
	6956.424	.144	7	29	−18.68	+1.57	C
1907							
May 17.....	7713.893	.....	9	20	−14.11	.....	C
	7713.909	.....	15	20	−22.24	.....	C
May 27.....	7723.701	.001	17	20	+ 1.52	.....	C
	.718	.018	13	21	+ 7.92	.....	C
	.734	.034	18	20	+ 6.33	.....	C
	.752	.052	18	20	+ 1.05	.....	C
	.769	.069	14	20	− 9.45	.....	C
	.788	.088	20	22	−19.36	.....	C
	7723.805	.105	19	20	−27.21	.....	C
Oct. 25.....	7874.512	.....	16	30	+ 5.34	.....	C
	7874.602	.....	16	40	+ 3.49	.....	C
Oct. 28.....	7877.573	.003	19	18	−12.60	.....	C
	.588	.018	18	18	− 8.15	.....	C
	.603	.033	18	16	− 1.31	.....	C
	.621	.051	17	14	+10.12	.....	C
	.631	.061	15	14	+ 7.31	.....	C
	.644	.074	15	13	+ 0.66	.....	C
	.657	.087	15	22	− 2.02	.....	C
	7877.678	.108	16	30	−11.29	.....	C

The observers at the Yerkes Observatory were: S. B. Barrett, P. Bourgeois, C. C. Crump, E. B. Frost, C. H. Gingrich, C. Hujer, O. J. Lee, S. A. Mitchell, F. E. Roach, H. F. Schwede, O. Struve, and F. R. Sullivan.

Frost (F) measured four of the series, Miss Helen Davis (D) three of the series, and Mr. John Allen (A) assisted with the measures of the 1919 plates. The values of the velocities for each complete variation of the radial velocity were plotted and the orbit was determined on the assumption that the star is a spectroscopic binary. Definitive elements for the 1919 series only are given. Table II also includes the incomplete series of May 17 and 27 and October 25 and 28, 1907.

In Figure 1 the nineteen different orbits are plotted for the different dates on which complete series of spectrograms were obtained. Table III contains a list of the elements of all the orbits thus far determined. It will be noted that in the group of orbits determined by the writer the values of γ range from $+1.8$ to -20.8 km/sec., with an average value of about -10 km/sec. The variation in K, the semi-amplitude, is from 9.5 to 22.8 km/sec., with an average value of 17 km/sec. The eccentricity (e) has as its greatest value 0.17. The orbit is so nearly circular that the values of ω and T cannot be fixed with certainty. The average value of $a \sin i$ seems to be 45,000 km. Attention should be called to the two orbits determined in September, 1919: one made by the writer and the other by Van Arnam. It is a coincidence that the same number of plates were used in each case, and that the probable errors are not of unlike value. These determinations would indicate that the variation in γ and e are quite rapid, 12 km/sec. being observed for γ and almost the maximum variation of e. Figure 2 contains a graphic representation of the change in γ; Figure 3, K; Figure 4, e; and Figure 5, ω.

Velocity of γ.—When this study was undertaken it was hoped that a period could be established for the variation of the velocity of the center of mass of the system. Such a variation had been detected by Professor Frost from early observations and was later confirmed by the writer in a study made at the University of Michigan. The data at hand do not seem sufficient to determine a period for this variation. Belopolsky proposed a period of nineteen years. Mendenhall suggested that "any period greater than fifteen years" would be admitted by his study. It will be noted from Figure 2 that during the years 1906–1909, γ had a variation of 7 km/sec. and that over

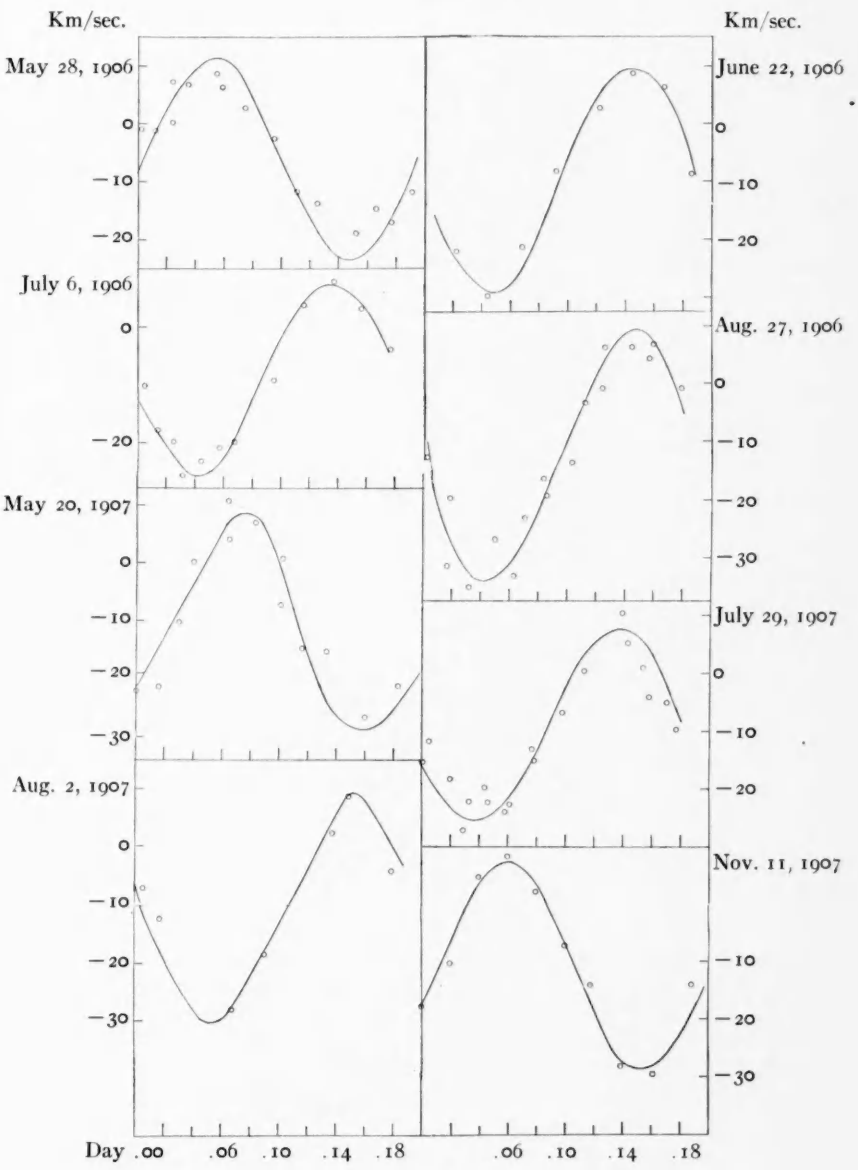

FIG. 1.—β Cephei

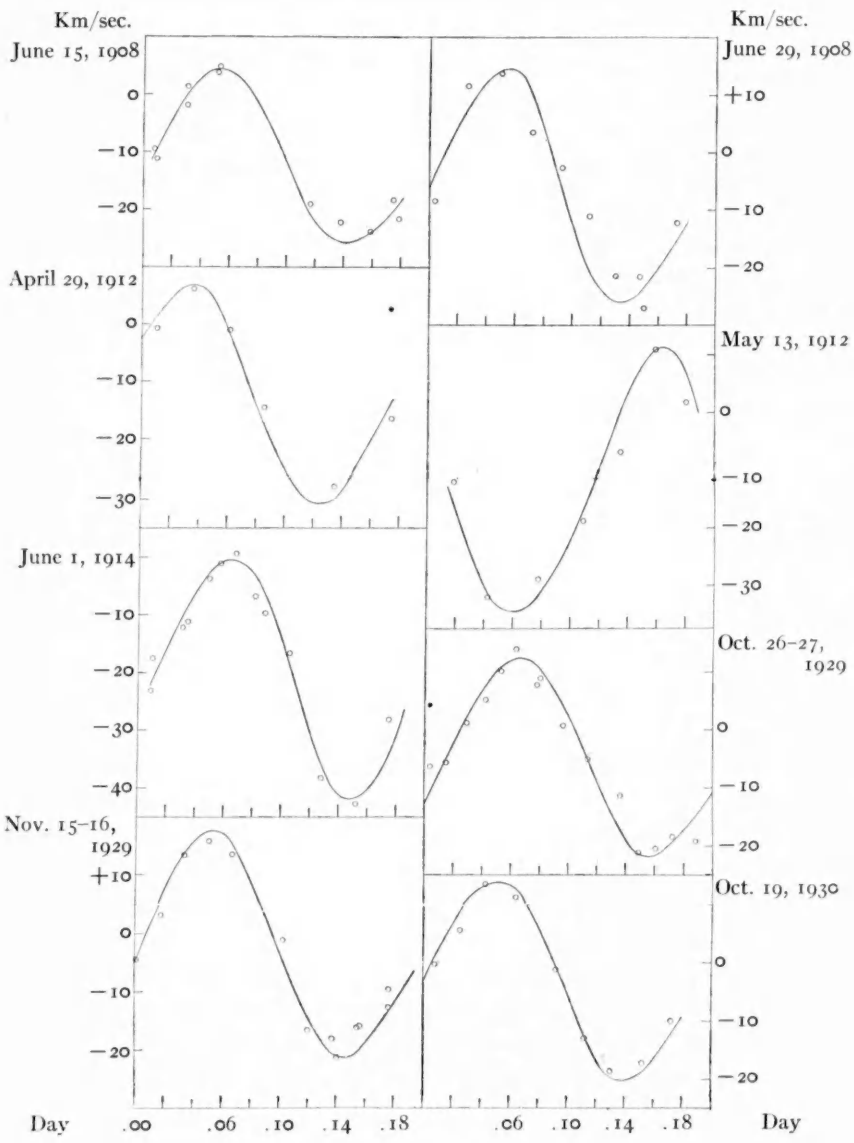
Km/sec.
June 15, 1908
0
−10
−20
April 29, 1912
0
−10
−20
−30
June 1, 1914
−10
−20
−30
−40
Nov. 15–16, 1929
+10
0
−10
−20
Km/sec.
June 29, 1908
+10
0
−10
−20
May 13, 1912
0
−10
−20
−30
Oct. 26–27, 1929
0
−10
−20
Oct. 19, 1930
0
−10
−20
Day
.00
.06
.10
.14
.18
.06
.10
.14
.18
Day

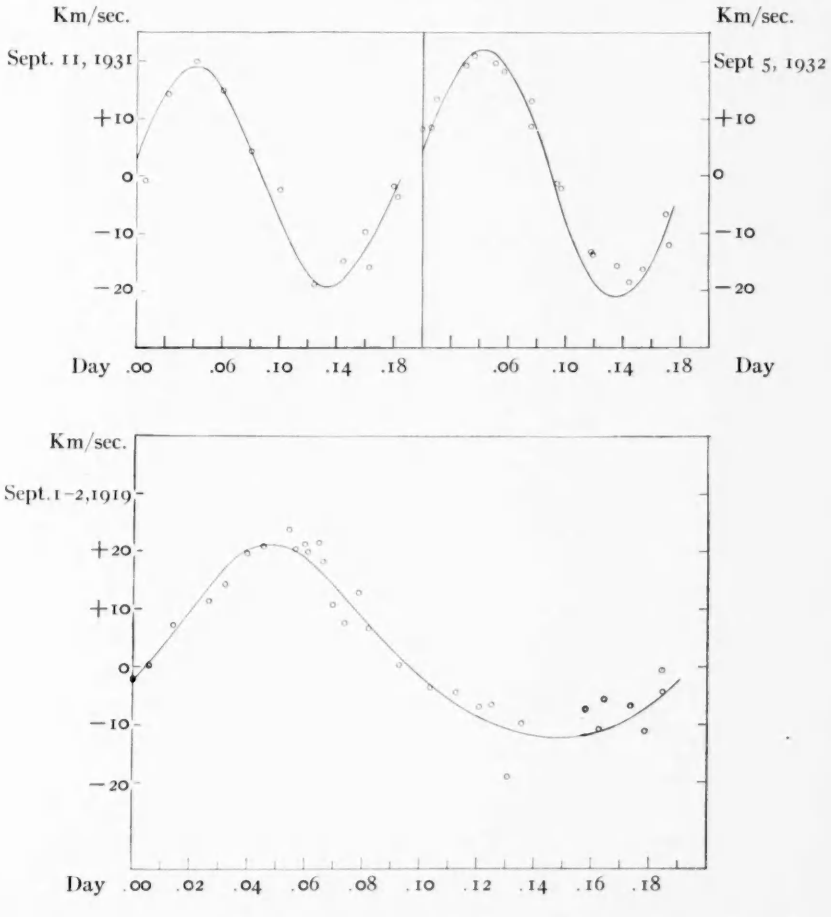

half of this complete range occurred in fourteen days, from June 15 to 29, 1908. From the observations made in 1919, the total range in sixteen days was approximately 12 km/sec., over half the entire variation observed. The entire difference from 1926 to 1932 is 6 km/sec., the same as that noted in 1906–1909, but the latter was between −6 and −13 km/sec., while the former was between −6 and +1 km/sec. Furthermore, a variation of more than half the value observed occurred within three months in 1931.

The semi-amplitude.—Henroteau suggested a short period of twenty-eight days for the variation of K, with an amplitude of 20

TABLE III

Date	Julian Day	γ in Km/Sec.	K in Km/Sec.	e	ω	$a \sin i$ 1000 Km	No. Plates	No. Prisms and A/Mm.	Velocity	Elements
1906	241+									
May 28	7359.810	− 5.75	17.22	.01	185	45	16	II 22	Crump	Crump
June 22	7384.727	− 9.2	19.00	.06	104	50	8	II 22	Crump	Crump
July 6	7398.679	− 9.0	16.40	.02	195	43	12	II 22	Frost; Crump	Crump
Aug. 27	7450.804	−12.7	21.68	.08	78	57	18	II 22	Davis; Crump	Crump
1907										
May 20	7716.706	−11.5	18.8	.14	63	49	13	II 22	Crump	Crump
July 29	7786.775	− 9.7	16.5	.05	6	43	20	II 22	Frost; Crump	Crump
Aug. 2	7790.775	−10.9	19.6	.02	11	51	8	II 22	Crump	Crump
Nov. 11	7891.789	−10.9	18.3	.02	112	48	10	II 22	Crump	Crump
1908										
June 15	8108.712	−11.35	14.95	.09	56	40	11	II 22	Frost; Crump	Crump
June 29	8122.811	− 6.49	20.2	.14	75	52	10	II 22	Frost; Crump	Crump
1912										
April 29	9522.831	−12.75	18.9	.04	36	49	7	II 22	Crump	Crump
May 13	9536.928	−13.1	22.78	.09	54	58	7	II 22	Davis; Crump	Crump
Aug. 8–Nov. 21	9638.812	−14.1	15.8	.04	3	41	163	I 44	Crump	Crump
Oct. 1	9638.820	−12.9	19.2	.05	17	50	(18)	I 44	Crump	Crump
1914	242+									
June 1	0285.725	−20.75	20.6	.10	102	54	13	II 22	Davis; Crump	Crump
Oct. 9–21	0415.285	−26.1	16.8	.16	184	43	35	III 30	Belopolsky;* Gerasimovič	Gerasimovič
1916										
Sept. 12–Oct. 31	1119.363	−32.4	19.0	.10	334	48	55	III 30	Belopolsky†	Belopolsky
Sept. 12–30	1119	−29.5	19.9	.0	.....	.....	(32)	III 30	Belopolsky‡	Mendenhall
Oct. 1–29	1119	−36.2	20.0	.0	.....	.....	(23)	III 30	Belopolsky‡	Mendenhall
1917										
Sept. 16–Oct. 31	1489.311	−22.5	18.0	.07	305	47	32	III 30	Belopolsky†	Belopolsky
1918										
May 15	1729.837	− 6.3	18.3	.07	305	48	6	III 11	Henroteau; Hobe and Mendenhall‡	Mendenhall
1919										
Sept. 1–2	2203.882	+ 1.8	16.7	.17	345	43	32	I 44	Crump	Crump
Sept. 17, 20–21	2219.789	−10.1	13.1	.02	359	34	32	.....	Van Arnam§	Van Arnam

* *Bulletin de l'Observatoire Central de Russie, Poulkovo*, **7**, No. 80.

† *Bulletin de l'Académie des Sciences de Russie*, 1918.

‡ *Lick Observatory Bulletin*, No. 418.

§ *Publications of the Dominion Astrophysical Observatory*, **4**, 171, 1929.

TABLE III—*Continued*

Date	Julian Day	γ in Km/Sec.	K in Km/Sec.	e	ω	$a \sin i$ 1000 Km	No. Plates	No. Prisms and A/Mm.	Velocity	Elements
1920	242+									
Jan. 19–Feb. 3	2343.741	−10.5	14.3	.14	230	37	71	III 33	Henroteau;‖ Henderson	Mendenhall
1921										
Nov. 6	3000.622	− 3.6	14.8	.05	78	39	16	III 11	Hobe; Mendenhall‡	Mendenhall
1922										
Feb. 16–April 18	3102.733	−14.2	13.1	.09	82	34	155	III 33	Henroteau¶	Mendenhall
Aug. 26, 27–Sept. 4	3293.739	− 9.6	9.5	.05	356	25	24	.....	Van Arnam§	Van Arnam
1923										
March 5–28	3484	− 6.8	10.6	.00	.....	28	68	III 33	Henroteau¶	Mendenhall
1926										
June 23–Dec. 31–Jan. 7	4796.832	− 5.1	15.4	.05	274	39	95	III 11	Mendenhall‡	Mendenhall
July 19–Aug. 14	4796.755	− 6.3	13.8	.08	220	36	17	III 22	Mendenhall‡	Mendenhall
1928										
Aug. 22	5480.203	− 0.7	15.5	.00	.....	41	33	III 20	Mitchell-Duncan**	Duncan-Mitchell
Sept. 10	5500.874	− 5.0	17.0	.02	12	45	8	III 11	Mendenhall‡	Mendenhall
1929										
Oct. 26–27	5913.134	− 4.6	16.9	.05	95	44	15	I 30	Crump	Crump
Nov. 15–16	5931.106	− 1.5	19.4	.02	46	51	13	I 30	Crump	Crump
1930										
Oct. 19	6269.095	− 3.1	17.4	.06	91	45	9	I 30	Crump	Crump
1931										
Aug. 16–Nov. 4	6580.566	− 4.6	16.9	.05	3	44	58	I 23	Kohl††	Kohl
Sept. 11	6596.130	− 0.3	18.9	.03	36	49	12	I 30	Crump	Crump
1932										
Sept. 5	6956.160	+ 1.5	21.6	.03	54	55	18	I 30	Crump	Crump

‖ *Publications of the Dominion Observatory*, **5**, 77, 1922.
¶ *Ibid.*, **9**, 36, 1925.
** *Astrophysical Journal*, **70**, 127, 1929.
†† *Astronomische Nachrichten*, **248**, No. 22, 1933.

km/sec. From the plot it seems that the range indicated by Henroteau is too great. Here again it is impossible to determine a period with the existing data. The range of possible periods is large and none of them is at all conclusive. It may be that this quantity varies in a more or less irregular manner.

The eccentricity.—The thirty-six values of the eccentricity, ranging from 0.00 to 0.17, are plotted in Figure 4. It will be readily seen from the velocity-curves which have been determined in this investigation that there is no question as to the reality of this variation. Mendenhall pointed out that the largest values of e seem to occur during intervals when there is rapid variation in γ and K. This seems to be confirmed by the present study.

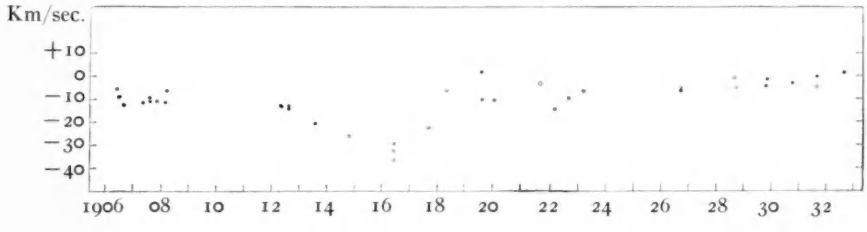

FIG. 2. γ

The longitude of periastron.—When the values of the eccentricity are small, it is evident that there must be great uncertainty in the values of ω and T. It is probably safe to conclude that only the quadrant in which ω is found has significance. The values of ω are given in Figure 5.

Secondary oscillation.—The writer discovered in his work in 1915 that the observations could be satisfied more adequately if account was taken of a secondary oscillation of a period equal to one-third of the original period. In this investigation it appears that there is evidence of a secondary oscillation but that the period varies.

The period.—The period for the variation of the velocity was given by Professor Frost in 1906 as .1904 day. Later, the writer determined for the interval 1906–1912 the average period to be .1904795 day. This period seemed very well established and most investigators have used it. Van Arnam (1919) used a period of .1904843 day in his reductions and Duncan and Mitchell (1928) suggested that a

period of .19047 day would satisfy their observations. It now seems certain that while the average period of .1904795 day satisfies the observations from 1906 to 1918, from that time on an average period of .1904851 day would be preferable. This fact was observed by Dr. Otto Kohl, using published data, together with observations made at the Berlin-Babelsberg Observatory. It seems reasonably

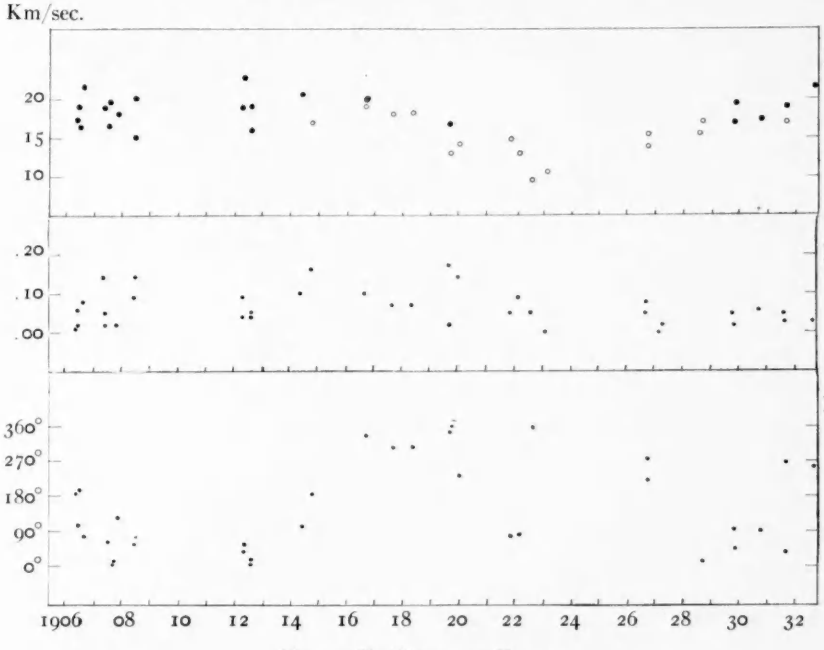

Fig. 3

Fig. 4

Fig. 5

FIG. 3. K; FIG. 4. e; FIG. 5. ω

certain that the average period has increased during the twenty-six years of observation.

As has already been stated, the series of plates secured on the nights of September 1 and 2, 1919, at the Observatory of the University of Michigan is the only series for which definitive elements were derived. The resulting elements with their probable errors are as follows:

$P = 0.1904795$
$K = 16.7 \pm 0.5$
$\gamma = +1.8 \pm 0.1$
$T = 1919$, Sept. 1, 13^h45^m48 E.S.T.
$e = 0.17 \pm 0.02$
$\omega = 345°.1 \pm 1°.8$
$a \sin i = 43{,}000$ km

A study was made to detect, if possible, a variation of the intensity and of the width of different lines in the spectra of a given series. The line λ 4471 (*He* I) was selected as a standard on each plate and eye estimates were made comparing it with lines λ 4552 (*Si* III), λ 4567 (*Si* III), λ 4638 (*O* II), λ 4641 (*O* II), and λ 4649 (*C* III). There was no marked variation from one plate of a given series to another. From the plates which were examined it seems safe to say that if there is a variation of the relative intensity of the lines, it is too slight to be detected with the eye. The measuring of the widths of the lines is beset with more difficulties than the estimates of relative intensities. No reliable results were obtained as to variation in the widths of the lines.

The study of the problem of β Cephei requires further data. It is hoped that photometric observations can be made simultaneously with spectroscopic observations. This would be a real help, and since the period of variation is so short, such a program could be carried out without much difficulty at an observatory equipped with both a photometer and a spectroscope. Various attempts have been made to explain the observed data but none has been completely satisfying.

YERKES OBSERVATORY
WILLIAMS BAY, WIS.
August 2, 1933

THE INTENSITIES OF SOME MULTIPLETS OF *Fe* II AND *Ti* II IN STELLAR SPECTRA

By C. T. ELVEY

ABSTRACT

The total absorptions of eight lines each of *Fe* II and *Ti* II were determined from spectrograms of three-prism dispersion for the stars 10 α Canis Minoris, 24 γ Geminorum, 33 α Persei, 41 Cygni, 50 α Cygni, 17 Leporis, 7 ε Aurigae, and 3 α Lyrae.

The relative intensities of these lines were compared with the square roots of the emission intensities as observed in the flash spectrum and marked deviations from the square-root law were found.

The abnormal enhancement of the strong lines in the spectrum of 17 Leporis with respect to the weak ones has been discussed by O. Struve.[1] The gradient of intensity within a multiplet of lines is much greater in this star than in other stars, such as the supergiant ε Aurigae. In comparing a given multiplet of *Fe* II Struve found that the ratio of intensity of some of the weakest members in ε Aurigae to those in 17 Leporis was as large as 4, while for the strongest members the ratio was unity. By making comparisons with the theoretical intensities of the lines of the multiplet, he found a marked deviation from the square-root law.

That this phenomenon is not confined to this peculiar star is shown by the abnormal intensity gradients in the multiplets of oxygen in the B-type stars, as reported by Struve.[2] Struve and Morgan[3] and Morgan[4] have called attention to the same effect in several A- and F-type stars. I have just investigated[5] the *Si* III triplet in six giant and five dwarf stars and have found deviations from the square-root law. R. v. d. R. Woolley[6] has investigated several multiplets of *Fe* I in the solar spectrum and has found deviations from the square-root law but different deviations are found for different multiplets. He attributes this to the neglect of "interlocking" in the theory of absorption intensities.

Since no explanation is available to throw light upon these ab-

[1] *Astrophysical Journal*, **76**, 85, 1932. [2] *Ibid.*, **74**, 260, 1931.

[3] *Proceedings of the National Academy of Science*, **18**, 590, 1932.

[4] *Astrophysical Journal*, **78**, 158, 1933.

[5] *Ibid.*, p. 219. [6] *Annals of the Solar Physics Observatory*, **3**, 79, 1933.

normal differences in intensities in stellar spectra, I have attempted to determine the departure from the square-root relationship for some selected multiplets of *Fe* II and *Ti* II. To begin with, I chose four stars of class F5 differing greatly in absolute magnitude, the

TABLE I*a*

TOTAL ABSORPTIONS

	1 10 α CMi	2 24 γ Gem	3 33 α Per	4 41 Cyg	5 50 α Cyg	6 17 Lep	7 7 ε Aur	8 7 ε Aur	9 3 α Lyr
	Fe II								
$b^4F-z^4F^\circ$:									
4472	0.13	0.05	0.25	0.22	0.14	0.13	0.28	0.25	0.018
4491	.15	.06	.30	.28	.33	.16	.53	.48	.049
4515	.16	.09	.34	.30	.38	.31	.60	.60	.051
4520	.15	.09	.34	.30	.38	.28	.61	.59	.052
$b^4F-z^4D^\circ$:									
4508	.16	.08	.33	.30	.41	.48	.63	.66	.069
4522	.22	.12	.40	.36	.47	.50	.69	.78	.064
4541	.13	.06	.29	.26	.27	.16	.46	.43	.033
4576	0.10	0.08	0.30	0.24	0.28	0.13	0.49	0.45	0.029
	Ti II								
4470	0.15	0.03	0.34	0.30	0.08	.....	0.34	0.30	0.011
4501	.23	.10	.48	.42	.20	.....	.75	.89	.062
4524	.18	.04	.32	.24	.03	.....	.16	.11	.012
4529	.18	.05	.34	.28	.06	.....	.42	.30	.018
4534	.34	.15	.54	.50	.30	.....	.83	.97	.072
4563	.25	.10	.46	.41	.20	.....	.82	0.95	.057
4572	.27	.12	.51	.46	.25	.....	.84	1.02	.070
4589	0.13	0.06	0.38	0.28	0.08	.....	0.53	0.53	0.020

dwarf α Canis Minoris at one end of the series and the supergiant 7 ε Aurigae at the other end. Four additional stars of interest were added. The intensities were determined from spectrograms obtained with the three-prism Bruce spectrograph. For the stars with faint lines Process plates were used whenever possible. The total absorptions were obtained by measuring, on a rather small-scale microphotogram, the average widths of the bases of the lines (applying a correction for dispersion) and their depths, and computing the area,

or total absorption, assuming the line to have the shape of a triangle. A number of comparisons were made of the intensities obtained by this method with those obtained by the usual one of measuring the entire profile on a large-scale microphotogram and then taking the

TABLE I*b*

RELATIVE INTENSITIES

	1 10 α CMi	2 24 γ Gem	3 33 α Per	4 41 Cyg	5 50 α Cyg	6 17 Lep	7 7 ε Aur	8 7 ε Aur	9 3 α Lyr
	Fe II								
$b^4F-z^4F^\circ$:									
4472	56	44	52	51	29	38	35	33	27
4491	65	53	62	65	68	46	67	64	73
4515	69	79	70	69	79	90	76	80	76
4520	65	79	70	69	79	81	77	78	78
$b^4F-z^4D^\circ$:									
4508	67	60	64	66	73	96	71	73	90
4522	92	90	77	79	84	100	77	86	84
4541	54	45	56	57	48	32	52	47	43
4576	42	60	58	53	50	26	55	50	38
	Ti II								
4470	51	27	59	61	39	14	43	35	20
4501	78	90	84	85	98	111	94	103	113
4524	61	36	56	49	15	9	20	13	22
4529	61	45	59	57	29	14	53	35	33
4534	115	135	94	102	146	148	104	112	131
4563	85	90	80	83	98	91	103	110	104
4572	91	108	89	93	122	112	105	118	128
4589	44	54	66	57	39	27	66	61	36

area with a planimeter. No systematic errors were found within the range of intensities measured.

The observed intensities of the lines are listed in Table I*a*. The values are total absorptions expressed in angstrom units. Table I*b* contains the relative intensities of the lines. Since a comparison is being made with emission intensities as observed in the flash spectrum by A. Pannekoek and M. G. J. Minnaert,[7] each multiplet or

[7] *Verhandelingen der Koninklijke Akademie van Wetenschappen te Amsterdam*, Eerste sectie, **13**, No. 5, 1928.

group of lines has had the total intensities in absorption adjusted in such a way that their sum equals the sum of the square roots of the flash intensities, each emission intensity having been multiplied by 100 in order to give convenient units. The flash intensities are listed in Table II. The intensities of the emission lines in the flash spectrum have been used, since they give a more consistent set of data than do the intensities measured in the laboratory. However, it should be noted that Pannekoek and Minnaert found the intensities in the flash spectrum to be proportional to the square root of the theoretical intensities, and consequently, wherever I have found an

TABLE II

INTENSITIES IN THE FLASH SPECTRUM

	Fe II				*Ti* II		
	Multiplet	I	$10\sqrt{I}$		Multiplet	I	$10\sqrt{I}$
4472.93.....	$b^4F-z^4F^\circ$	22	47	4470.88.....	$a^4P-z^2D^\circ$	12	35
4491.41.....	$b^4F-z^4F^\circ$	42	65	4501.29.....	$a^2G-z^2F^\circ$	121	110
4515.33.....	$b^4F-z^4F^\circ$	49	70	4524.73.....	$b^4P-z^2D^\circ$	11	33
4520.24.....	$b^4F-z^4F^\circ$	52	72	4529.49.....	$a^2H-z^2G^\circ$	14	37
4508.29.....	$b^4F-z^4D^\circ$	46	68	4533.97.....	$a^2P-z^2D^\circ$	141	119
4522.64.....	$b^4F-z^4D^\circ$	66	81	4563.76.....	$a^2P-z^2D^\circ$	93	96
4541.52.....	$b^4F-z^4D^\circ$	28	53	4571.97.....	$a^2H-z^2G^\circ$	101	100
4576.31.....	$b^4F-z^4D^\circ$	28	53	4589.96.....	$a^2P-z^2D^\circ$	34	58

agreement of the total absorptions with the square roots of the flash intensities it will be with the fourth root of the theoretical intensities.

The data of Table I*b* are shown in the form of graphs in Figures 1 and 2. The ordinates are the square roots of the emission intensities and the abscissae are the relative intensities in absorption. The dashed line at 45° represents exact correlation with the square-root law. The numbers on the diagrams correspond with the numbers of the stars in the table. For *Fe* II, four lines each of two multiplets were used, the dots in Figure 1 representing $b^2F-z^2F^\circ$, and the circles $b^4F-z^4D^\circ$. In the case of *Ti* II, lines had to be chosen from several multiplets and no attempt has been made to show them separately.

The deviations from the square-root law for *Fe* II are in the direction of a larger gradient for the relative intensities within a multiplet, that is, there is a tendency for the intensities in absorption to be

proportional to the emission intensities instead of to their square roots. The greatest deviation is for 17 Leporis (No. 6). There is considerable scatter in the observations, owing to our having only two three-prism spectrograms, both of poor quality. J. A. Hynek[8]

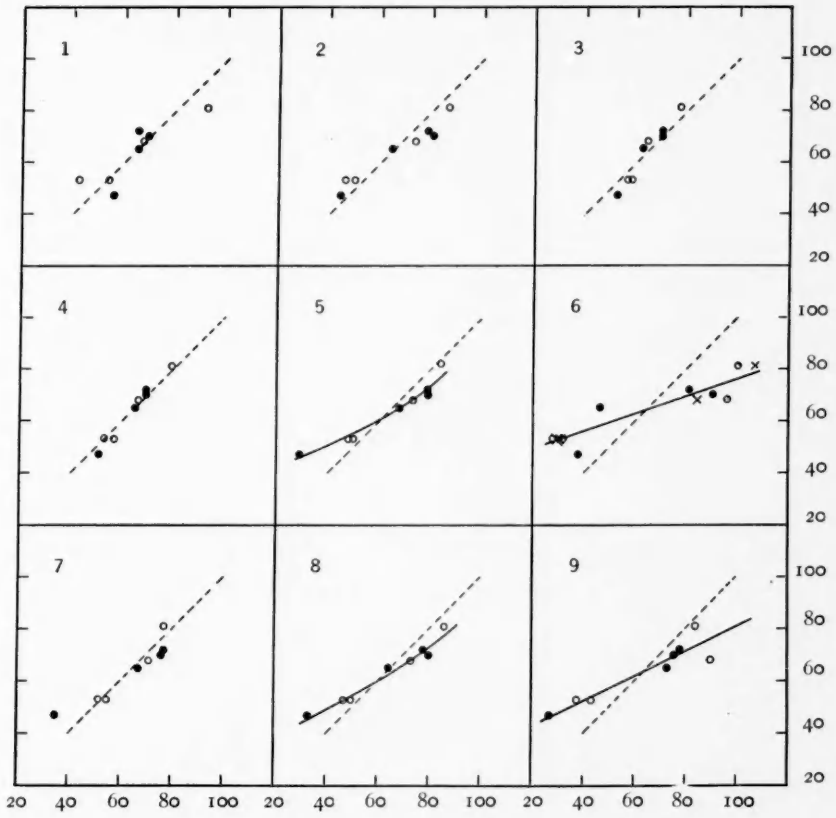

FIG. 1.—Relative intensities of *Fe* II lines in stellar spectra (abscissae) compared with square roots of emission intensities in the flash spectrum (ordinates). The diagrams are for the following stars: 1, α CMi.; 2, γ Gem.; 3, α Per.; 4, 41 Cyg.; 5, α Cyg.; 6, 17 Lep.; 7, ε Aur. (lines symmetrical); 8, ε Aur. (lines asymmetrical); and 9, α Lyr.

has measured the intensities of the lines in this star on nine spectrograms of single-prism dispersion and for the one multiplet of *Fe* II his observations are represented by crosses. The peculiar spectral changes in this star have been attributed by Struve[9] to the ejection

[8] *Astrophysical Journal*, **78**, 54, 1933.

[9] *Loc. cit.*

of shells of gas from its surface, and, consequently, we would hardly expect this star to have a normal atmosphere in a steady state, but undoubtedly one in which there is considerable turbulence.

The next largest deviations are shown by α Lyrae (No. 9), a normal star of class A0, and by α Cygni (No. 5), an A2 supergiant. For

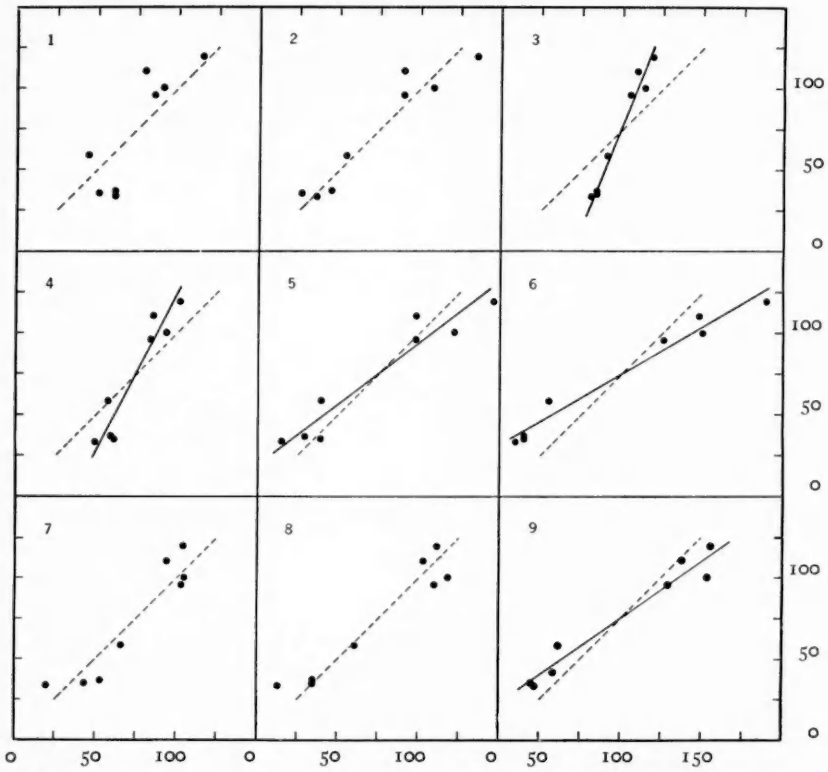

FIG. 2.—Relative intensities of *Ti* II lines in stellar spectra (abscissae) compared with the square roots of emission intensities in the flash spectrum (ordinates). The diagrams are for the following stars: 1, α CMi.; 2, γ Gem.; 3, α Per.; 4, 41 Cyg.; 5, α Cyg.; 6, 17 Lep.; 7, ε Aur. (lines symmetrical); 8, ε Aur. (lines asymmetrical); and 9, α Lyr.

α Lyrae the observed intensities depend upon one spectrogram, an excellent one, however, made on Process emulsion; on the other hand, the lines are weak, and this adds uncertainty to the measures. The first four stars on the list show rather good agreement with the square-root law for the *Fe* II lines. The first one, α Canis Minoris, is a dwarf of class F5; γ Geminorum (No. 2) is a normal star of class

A0; α Persei and 41 Cygni (Nos. 3 and 4) are giants of class F5. It might be noted, however, that for γ Geminorum the best fit of the observations would be obtained if the dashed line were rotated clockwise, and for the two giants if it were rotated counterclockwise.

Numbers 7 and 8 are for the star 7 ε Aurigae, the F5 supergiant, which during its last eclipse showed decided asymmetries of certain spectral lines at the partial phases.[10] Comparisons with the emission intensities were made separately for spectrograms showing the lines symmetrical (No. 7) and asymmetrical (No. 8). There is a definite tendency for the asymmetrical lines to show a deviation from the square-root law in the direction of larger gradient.

The results for the *Ti* II lines are shown in Figure 2, the arrangement of the diagram being the same as that of Figure 1. Here we note some striking differences from the results obtained for *Fe* II. The first star, α Canis Minoris, shows a fairly large scatter in the observations, owing to blends occurring in a spectrum so rich in lines that very little can be said concerning them. γ Geminorum shows a very good agreement with the square-root law, while the two F5 giants, α Persei and 41 Cygni, show marked deviations in the direction of a very small gradient for the relative intensities. This has been observed visually by Morgan.[11] The stars α Cygni, 17 Leporis (from Hynek's observed intensities), and α Lyrae show deviations of about the same order of magnitude, making the gradient larger than the square-root law requires. For ε Aurigae the same effect is noticed as in *Fe* II, but it is not as noticeable on the diagrams because of the scatter in the observations. However, by comparing each line it is seen that there is a deviation for the asymmetrical lines in the direction of a greater gradient.

The data given above are still too meager to draw definite conclusions as to the cause of the observed deviations from the square-root law. However, they show that very likely at least two factors enter: the known deviation due to the low concentration of atoms (weak lines)[12] and an additional effect seen especially in 17 Leporis.

[10] *Publications of the Yerkes Observatory*, **7**, 81, 1932.

[11] *Loc. cit.*

[12] This effect has been studied both observationally and theoretically by M. G. J. Minnaert and his colleagues, *Zeitschrift für Astrophysik*, **1**, 192, 1930; *ibid.*, **2**, 165, 1931; *Proceedings Koninklijke Akademie van Wetenschappen te Amsterdam*, **34**, 542, 1931.

The latter is possibly due to turbulence. An effect of increased gradient is noticed also in ϵ Aurigae when the lines become asymmetrical during the partial phases of the eclipse. A reasonable hypothesis to explain the asymmetries is that the eclipse is caused by a rotating star which has a very extensive atmosphere producing additional absorption lines somewhat displaced with respect to the lines of the primary star. The total absorption of the combined lines would show an increased gradient similar to that produced by turbulence.

YERKES OBSERVATORY
September 23, 1930

NOTES

THE ATMOSPHERIC OZONE ABSORPTION IN THE VISIBLE SPECTRUM

ABSTRACT

In spectrograms of the light from the eastern sky before sunrise, pronounced absorption shows at the positions of the two main ozone bands in the orange and yellow and is probably due principally to the intensification of this very weak absorption in the long paths occasioned by multiple scattering.

Spectrograms of the light from the eastern sky before sunrise have been taken at the station of the Smithsonian Astrophysical Observatory at Table Mountain, California (altitude 7,500 ft.), in an effort to obtain in a simple way distinct photographic records of the absorption of atmospheric ozone which lies in the orange-and-yellow portion of the spectrum. These Chappuis bands have been found in the solar spectrum in the bolometric measurements of Fowle[1] and of Lindholm[2] by Cabannes and Dufay,[3] and in the photographic measurements of Plaskett[4] by Dufay.[5] In 1884 Schoene[6] reported the visual observation of these bands in the light of the eastern sky before

[1] *Ap. J.*, **38**, 392, 1913.

[2] *Nova Acta Regiae Societatis Scientiarum Upsaliensis* (4th ser.), **3**, 1913.

[3] CR, **179**, 191, 1924; *J. de Phys. et le Radium* (6), **7**, 257 (1926).

[4] *DAO*, Victoria, **2**, 213, 1923. [5] *J. de Phys. et le Radium* (7), **1**, S31, 1930.

[6] *J. Russ. Phys.-Chem. Soc.*, **16**, Part IX, 250, December 20, 1884; *J. Chem. Soc.*, **48**, 713, 1884; *Chem. News*, **69**, 289, 1894.

sunrise under abnormally favorable weather conditions. The present experiments were undertaken because it seemed that multiple scattering might very well lead to a pronounced strengthening of these bands in the atmosphere. Considerably before sunrise the atmosphere in the east receives its illumination scattered from more easterly atmosphere which itself is illuminated by sunlight that has passed very obliquely through considerable paths of the higher atmosphere still farther to the east. This scattered solar radiation should suffer rather large absorption by ozone. Diurnal changes in the atmospheric ozone could evidently also play a part.

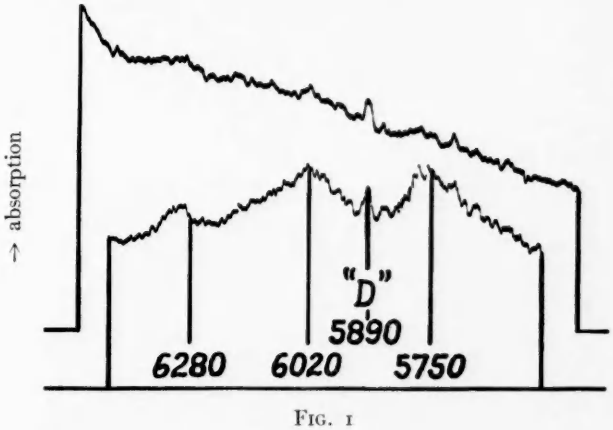

FIG. 1

The spectrograms taken at Table Mountain appear to show the two principal bands clearly. They were made with a very simple apparatus consisting of a small direct-vision spectroscope (transmission grating replica, Cenco "Wallace" type) affixed to a camera box, and adjusted so that the sodium D lines were in focus on the plate. The figure shows a microphotometer record of such a spectrogram (lower), and another of north-sky light for comparison taken with the sun in the sky. Sodium D shows as a small but unmistakable absorption peak. On both sides, absorption at the positions of the two main ozone bands[7] stands out clearly in the record of the light of the eastern sky before sunrise. The third oxygen band (edge at λ 6278, degrades to the red) can be seen. Weak absorption

[7] See, e.g., Wulf, *Proc. Nat. Acad. Sci.*, **16**, 507, 1930.

due to water vapor also occurs in the general region of the ozone bands. Two factors make it probable, however, that this has not led to confusion here: first, the spectrograms were made under favorable conditions of low atmospheric water, and, second, the weak water band in this region lies rather between the two ozone bands, at approximately λ 5900, thus not seriously affecting their identification. The plates indicate that the light from the eastern sky before sunrise does show the ozone absorption quite strongly. The study of the scattered light is being continued.

OLIVER R. WULF,[8] ALFRED F. MOORE, AND
EUGENE H. MELVIN

SMITHSONIAN INSTITUTION AND BUREAU
OF CHEMISTRY AND SOILS
Washington, D.C.
December, 8, 1933

ERRATUM

Vol. 78, No. 1, July 1933, p. 59, eighteenth line from top, *read* 10^{-4} *for* 10^{-8}.

[8] Fellow of the John Simon Guggenheim Memorial Foundation during part of this work.